Response to the comments of the editor:

We thank the editor for the helpful comments.

Comment: The use of verb tenses in the abstract is not consistent: the 1st sentence is in simple past, the 2nd, 3rd, and 4th are in present, and the 5th is in the past again. I would follow up on the suggestion of one of the reviewers and make the use of tenses more uniform. Simple past is more appropriate for observations done in the experiment or doing the data analysis.

In Figure 5, the color used for ozonolysis and color used for measured OH are hard to tell apart. I would recommend using something like bight green for ozonolysis since its contribution is small and hard to miss in the figure.

Response: Changes are implemented as suggested.

Investigation of the oxidation of methyl vinyl ketone (MVK) by OH radicals in the atmospheric simulation chamber SAPHIR

Hendrik Fuchs[1], Sascha Albrecht[1], Ismail–Hakki Acir[1, a], Birger Bohn[1], Martin Breitenlechner[2], Hans-Peter Dorn[1], Georgios I. Gkatzelis[1], Andreas Hofzumahaus[1], Frank Holland[1], Martin Kaminski[1, b], Frank N. Keutsch[2], Anna Novelli[1], David Reimer[1], Franz Rohrer[1], Ralf Tillmann[1], Luc Vereecken[1], Robert Wegener[1], Alexander Zaytsev[2], Astrid Kiendler-Scharr[1], and Andreas Wahner[1]

[1]Institute of Energy and Climate Research, IEK-8: Troposphere, Forschungszentrum Jülich GmbH, Jülich, Germany
[2]School of Engineering and Applied Sciences and Department of Chemistry and Chemical Biology, Harvard University, Cambridge, MA, USA
[a]now at: Institute of Nutrition and Food Sciences, Food Chemistry, University of Bonn, Germany
[b]now at: Bundesamt für Verbraucherschutz, Abteilung 5 – Methodenstandardisierung, Germany

Correspondence to: Hendrik Fuchs
(h.fuchs@fz-juelich.de)

Abstract. The photooxidation of methyl vinyl ketone (MVK) was investigated in the atmospheric simulation chamber SAPHIR for conditions at which organic peroxy radicals (RO_2) mainly reacted with NO ("high NO" case) and for conditions at which other reaction channels could compete ("low NO" case). Measurements of trace gas concentrations were~~are~~ compared to calculated concentration time series applying the Master Chemical Mechanism (MCM version 3.3.1). Product yields of methylglyoxal and glycolaldehyde were~~are~~ determined from measurements. For the high NO case, the methylglyoxal yield was~~is~~ (19 ± 3) % and the glycolaldehyde yield was~~is~~ (65 ± 14) % consistent with recent literature studies. For the low NO case, the methylglyoxal yield reduced to (5 ± 2) % because other RO_2 reaction channels that do not form methylglyoxal became~~become~~ important. Consistent with literature data, the glycolaldehyde yield of (37 ± 9) % determined in the experiment was~~is~~ not reduced as much as implemented in the MCM suggesting additional reaction channels producing glycolaldehyde. At the same time, direct quantification of OH radicals in the experiments shows the need for an enhanced OH radical production at low NO conditions similar to previous studies investigating the oxidation of the parent VOC isoprene and methacrolein, the second major oxidation product of isoprene. For MVK the model–measurement discrepancy was~~is~~ up to a factor of 2. Product yields and OH observations were~~are~~ consistent with assumptions of additional RO_2 plus HO_2 reaction channels as proposed in literature for the major RO_2 species formed from the reaction of MVK with OH. This study, however, shows that also HO_2 radical concentrations are underestimated by the model, suggesting that additional OH is not directly produced from RO_2 radical reactions, but indirectly via increased HO_2. Quantum chemical calculations show that HO_2 could be produced from a fast 1,4-H shift of the second most important MVK derived RO_2 species (reaction rate constant $0.003\,s^{-1}$). However, additional HO_2 from this reaction was~~is~~ not sufficiently large to bring modelled HO_2 radical concentrations into agreement with measurements due to the small yield of this RO_2 species. An additional reaction channel of the major RO_2 species with a reaction rate constant of $(0.006 \pm 0.004)\,s^{-1}$ would be required that produces concurrently HO_2 radicals and glycolaldehyde to achieve model–measurement agreement. A unimolecular reaction similar to the 1,5-H shift reaction that was proposed in literature for

RO_2 radicals from MVK would not explain product yields for conditions of experiments in this study. A set of H-migration reactions for the main RO_2 radicals were investigated by quantum chemical and theoretical kinetic methodologies, but did not reveal a contributing route to HO_2 radicals or glycolaldehyde.

1 Introduction

Isoprene (C_5H_8) emitted by plants (Guenther et al., 2012) has the highest emission rate among non-methane organic compounds. Isoprene is mainly oxidized by the photochemically generated hydroxyl radical (OH) forming the first-generation organic compounds methacrolein (MACR), methyl vinyl ketone (MVK), formaldehyde (HCHO and isoprene hydroxyperoxides (ISOPOOH) (e.g. Karl et al., 2006). The latter ones are formed without the involvement of nitric oxide (NO) so that ISOPOOH becomes increasingly important with decreasing concentrations of nitrogen oxides (St. Clair et al., 2015) which are mainly released by anthropogenic activities. The formation of MVK and MACR is accompanied by the production of HO_2, which can further recycle OH, whereas ISOPOOH formation is a radical termination reaction. However, field studies have shown that also in environments where NO concentrations are less than a few 100 pptv a high OH regeneration rate can be maintained which is not explained by chemical models (Tan et al., 2001; Lelieveld et al., 2008; Hofzumahaus et al., 2009; Whalley et al., 2011). The gap between measured and modelled OH is correlated with the abundance of isoprene (Lu et al., 2012). Since then, it has been recognized that organic peroxy radical (RO_2) pathways which do not require NO as reaction partner can also significantly recycle OH (Wennberg et al., 2018). These reactions include

- hydrogen-shift reactions of RO_2 radicals forming OH or HO_2,
- reaction of peroxy radicals with HO_2.

These pathways have both been identified in the oxidation chain of isoprene (Peeters et al., 2009, 2014). 1,6 H-shift of RO_2 formed in the reaction of isoprene with OH leads to the formation of hydroxyperoxy aldehydes (HPALD) and HO_2. The photolysis of HPALD gives even additional OH radicals. Its relevance for the atmosphere has been shown in laboratory experiments (Crounse et al., 2011; Wolfe et al., 2012) and chamber experiments (Fuchs et al., 2013). In the supplement of the first publication of the LIM (Peeters et al., 2009) the authors also suggested that a 1,5-H-shift reaction could be relevant for MVK and MACR. For MACR, however, an 1,4 H-shift reaction for RO_2 was found, which efficiently recycles OH (Crounse et al., 2012). Its impact on the radical budget has been shown in chamber experiments (Fuchs et al., 2014). H-shift reactions have also been proposed to be important for RO_2 radicals which are formed in the oxidation chain of ISOPOOH (D'Ambro et al., 2017) also potentially enhancing the OH regeneration rate.

The reaction of peroxy radicals with HO_2 forms not only hydroxyperoxides, but also OH together with an alkoxy radical. This was shown for the acetylperoxy radical with an OH yield of 50 % (Dillon and Crowley, 2008; Winiberg et al., 2016). In a recent study by Praske et al. (2015), product yields from the reaction of MVK derived peroxy radicals with HO_2 were investigated. Similar to the acetylperoxy radical, product yields demonstrated that only one third of the reaction yields hydroxyperoxides and that two additional reaction channels exist, both of which could lead to the reformation of OH.

In this study, the oxidation of MVK by OH was investigated in the atmospheric simulation chamber SAPHIR (Simulation of Atmospheric PHotochemistry In a Large Reaction Chamber) at Forschungszentrum Jülich. Experiments were performed under controlled conditions with atmospheric trace gas and radical concentrations. In these experiments, not only organic compounds like in previous studies were measured, but also radical species (OH, HO_2, and RO_2) allowing for an analysis

of the OH budget. In the low NO case, NO mixing ratios were kept below 100 pptv so that different RO_2 radical reactions, i.e. reaction with HO_2 and unimolecular isomerization reactions, can compete. Measured time series of radical concentrations are compared to model calculations applying the Master Chemical Mechanism version 3.1.1 (MCM, 2017) and modifications suggested in literature.

2 Methods

2.1 Simulation experiment in SAPHIR

Experiments were performed in the outdoor atmospheric simulation chamber SAPHIR. Details of the chamber can be found in previous publications (e.g. Rohrer et al., 2005). SAPHIR has a cylindrical shape (length 18 m, diameter 5 m, volume 270 m^3) and consists of a double-wall FEP (fluorethylene-propylene) film. A small overpressure (45 Pa) prevents ambient air entering the chamber. The replenishment flow that is required to maintain this pressure leads to a dilution of all trace gases by approximately 3 to 5 % per hour. A shutter system shades the chamber before the photooxidation experiment is started. Natural sunlight is used to irradiate the mixture. Small sources of nitrous acid (HONO) and formaldehyde (HCHO) are present in the sunlit chamber (100 to 200 pptv/h). The photolysis of HONO is typically the primary source for OH radicals and nitrogen oxides.

In total, four experiments were conducted in this study, two of them at low NO (23 June 2016: NO<70 pptv and 23 May 2017: NO<40 pptv) and two of them at high NO conditions (20 August 2014: 0.7 to 6 ppbv NO and 17 May 2017: approximately 0.1 to 0.4 ppbv NO). Results from experiments performed at similar conditions gave consistent results. The discussion of results focus on the two experiments for which the number of trace gas measurements was highest and results for the other experiments are shown in the Supporting Information.

The experiments started with cleaning the chamber air by flushing out impurities from previous experiments until trace gas concentrations were below the detection limit of the instruments. The chamber air was first humidified by flushing water vapour from boiling water into the dark chamber (relative humidity approximately 70 %). In the low NO experiments, approximately 140 ppbv ozone produced from a silent discharge ozoniser (O3onia) was injected in the dark, in order to suppress NO concentrations. In contrast, 6 to 10 ppbv of NO_2 or NO were injected from a gas mixture in case of the high NO experiments. In one of the two low NO experiments (23 May 2017), 20 ppbv MVK (Sigma-Aldrich, purity 99 %) in water was injected in the dark chamber from a Liquid Calibration Unit (LCU, Ionicon). MVK (1.5 ppbv) was reinjected after 3.5 hours of photooxidation. In the other experiments, MVK was injected several times during the experiment after an initial phase of illumination of the chamber air without additional OH reactants by injecting liquid MVK into a heated inlet line that is flushed by synthetic air. This procedure was similar to that applied in previous studies (e.g. Fuchs et al., 2013, 2014; Kaminski et al., 2017). The photooxidation of MVK was then observed for several hours. No significant particle formation was observed in the experiments so that only gas-phase chemistry needs to be considered in the evaluation.

2.2 Instrumentation

Trace gas concentrations were measured with a comprehensive set of instruments. Nitric oxide (NO) was detected by chemiluminescence (Eco Physics) and nitrogen dioxide (NO_2) by the same instrument but with a blue-light converter in the inlet. In one of the experiments (17 May 2017), no NO_x measurements were available. A cavity ring-down instrument (Picarro) monitored water vapour and carbon monoxide and a UV photometer (Ansyco) detected ozone.

The total OH reactivity (inverse lifetime of OH) was measured by a pump-probe method (Lou et al., 2010; Fuchs et al., 2017), in which the decay of OH radicals produced by laser flash photolysis of ozone is observed by laser-induced fluorescence (LP-LIF). OH reactivity gives a measure of all OH reactant concentrations, so that potential gaps in the detection of e.g. organic compounds that are relevant for the radical chemistry can be identified (e.g. Nölscher et al., 2012). Unfortunately, the instrument failed in 2014, so that OH reactivity was only measured in one of the two high NO experiments.

Organic compounds were measured by a proton-transfer time-of-flight mass spectrometer (PTR-TOF-MS, Ionicon), which was calibrated to quantify MVK. Methylglyoxal ($CHOCOCH_3$, MGLYOX), and glycolaldehyde ($HOCH_2CHO$) were quantified in one low and one high NO experiment. In the other two experiments, performed in different years, the PTR-TOF-MS was calibrated for MVK, but not for methylglyoxal and glycolaldehyde for all experiments so that these species could not be quantified in all experiments. Acetic acid was detected on the same mass as glycolaldehyde in the PTR-TOF-MS instrument. However, model calculations suggest that the contribution of acetic acid was less than 10 % of the total signal. Therefore, measurements represent glycolaldehyde concentrations reasonably well.

A second PTR-TOF-MS instrument (PTR-3, Ionicon) quantified MVK concentrations in the experiment on 23 May 2017. Measurements of both instruments agreed within 20 %. In addition to direct measurements of MVK concentrations, measurements of the OH reactivity can be used to calculate the MVK concentration that was injected in the experiments because the increase in OH reactivity at that point in time can be attributed to the MVK concentration increase. The comparison with the increase in MVK measurements by the PTR-TOF-MS instrument shows good agreement.

In the experiments in 2017, formaldehyde was measured by the same differential optical absorption spectroscopy (DOAS) instrument that also detects OH radicals in the chamber (Dorn et al., 1995). In the other years, HCHO was measured by a Hantzsch monitor. The 1σ-precision of the formaldehyde measurement of 230 pptv is less than that of the Hantzsch monitor (20 pptv), but it is sufficiently high for the detection of HCHO in the experiments here.

OH was detected by DOAS (Dorn et al., 1995) in all experiments except for the high NO experiment in 2014. In addition, OH, HO_2 and RO_2 radicals were measured by laser-induced fluorescence (LIF). The instrument has been described in detail elsewhere (Fuchs et al., 2008, 2011, 2016). OH concentrations measured by LIF in the SAPHIR chamber have been shown to agree with measurements by DOAS in several comparison exercises (e.g. Schlosser et al., 2009; Fuchs et al., 2012). Good agreement was also observed in this work so that significant potential artefacts in the LIF detection scheme as reported for some instruments in the field (Mao et al., 2012; Novelli et al., 2014; Rickly and Stevens, 2018) can be excluded.

HO_2 and RO_2 are chemically converted to OH by the reaction with NO prior to OH detection by laser-induced fluorescence in the LIF instrument. The conversion of RO_2 requires at least two subsequent reactions with NO. First, RO_2 is converted by

added NO to HO_x in a flow reactor upstream of the fluorescence cell. Added CO in the reactor ensures that the HO_x consists predominantly of HO_2, which has a small wall loss compared to OH. The reactor is operated at higher pressure (25 hPa) compared to the low-pressure (4 hPa) LIF detection cell (Fuchs et al., 2009). The HO_x is sampled from the reactor into the LIF detection cell where HO_2 is converted by a large excess of added NO to OH. Operational parameters of the RO_2 system are optimized for the efficient detection of RO_2 radicals that have a similar reaction rate with NO as methylperoxy radicals. As a consequence, RO_2 radicals are not efficiently detected, if their reaction with NO does not directly and quantitatively result in the production of HO_2. This is for example the case for the peroxy radical $HMVKBO_2$ (as named in the MCM) that is formed from the reaction of MVK with OH (see below for details). This has to be taken into account, if measured RO_2 radicals are compared with model calculations.

The HO_2 detection cell consists of a fluorescence cell, in which HO_2 reacts with excess NO that is injected behind the inlet nozzle. As shown for several LIF instruments, the HO_2 signal can also contain contributions from RO_2 radicals that rapidly form HO_2 in the reaction with NO (Fuchs et al., 2011; Whalley et al., 2013; Lew et al., 2018). This applies for those RO_2 radicals which form an alkoxy radical (RO) in the reaction with NO that rapidly produces HO_2 and other products. The interferences from RO_2 can be minimized, however, if the instrument is operated with an NO concentration, for which the HO_2 to OH conversion efficiency is only approximately less than 10 %. In this case, the RO_2 to OH conversion efficiency becomes much smaller for all RO_2 species, because the two reactions with NO needed to produce OH limit the overall conversion efficiency. In this study, the HO_2 channel of the LIF instrument was operated such that RO_2 interferences can be assumed to be negligible.

In one of the experiments (23 May 2017), HO_2 was additionally detected by a newly developed chemical ionization mass spectrometry (CIMS) instrument using Br^- as ionization reagent. HO_2 is detected as cluster ion similar to the approaches reported by Veres et al. (2015); Sanchez et al. (2016) using an I^- and Br^- CIMS, respectively. Details of this new instrument will be presented in a separate publication. HO_2 measurements of the CIMS instrument agreed with $[HO_2]$ detected by the LIF instrument within 15 %.

Solar radiation was measured outside the chamber using a spectroradiometer. Photolysis frequencies are then calculated by applying a model to transfer outside conditions to conditions inside the chamber (Bohn et al., 2005; Bohn and Zilken, 2005). Latest recommendations for absorption spectra and photolysis yields are used.

2.3 Model calculations

Model calculations were performed using the Master Chemical Mechanism in its latest version 3.3.1 (MCM, 2017). A simplified reaction scheme is shown in Fig. 1. The MCM mechanism was modified (MCM*) to take results reported in literature into account and findings in this work. Details are listed in Table 1.

Chamber specific properties were added such as dilution of traces gases due to the replenishment flow. Sources for HONO and HCHO production from the chamber were parametrized as described in previous publications (e.g. Fuchs et al., 2014; Kaminski et al., 2017).

Model calculations were constrained to physical parameters (pressure, temperature, photolysis frequencies, dilution rate of trace gases). A small, constant background OH reactivity of unknown OH reactants that was measured by the OH reactivity instrument after humidification of the chamber air was modelled as an OH reactant that converts OH to HO_2. However, the magnitude of this background reactivity was small ($< 1\,s^{-1}$) compared to the OH reactivity from MVK during the experiment ($> 15\,s^{-1}$) so that it did not affect the chemistry.

Injections of trace gases were modelled as sources during the time of injection, but injected trace gases were not constrained to measured values at later times. $[NO]$, $[NO_2]$ and $[O_3]$ were only constrained to measurements for the high NO_x experiment, because differences between modelled and measured values would have led to significant differences in other observables. No modelling could be performed for one of the high NO experiments (17 May 2017) due to the lack of NO_x measurements. No measurements for the reaction rate constants of RO_2 species from MVK exist. The sensitivity of model results to a change of the RO_2 reaction rate constants, however, is rather small so that their uncertainties could not explain observed model-measurements discrepancies.

2.4 Quantum-chemical calculations

A set of H-migration reactions for the main MVK-derived peroxy radicals was investigated by quantum chemical and theoretical kinetic methodologies. The reactions studied included migration of hydroxyl, of $\alpha-$OH, and of methyl H-atoms; direct HO_2 elimination forming an enol was also investigated (Table 2).

Several methodologies were applied, as detailed in the supporting information. From these data, the M06-2X/cc-pVTZ rovibrational data (Dunning, 1989; Zhao and Truhlar, 2008), with CCSD(T)/aug-schwartz4(DT) single point energy calculations extrapolated to the basis set limit (Purvis and Bartlett, 1982; Martin, 1996) were selected. All quantum chemical calculations were performed using the Gaussian-09 program suite (Frisch et al., 2010). The high-pressure rate coefficients for each of the elementary processes was then calculated using multi-conformer canonical transition state theory, MC-CTST (Vereecken and Peeters, 2003; Zheng and Truhlar, 2013) based on a rigid rotor harmonic oscillator paradigm, an exhaustive search of the reactants and TS conformers, and asymmetric Eckart tunneling and WKB zero-curvature (ZCT) tunneling. For the 1,4- and 1,6-H-shift in $HMVKAO_2$, a large difference between Eckart and ZCT tunneling was found; the geometric average is reported here (see Supporting Information).

3 Results

3.1 Product yields

The reaction of OH with MVK leads to the addition of OH to either one of the double-bonded C-atoms so that two different RO_2 radical species can be formed (Fig. 1):

$$MVK + OH \rightarrow HMVKAO_2 \quad (\text{yield} : 0.3) \tag{R1}$$

$$MVK + OH \rightarrow HMVKBO_2 \quad (\text{yield} : 0.7) \tag{R2}$$

Yields are from current recommendations (Atkinson et al., 2006) that are also used in the MCM. The further reaction chain with NO gives glycolaldehyde and an acetylperoxy radical for $HMVKBO_2$ and methylglyoxal, formaldehyde and HO_2 for $HMVKAO_2$. In the low NO experiment (23 May 2017), approximately 30 % of the RO_2 reacted with NO assuming that the reaction with HO_2 was the only competing reaction. In contrast, more than 90 % of RO_2 reacted with NO in the high NO experiment. Mixing ratios of the major products formaldehyde, glycolaldeyde and methylglyoxal increased to 6, 8, and 1.3 ppbv, respectively, in the high NO experiment when 13 ppbv MVK was oxidized (Fig. 2). Less of these products was observed in the low NO experiment with 4.5 ppbv formaldehyde, 5 ppbv glycolaldehyde and 1 ppbv methylglyoxal (Fig. 3) when 17 ppbv MVK is oxidized. The smaller concentrations of these products in the low NO case might be expected, because other products can be formed in the competing RO_2 reaction channels (Fig. 1).

Because part of the products are oxidized during the experiment, a correction procedure described in detail by Galloway et al. (2011) and Kaminski et al. (2017) is applied, in order to calculate products yields originating from the oxidation of MVK. This correction takes loss of products due to the reaction with OH and photolysis into account and also small production from chamber sources. The relationship between consumed MVK and corrected product concentrations gives the yield of the product species (Table 3, Figure in Supporting Information).

For the high NO experiment, when RO_2 nearly exclusively reacted with NO, the ratio of product yields for glycolaldehyde (0.65 ± 0.14) and methylglyoxal (0.19 ± 0.03) can be related to the branching ratio of the MVK reaction with OH (Reactions R1 and R2), because these products are formed in either one of the two reaction channels. The values derived from this experiment agree within their uncertainties with studies by Galloway et al. (2011); Tuazon and Atkinson (1989); Praske et al. (2015) all reporting lower methylglyoxal yields than suggested by current recommendations (Atkinson et al., 2006). This indicates that the branching ratio assumed in the MCM of 0.7:0.3 needs to be shifted towards $HMVKBO_2$. Praske et al. (2015) suggests a branching ratio of 0.76:0.24. The formaldehyde yield of 0.73 ± 0.15 is higher than the methylglyoxal yield, because formaldehyde is not only a co-product of methylglyoxal in the reaction chain of $HMVKAO_2$ (Fig. 1), but can also be formed from secondary products in the oxidation scheme of MVK. This might also explain why the HCHO yield in this chamber experiment is higher than that in the study by Tuazon and Atkinson (1989). Product yields reported by Grosjean et al. (1993) differ for all three species (largest difference for formaldehyde) from the other studies for unclear reasons.

In the low NO case, other RO_2 reaction channels than reaction with NO gain in importance. Lower yields of methylglyoxal (0.05 ± 0.002) and glycolaldehyde (0.37 ± 0.09) compared to the high NO experiment are therefore found in this case. However, the relative decrease of glycolaldehyde is much smaller than that of methylglyoxal. This indicates that glycolaldehyde is also formed from other reaction channels than the reaction of $HMVKBO_2$ with NO. This agrees with results reported by Praske et al. (2015). In that study, a glycolaldehyde yield of 0.38 ± 0.05 was determined in experiments, in which RO_2 exclusively reacted with HO_2.

3.2 Modelled and measured time series of radical concentrations

Time series of trace gas and radical concentrations are shown together with model calculations using the MCM without modifications for one of the high NO experiments (Fig. 2, 20 August 2014) and for one of the low NO experiments (Fig. 3, 23 May

2017). Although the instrumentation that performed measurements in the experiments were partly different specifically for experiments done in different years, consistent results are obtained. In addition, parameters that are measured by two instruments agree within their combined uncertainties.

MVK (12 ppbv) was injected at two times into the sunlit chamber in the high NO experiment (Fig. 2). Approximately half of the MVK reacted away before the second MVK addition was done. The NO mixing ratio decreased over the course of the experiment from nearly 6 to 0.5 ppbv, but was sufficiently high that 90 % of HO_2 reacted with NO for most of the time. OH concentrations ranged from (2–4)$\times 10^6$ cm^{-3} modulated by changes of the OH reactivity and radiation. Model calculations of [OH] agree with measurements within 20 % at all times during the oxidation of MVK. This corresponds to a good description of the measured MVK concentration by the model (deviations less than 5 %) demonstrating that the OH concentration fits the observed oxidation rate of MVK.

HO_2 and RO_2 radical concentrations were rather small ($< 2 \times 10^8$ cm^{-3}) due to their fast loss in the presence of high NO. Measured and modelled HO_2 concentrations show good agreement until the NO mixing ratio decreased below 0.5 ppbv (at 11:00, Fig 2). In the case of RO_2, the model yields significantly larger concentrations than measurements. This discrepancy is plausible due to the incomplete conversion of the peroxy radical $HMVKBO_2$ in the pre-reactor. The transformation to HO_2 requires more than one NO reaction step and therefore remains incomplete during the transit through the reactor. If the modelled concentration of $[HMVKBO_2]$ is subtracted from the total modelled $[RO_2]$, good model–measurement agreement is obtained.

Overall, the good agreement between modelled and measured radical concentrations demonstrates that radical chemistry during the oxidation of MVK is well described by state-of-the-art chemical models, if RO_2 radicals are mainly lost in the reaction with NO.

In the low NO experiment (Fig. 3), approximately 20 ppbv of MVK was injected, before photooxidation started. As a consequence of the low NO (< 40 pptv), RO_2 radicals formed in the reaction of MVK with OH not only reacted with NO, but reaction with HO_2 and RO_2 were competitive. Model calculations using the MCM (Fig. 3) suggest that at least half of the RO_2 reacted with HO_2 and a smaller fraction (10 to 20 %) with other RO_2 radicals.

After nearly 6 hours of oxidation, only 4 ppbv MVK was left in the presence of (2–4)$\times 10^6$ cm^{-3} OH. The amount of MVK that is injected in the model is adjusted to the increase in OH reactivity during the time of injection. The 10 % discrepancy to measured MVK mixing ratios is within the uncertainty of the PTR-TOF-MS calibration. However, the decay of the measured [MVK] is slightly faster than the decay in the model specifically during the first two hours of oxidation. This corresponds to modelled OH concentrations, which are up to a factor of 2 smaller than measured OH concentrations during this time. At later times of the experiment, measured and modelled [OH] as well as the relative change in [MVK] are matched. Differences between measured and modelled OH concentrations in the first phase of the experiment are accompanied by HO_2 concentrations, which are approximately 2×10^8 cm^{-3} lower in the model compared to measured values. Measured $[HO_2]$ increased from (4–8)$\times 10^8$ cm^{-3} during the first 2 hours. Modelled values match measurements at later times of the experiment like observed for [OH]. The concurrent underestimation of [OH] and $[HO_2]$ suggests that a radical source is missing in the model.

In a sensitivity run (MCM*), modifications of reactions that are reported in literature, but do not directly affect the fate of RO_2 are implemented:

- The reaction rate constant of glycolaldehyde with OH is lowered by 20 % following measurements by Karunanandan et al. (2007).
- Following the results of the product analysis (see above), the branching ratio of Reaction R1 and R2 is changed from 0.3:0.7 to 0.24:0.76 as suggested by Praske et al. (2015).
- OH yield from ozonolysis of MVK is lowered to 16 % as determined by Aschmann et al. (1996); Paulson et al. (1998) compared to 36 % assumed in the MCM.

Details are listed in Table 1. Differences to results with the current version of the MCM are rather small (not shown here) so that these modifications do not significantly affect the model–measurement agreement. They are included in the sensitivities model runs shown below.

4 Discussion

4.1 Additional RO_2+HO_2 reactions

Product yields indicate that an additional source for glycolaldehyde that is not included in the MCM is required to explain observations in the low NO experiment. This is consistent with chamber experiments by Praske et al. (2015), which were performed under conditions that RO_2 exclusively reacted with HO_2. In this case, the glycolaldehyde yield is expected to be small, because glycolaldehyde is mainly formed in the subsequent reaction of RO_2 with NO (Fig. 1). In that study, also a $C_4\alpha-\mathrm{diketone}$ ($CH_3COCOCH_2OH$, MCM name: BIACETOH) was measured with a yield of 0.14. From these product yields, the authors suggest that there are reaction channels of the $HMVKBO_2$ plus HO_2 reaction in addition to the formation of hydroxyperoxides (Praske et al., 2015):

$$HMVKBO_2 + HO_2 \rightarrow HMVKBOOH \quad (\mathrm{yield}: 0.34) \tag{R3}$$

$$HMVKBO_2 + HO_2 \rightarrow HMVKBO + OH \quad (\mathrm{yield}: 0.48) \tag{R4}$$

$$HMVKBO_2 + HO_2 \rightarrow BIACETOH + OH + HO_2 \quad (\mathrm{yield}: 0.18) \tag{R5}$$

Including Reactions R3–R5 in the MCM* mechanism (M1 Table 1) results in an improved description of observations for the low NO experiment (Fig. 4). Modelled [OH] agrees with measurements within 20 %. The largest increase of modelled [OH] is obtained 1 to 2 hours after starting the oxidation due to the additional radical regeneration from Reactions R4 and R5. The model–measurement agreement is worsened for $[RO_2]$ compared to the MCM model run, but still within the uncertainty of the measurement. The additional production of glycolaldehyde from the subsequent chemistry of Reaction R4 brings modelled organic product species into agreement with measurements within 20 % so that all observations except for $[HO_2]$ can be explained by the new reactions of $HMVKBO_2$ with HO_2. HO_2 concentrations, however, are still significantly lower in the model

compared to measurements. Results are consistent with experiments by Praske et al. (2015), but a potential underestimation of $[HO_2]$ could not be recognized, because HO_2 radicals were not measured in their experiments.

4.2 RO_2 isomerization reactions

RO_2 isomerization reactions have been shown to be of importance for the atmospheric fate of RO_2 from isoprene (Peeters et al., 2014). Peeters et al. (2009) also suggested from quantum-chemical calculations that $HMVKBO_2$ undergoes a fast 1,5-H shift with subsequent decomposition (Fig. 1 and Table 1):

$$HMVKBO_2 \quad \rightarrow \quad MGLYOX + HCHO + OH. \tag{R6}$$

Here, the possibility of RO_2 isomerization reactions for both major RO_2 species formed from the reaction of MVK with OH were investigated in detail by means of quantum-chemical calculations.

Table 2 shows the reaction pathways that were examined for the $HMVKAO_2$ and $HMVKBO_2$ peroxy radicals. More information can be found in the Supporting Information. For both radicals, 1,5-H-migration of the hydroxyl H-atom is energetically most favourable with a barrier of 22 $\mathrm{kcal\,mol^{-1}}$. The predicted reaction rate constant remains below $5 \times 10^{-4}\,\mathrm{s^{-1}}$, mostly due to limited tunnelling owing to the large reaction endothermicity, and the broad energy barrier protruding less than 2 $\mathrm{kcal\,mol^{-1}}$ above the reaction products. The concomitant low energy barrier for the reverse H-migration in the product implies that the reaction might be competitive against the alkoxy product decomposition with estimated barriers 4 $\mathrm{kcal\,mol^{-1}}$ (Vereecken and Peeters, 2009). Most of the other reactions considered are several orders of magnitude slower and can be neglected. The predicted rates for all processes considered remain over an order of magnitude below that required to fit the measured OH, HO_2, and glycolaldehyde concentrations so that these H-migration reactions do not have a discernible impact on the MVK oxidation chemistry radical budget or product yields at room temperature. As such, the subsequent chemistry after these reactions was not investigated.

The isomerization rate constant estimated by Peeters et al. (2009) for Reaction R6 of 0.01 $\mathrm{s^{-1}}$ is about two orders of magnitude faster than calculated here. This is mainly related to the higher energy barriers found at the levels of theory applied in this work. The small reaction rate constant for this reaction is consistent with the small product yield for methylglyoxal found in the low NO experiment, which would need to be significantly higher than calculated, if Reaction R6 was competitive with the other RO_2 reaction channels. A similar conclusion was drawn from product yields obtained in the study by Praske et al. (2015).

The fastest reaction rate coefficient of RO_2 isomerization reactions calculated here is found to be the $HMVKAO_2$ 1,4-H-migration of the hydrogen atoms adjacent to the $-OH$ group, followed by H abstraction at the $-OH$ site by O_2 forming HO_2 together with a bi-ketone (named BIACETOOH in the MCM):

$$HMVKAO_2 + (O_2) \quad \rightarrow \quad HO_2 + BIACETOOH \tag{R7}$$

A reaction rate constant of 0.003 $\mathrm{s^{-1}}$ is calculated making this reaction competitive with the reaction of $HMVKAO_2$ with HO_2 and NO in the low NO experiments. Approximately 20 to 30 % of the $HVMKAO_2$ undergoes the 1,4-H shift reaction in this

experiment. However, the resulting increase of the HO_2 concentration is rather small ($< 0.5 \times 10^8\,cm^{-3}$) because of the small $HMVKAO_2$ yield in the reaction of MVK with OH. This reaction is included in the model sensitivity runs M2.

4.3 Potential additional RO_2 reaction channel

A fast conversion of $HMVKBO_2$ to HO_2 would be required to fit HO_2 measurements. Glycolaldehyde would need to be a co-product to match measured values:

$$HMVKBO_2 + (X) \quad \rightarrow \quad HO_2 + products \tag{R8}$$

X represents an unknown reaction partner not needed in case of a unimolecular reaction. M2 in Fig. 4 gives the model result, if Reaction R8 is included in the MCM* in addition to the 1,4-H shift of $HMVKAO_2$ (Reaction R7) and the additional channels of the reaction of $HMVKBO_2$ with HO_2 (Reactions R3–R5).

In order to fit HO_2 and glycolaldehyde concentration measurements, a reaction rate constant of $0.006 \pm 0.004\,s^{-1}$ is required. This reaction rate makes the Reaction R8 competitive with the reaction of RO_2 with NO (reaction rate approximately $0.004\,s^{-1}$) and HO_2 (reaction rate approximately $0.008\,s^{-1}$). In M2, 40 % of $HMVKBO_2$ reacts with HO_2 and 30 % of $HMVKBO_2$ forms directly HO_2 and glycolaldehyde in Reaction R8 for conditions of this experiment. In comparison, 60 % of $HMVKBO_2$ reacts with HO_2 in the model run M1. The overall effect on the [OH], however, is similar in both model runs so that modelled [OH] becomes consistent with measurements. This is due to the conversion of HO_2 produced in Reaction R8 to OH. Overall, however, the major difference in the results of M1 and M2 is in the improved model–measurement agreement of $[HO_2]$.

Unfortunately, experiments here do not give hints about the exact nature of Reaction R8. Quantum-chemical calculations (see above) shows that Reaction R8 cannot be a unimolecular reaction such as H-atom migration, because they are not fast enough to compete with other RO_2 reaction channels. Photolysis of RO_2 that could results in OH/HO_2 have been observed for acetylperoxy radicals (Cox et al., 1990) and isoprene derived RO_2 (Hansen et al., 2017). However, the reaction rate constant of $0.006 \pm 0.004\,s^{-1}$ needed here to explain observations would require an unrealistically high absorption cross section. A reaction partner in Reaction R8 could also be a RO_2 radical. In this case, however, products of the $HMVKBO_2$ plus RO_2 reaction that are assumed in the MCM would need to be changed according to Reaction R8 and the reaction rate constant would need to be increased by a large factor of 20 to 50 compared to recommendations for RO_2 self-reaction rate constants in order to make this reaction competitive with the other RO_2 reaction channels.

4.4 Model–measurement agreement of nitrogen oxide species

So far, only radicals and organic products have been discussed. However, there is also disagreement between measured and modelled NO_2 mixing ratios. The NO_2 concentration produced by the model is 30 % smaller in the low NO experiment (23 May 2017)) compared to measured values. This discrepancy increases to 40 %, if the OH concentration and therefore the MVK oxidation rate is increased. This is due to the increased production of peroxy radicals, which form peroxy acyl nitrate (PAN) or PAN like species, which act as nitrogen oxide reservoirs. Acetylperoxy radicals forming PAN are mainly produced from

$HVMKBO_2$ as a co-product of glycolaldehyde, but another PAN-like species (MCM name PHAN) is additionally produced by the oxidation of glycolaldehyde. If no production of PHAN is assumed, measured and modelled NO_2 mixing ratios agree within 100 pptv (M2 in Fig. 4), less than the accuracy of the NO_x formation in the chamber. However, also reduction of the production of acetylperoxy radicals could improve the model–measurement agreement. The change in NO and peroxy radical concentrations is rather small, because of the suppression of NO by O_3 and the overall small turnover rate of HO_2 and NO. More specific experiments concerning the NO_x budget would be required to decide, which NO_x reservoir species is overestimated by the model.

4.5 OH budget analysis

OH is in steady state because of its short lifetime, so that its rates of production and destruction are equal. Therefore, OH reactivity together with OH concentration measurements allows determination of the total OH production rate from only two measured quantities. Under conditions with high NO concentrations, only few chemical reactions are typically controlling the OH production. The dominating process is usually the recycling of HO_2 by its reaction with NO. In addition, photolysis of ozone and HONO make significant contributions. For low NO conditions and in the presence of high VOC concentrations, field and chamber experiments often show larger total OH productions rates (derived from measured OH and OH reactivity) than can be explained by the above processes. Under these conditions, other OH sources linked to the degradation of VOCs become relevant.

Figure 5 shows the OH budget for the low NO experiment (23 May 2017) using model results (M2, Table 1) to calculate contributions to the OH production. In addition, total OH production is calculated from measured and modelled OH concentrations and OH reactivity. Results from calculations using either modelled or measured values give similar numbers that agree within the uncertainty of the calculation of 20 %.

The OH production rate is dominated by HO_2 recycling reactions and primary OH production (HONO and O_3 photolysis). These contributions explain 70 to 80 % of the total OH production during the MVK oxidation. The model would give lower OH production compared to calculations using measurements if Reaction R8 was not included because HO_2 concentrations and therefore OH recycling by HO_2 would be underpredicted in this case. This reaction is responsible for approximately half of the HO_2 concentration during the first two hours of MVK oxidation. This demonstrates the importance of including all HO_2 sources in models.

Another 10 to 15 % of the total OH production rate is due to the OH formation from the additional HO_2 plus RO_2 reaction channel suggested by Praske et al. (2015) (Reaction R4). A large number of other OH forming reactions included in the model such as photolysis of hydroxyperoxides fills the remaining gap between these major contributions and the total calculated OH production.

5 Summary and conclusions

The photooxidation of MVK, one of the major oxidation products of isoprene, was investigated at atmospheric conditions in the simulation chamber SAPHIR. NO was varied from high to low concentrations. For high NO, RO_2 is mainly lost in the reaction with NO and current chemical models can describe radical concentrations within 20 %. Product yields of the major oxidation products glycolaldehyde (0.65 ± 0.14) and methylglyoxal (0.19 ± 0.03) are consistent with previous measurements (Tuazon and Atkinson, 1989; Galloway et al., 2011; Praske et al., 2015).

OH radical concentrations are underestimated (maximum factor 2) by the MCM at low NO concentrations ($< 100\,\mathrm{pptv}$), when other RO_2 reaction channels can compete with the reaction of RO_2 with NO. At the same time, also HO_2 and glycolaldehyde concentrations are smaller in the model compared to measurements. Only part of the model–measurements discrepancies can be explained by findings in recent studies investigating the MVK photooxidation. The higher glycolaldehyde yield is consistent with a study by Praske et al. (2015). The additional channels for the RO_2 plus HO_2 reaction suggested by these authors can reproduce glycolaldehyde and OH concentrations, but do not explain the model–measurement discrepancy for replaced$[HO_2]HO_2$.

The possibility of RO_2 isomerization reactions for both major RO_2 species formed from the reaction of MVK with OH were investigated in detail by means of quantum-chemical calculations. Additional HO_2 can be produced from the 1,4-H shift reaction of$HVMKAO_2$. The reaction rate constant of $0.003\,\mathrm{s}^{-1}$ is competitive with other RO_2 reaction channels at low NO conditions. The overall impact, however, is small due to the small $HMVKAO_2$ yield. Other reactions considered here can be neglected for atmospheric conditions. This also includes the isomerization reaction suggested by Peeters et al. (2009) (Reaction R6). The rate constant for this reaction is about two orders of magnitude smaller than calculated by Peeters et al. (2009) due to the higher energy barriers found at the higher levels of theory applied in this work.

Because HO_2 and glycolaldehyde concentrations are underestimated at the same time, a reaction that converts RO_2 to HO_2 and glycolaldehyde (Reaction R8) would explain observations in these experiments. A reaction rate constant of $0.006 \pm 0.004\,\mathrm{s}^{-1}$ is required to bring measured and modelled values into agreement. Unimolecular H-shift reactions are found to be too slow. Alternatively, reaction of $HMVKBO_2$ with RO_2 that would produce directly HO_2 and glycolaldehyde would explain $[HO_2]$ observations and would give similar OH and glycolaldehyde concentrations as the mechanism by Praske et al. (2015). However, not only product species would need to be different from what is described in the MCM, but also the reaction rate constants would need to be increased by a large factor of 20 to 50 for the $HMVKBO_2$ plus RO_2 reaction. More studies will be needed to explore the exact role of HO_2 in the MVK oxidation scheme. In addition, open questions remain concerning the fate of nitrogen oxides in the MVK oxidation scheme. The MCM suggests the built-up of nitrogen oxide reservoirs by the formation of PAN and PAN-like species. Experiments here indicate that these reservoirs are less important.

The need for an additional HO_2 source was also found in the oxidation of monoterpenes. Field studies, in which OH reactivity was dominated by monoterpenes, showed that models underestimate HO_2 and OH concentrations (Kim et al., 2013; Hens et al., 2014). A chamber study investigating the photochemistry of $\beta-$pinene found that an additional HO_2 source is

required to explain observed HO_2 and OH and suggested a rearrangement of radical intermediates as explanation (Kaminski et al., 2017).

The impact on the OH recycling efficiency and observed organic products in the MVK oxidation are the same regardless whether OH is directly produced from HO_2 plus RO_2 like in the Praske et al. (2015) mechanism or if OH is produced from enhanced HO_2 as suggested by experiments here. The enhanced OH recycling is demonstrated in this study by the direct quantification of the OH radical concentration during the photochemical oxidation of MVK. Similar as for isoprene (Peeters et al., 2014; Fuchs et al., 2013) and the second major organic product from isoprene oxidation, methacrolein, (Crounse et al., 2011; Fuchs et al., 2014), HO_x radicals are faster recycled in the MVK oxidation scheme than previously assumed. For all three species, OH concentrations are found to be a factor 2 to 3 higher than calculated by models for atmospheric conditions with low NO concentrations. Current state-of-the-art models increased already OH production for isoprene and methacrolein oxidation by including additional reaction pathways. The study here shows that this is also needed for the MVK oxidation scheme.

Competing interests. The authors declare to have no competing interests.

Data availability. Data of the experiments in the SAPHIR chamber used in this work is available on the EUROCHAMP data homepage (https://data.eurochamp.org/).

Acknowledgements. This project has received funding from the European Research Council (ERC) under the European Union's Horizon 2020 research and innovation programme (SARLEP grant agreement No. 681529) and from the European Commission (EC) under the European Union's Horizon 2020 research and innovation programme (Eurochamp 2020 grant agreement No. 730997). The authors thank the Forschungszentrum Jülich for travel support under the project "Seed Money". Frank N. Keutsch and Alex Zaytsev were supported by the National Science Foundation (AGS 1628491 and 1628530). Martin Breitenlechner was supported by the Austrian Science Fund (FWF), Erwin Schrödinger Stipendium, Grant No. J-3900. The authors thank Thomas Mentel, Yare Baker and Sungah Kang from Forschungszentrum Jülich for supporting the HO_2 CIMS measurements.

References

Aschmann, S. M., Arey, J., and Atkinson, R.: OH radical formation from the gas-phase reactions of O_3 with methacrolein and methyl vinyl ketone, Atmos. Environ., 30, 2939–2943, https://doi.org/10.1016/1352-2310(96)00013-1, 1996.

Atkinson, R., Baulch, D. L., Cox, R. A., Crowley, J. N., Hampson, R. F., Hynes, R. G., Jenkin, M. E., Rossi, M. J., Troe, J., and Subcommittee, I.: Evaluated kinetic and photochemical data for atmospheric chemistry: Volume II - gas phase reactions of organic species, Atmos. Chem. Phys., 6, 3625–4055, https://doi.org/10.5194/acp-6-3625-2006, 2006.

Bohn, B. and Zilken, H.: Model-aided radiometric determination of photolysis frequencies in a sunlit atmosphere simulation chamber, Atmos. Chem. Phys., 5, 191–206, https://doi.org/10.5194/acp-5-191-2005, 2005.

Bohn, B., Rohrer, F., Brauers, T., and Wahner, A.: Actinometric measurements of NO_2 photolysis frequencies in the atmosphere simulation chamber SAPHIR, Atmos. Chem. Phys., 5, 493–503, https://doi.org/10.5194/acp-5-493-2005, 2005.

Cox, R. A., Munk, J., Nielsen, O. J., Pagsberg, P., and Ratajczak, E.: Ultraviolet absorption spectra and kinetics of acetonyl and acetonylperoxy radicals, Chem. Phys. Lett., 173, 206–210, https://doi.org/10.1016/0009-2614(90)80079-S, 1990.

Crounse, J. D., Paulot, F., Kjaergaard, H. G., and Wennberg, P. O.: Peroxy radical isomerization in the oxidation of isoprene, Phys. Chem. Chem. Phys., 13, 13 607–13 613, https://doi.org/10.1039/C1CP21330J, 2011.

Crounse, J. D., Knap, H. C., Ornso, K. B., Jorgensen, S., Paulot, F., Kjaergaard, H. G., and Wennberg, P. O.: On the atmospheric fate of methacrolein: 1. Peroxy radical isomerization following addition of OH and O_2, J. Phys. Chem. A, 116, 5756–5762, https://doi.org/10.1021/jp211560u, 2012.

D'Ambro, E. L., Moller, K. H., Lopez-Hilfiker, F. D., Schobesberger, S., Liu, J., Shilling, J. E., Lee, B. H., Kjaergaard, H. G., and Thornton, J. A.: Isomerization of second-generation isoprene peroxy radicals: epoxide formation and implications for secondary organic aerosol yields, Environ Sci. Technol., 51, 4978–4987, https://doi.org/10.1021/acs.est.7b00460, 2017.

Dillon, T. J. and Crowley, J. N.: Direct detection of OH formation in the reactions of HO_2 with $CH_3C(O)O_2$ and other substituted peroxy radicals, Atmos. Chem. Phys., 8, 4877–4889, https://doi.org/10.5194/acp-8-4877-2008, 2008.

Dorn, H.-P., Brandenburger, U., Brauers, T., and Hausmann, M.: A new in-situ laser long-path absorption instrument for the measurement of tropospheric OH radicals, J. Atmos. Sci., 52, 3373–3380, 1995.

Dunning, T. H.: Gaussian basis sets for use in correlated molecular calculations. I. The atoms boron through neon and hydrogen, J. Chem. Phys., 90, 1007–1023, https://doi.org/10.1063/1.456153, 1989.

Frisch, M. J., Trucks, G. W., Schlegel, H. B., Scuseria, G. E., Robb, M. A., Cheeseman, J. R., Scalmani, G., Barone, V., Mennucci, B., Petersson, G. A., Nakatsuji, H., Caricato, M., Li, X., Hratchian, H. P., Izmaylov, A. F., Bloino, J., Zheng, G., Sonnenberg, J. L., Hada, M., Ehara, M., Toyota, K., Fukuda, R., Hasegawa, J., Ishida, M., Nakajima, T., Honda, Y., Kitao, O., Nakai, H., Vreven, T., A., M. J. J., Peralta, J. E., Ogliaro, F., Bearpark, M., Heyd, J. J., Brothers, E., Kudin, K. N., Staroverov, V. N., Keith, T., Kobayashi, R., Normand, J., Normand, J., Raghavachari, K., Rendell, A., Burant, J. C., Iyengar, S. S., Tomasi, J., Cossi, M., Rega, N., Millam, J. M., Klene, M., Knox, J. E., Cross, J. B., Bakken, V., Adamo, C., Jaramillo, J., Gomperts, R., Stratmann, R. E., Yazyev, O., Austin, A. J., Cammi, R., Pomelli, C., Ochterski, J. W., Martin, R. L., Morokuma, K., Zakrzewski, V. G., Voth, G. A., Salvador, P., Dannenberg, J. J., Dapprich, S., Daniels, A. D., Farkas, O., Foresman, J. B., Ortiz, J. V., Cioslowski, J., Fox, D. J., and Pople, J. A.: Gaussian 09, Revision B.01, Gaussian Inc., Wallington CT., 2010.

Fuchs, H., Hofzumahaus, A., and Holland, F.: Measurement of tropospheric RO_2 and HO_2 radicals by a laser-induced fluorescence instrument, Rev. Sci. Instrum., 79, 084 104, https://doi.org/10.1063/1.2968712, 2008.

Fuchs, H., Dube, W. P., Lerner, B. M., Wagner, N. L., Williams, E. J., and Brown, S. S.: A sensitive and versatile detector for atmospheric NO_2 and NO_x based on blue diode laser cavity ring-down spectroscopy, Environ. Sci. Technol., 43, 7831–7836, https://doi.org/10.1021/es902067h, 2009.

Fuchs, H., Bohn, B., Hofzumahaus, A., Holland, F., Lu, K. D., Nehr, S., Rohrer, F., and Wahner, A.: Detection of HO_2 by laser-induced fluorescence: calibration and interferences from RO_2 radicals, Atmos. Meas. Tech., 4, 1209–1255, https://doi.org/10.5194/amt-4-1209-2011, 2011.

Fuchs, H., Dorn, H. P., Bachner, M., Bohn, B., Brauers, T., Gomm, S., Hofzumahaus, A., Holland, F., Nehr, S., Rohrer, F., Tillmann, R., and Wahner, A.: Comparison of OH concentration measurements by DOAS and LIF during SAPHIR chamber experiments at high OH reactivity and low NO concentration, Atmos. Meas. Tech., 5, 1611–1626, https://doi.org/10.5194/amt-5-1611-2012, 2012.

Fuchs, H., Hofzumahaus, A., Rohrer, F., Bohn, B., Brauers, T., Dorn, H.-P., Häseler, R., Holland, F., Kaminski, M., Li, X., Lu, K., Nehr, S., Tillmann, R., Wegener, R., and Wahner, A.: Experimental evidence for efficient hydroxyl radical regeneration in isoprene oxidation, Nature Geosci., 6, 1023–1026, https://doi.org/10.1038/NGEO1964, 2013.

Fuchs, H., Acir, I. H., Bohn, B., Brauers, T., Dorn, H. P., Häseler, R., Hofzumahaus, A., Holland, F., Kaminski, M., Li, X., Lu, K., Lutz, A., Nehr, S., Rohrer, F., Tillmann, R., Wegener, R., and Wahner, A.: OH regeneration from methacrolein oxidation investigated in the atmosphere simulation chamber SAPHIR, Atmos. Chem. Phys., 14, 7895–7908, https://doi.org/10.5194/acp-14-7895-2014, 2014.

Fuchs, H., Tan, Z., Hofzumahaus, A., Broch, S., Dorn, H. P., Holland, F., Künstler, C., Gomm, S., Rohrer, F., Schrade, S., Tillmann, R., and Wahner, A.: Investigation of potential interferences in the detection of atmospheric RO_X radicals by laser-induced fluorescence under dark conditions, Atmos. Meas. Tech., 9, 1431–1447, https://doi.org/10.5194/amt-9-1431-2016, 2016.

Fuchs, H., Novelli, A., Rolletter, M., Hofzumahaus, A., Pfannerstill, E. Y., Kessel, S., Edtbauer, A., Williams, J., Michoud, V., Dusanter, S., Locoge, N., Zannoni, N., Gros, V., Truong, F., Sarda-Esteve, R., Cryer, D. R., Brumby, C. A., Whalley, L. K., Stone, D., Seakins, P. W., Heard, D. E., Schoemaecker, C., Blocquet, M., Coudert, S., Batut, S., Fittschen, C., Thames, A. B., Brune, W. H., Ernest, C., Harder, H., Muller, J. B. A., Elste, T., Kubistin, D., Andres, S., Bohn, B., Hohaus, T., Holland, F., Li, X., Rohrer, F., Kiendler-Scharr, A., Tillmann, R., Wegener, R., Yu, Z., Zou, Q., and Wahner, A.: Comparison of OH reactivity measurements in the atmospheric simulation chamber SAPHIR, Atmos. Meas. Tech., 10, 4023–4053, https://doi.org/10.5194/amt-10-4023-2017, 2017.

Galloway, M. M., Huisman, A. J., Yee, L. D., Chan, A. W. H., Loza, C. L., Seinfeld, J. H., and Keutsch, F. N.: Yields of oxidized volatile organic compounds during the OH radical initiated oxidation of isoprene, methyl vinyl ketone, and methacrolein under high-NO_X conditions, Atmos. Chem. Phys., 11, 10 779–10 790, https://doi.org/10.5194/acp-11-10779-2011, 2011.

Grosjean, D., Williams, E. L., and Grosjean, E.: Atmospheric chemistry of isoprene and of its carbonyl products, Environ Sci. Technol., 27, 830–840, https://doi.org/10.1021/es00042a004, 1993.

Guenther, A. B., Jiang, X., Heald, C. L., Sakulyanontvittaya, T., Duhl, T., Emmons, L. K., and Wang, X.: The model of emissions of gases and aerosols from nature version 2.1 (MEGAN2.1): an extended and updated framework for modeling biogenic emissions, Geosci. Model Dev., 5, 1471–1492, https://doi.org/10.5194/gmd-5-1471-2012, 2012.

Hansen, R. F., Lewis, T. R., Graham, L., Whalley, L. K., Seakins, P. W., Heard, D. E., and Blitz, M. A.: OH production from the photolysis of isoprene-derived peroxy radicals: cross-sections, quantum yields and atmospheric implications, Phys. Chem. Chem. Phys., 19, 2332–2345, https://doi.org/10.1039/C6CP06718B, 2017.

Hens, K., Novelli, A., Martinez, M., Auld, J., Axinte, R., Bohn, B., Fischer, H., Keronen, P., Kubistin, D., Nölscher, A. C., Oswald, R., Paasonen, P., Petäjä, T., Regelin, E., Sander, R., Sinha, V., Sipilä, M., Taraborrelli, D., Tatum Ernest, C., Williams, J., Lelieveld, J., and Harder,

H.: Observation and modelling of HO_X radicals in a boreal forest, Atmos. Chem. Phys., 14, 8723–8747, https://doi.org/10.5194/acp-14-8723-2014, 2014.

Hofzumahaus, A., Rohrer, F., Lu, K., Bohn, B., Brauers, T., Chang, C.-C., Fuchs, H., Holland, F., Kita, K., Kondo, Y., Li, X., Lou, S., Shao, M., Zeng, L., Wahner, A., and Zhang, Y.: Amplified trace gas removal in the troposphere, Science, 324, 1702–1704, https://doi.org/10.1126/science.1164566, 2009.

Kaminski, M., Fuchs, H., Acir, I. H., Bohn, B., Brauers, T., Dorn, H. P., Häseler, R., Hofzumahaus, A., Li, X., Lutz, A., Nehr, S., Rohrer, F., Tillmann, R., Vereecken, L., Wegener, R., and Wahner, A.: Investigation of the β-pinene photooxidation by OH in the atmosphere simulation chamber SAPHIR, Atmos. Chem. Phys., 17, 6631–6650, https://doi.org/10.5194/acp-17-6631-2017, 2017.

Karl, M., Dorn, H.-P., Holland, F., Koppmann, R., Poppe, D., Rupp, L., Schaub, A., and Wahner, A.: Product study of the reaction of OH radicals with isoprene in the atmosphere simulation chamber SAPHIR, J. Atmos. Chem., 55, 167–187, https://doi.org/10.1007/s10874-006-9034-x, 2006.

Karunanandan, R., Hölscher, D., Dillon, T. J., Horowitz, A., Crowley, J. N., Vereecken, L., and Peeters, J.: Reaction of HO with glycolaldehyde $HOCH_2CHO$: Rate coefficients (240-362 K) and mechanism, J. Chem. Phys. A, 111, 897–908, https://doi.org/10.1021/jp0649504, 2007.

Kim, S., Wolfe, G. M., Mauldin, L., Cantrell, C., Guenther, A., Karl, T., Turnipseed, A., Greenberg, J., Hall, S. R., Ullmann, K., Apel, E., Hornbrook, R., Kajii, Y., Nakashima, Y., Keutsch, F. N., DiGangi, J. P., Henry, S. B., Kaser, L., Schnitzhofer, R., Graus, M., and Hansel, A.: Evaluation of HO_X sources and cycling using measurement-constrained model calculations in a 2-methyl-3-butene-2-ol (MBO) and monoterpene (MT) dominated ecosystem, Atmos. Chem. Phys., 13, 2031–2044, https://doi.org/10.5194/acp-13-2031-2013, 2013.

Lelieveld, J., Butler, T. M., Crowley, J. N., Dillon, T. J., Fischer, H., Ganzeveld, L., Harder, H., Lawrence, M. G., Martinez, M., Taraborrelli, D., and Williams, J.: Atmospheric oxidation capacity sustained by a tropical forest, Nature, 452, 737–740, https://doi.org/10.1038/nature06870, 2008.

Lew, M. M., Dusanter, S., and Stevens, P. S.: Measurement of interferences associated with the detection of the hydroperoxy radical in the atmosphere using laser-induced fluorescence, Atmos. Meas. Tech., 11, 95–108, https://doi.org/10.5194/amt-11-95-2018, 2018.

Lou, S., Holland, F., Rohrer, F., Lu, K., Bohn, B., Brauers, T., Chang, C. C., Fuchs, H., Häseler, R., Kita, K., Kondo, Y., Li, X., Shao, M., Zeng, L., Wahner, A., Zhang, Y., Wang, W., and Hofzumahaus, A.: Atmospheric OH reactivities in the Pearl River Delta - China in summer 2006: measurement and model results, Atmos. Chem. Phys., 10, 11 243–11 260, https://doi.org/10.5194/acp-10-11243-2010, 2010.

Lu, K. D., Rohrer, F., Holland, F., Fuchs, H., Bohn, B., Brauers, T., Chang, C. C., Häseler, R., Hu, M., Kita, K., Kondo, Y., Li, X., Lou, S. R., Nehr, S., Shao, M., Zeng, L. M., Wahner, A., Zhang, Y. H., and Hofzumahaus, A.: Observation and modelling of OH and HO_2 concentrations in the Pearl River Delta 2006: a missing OH source in a VOC rich atmosphere, Atmos. Chem. Phys., 12, 1541–1569, https://doi.org/10.5194/acp-12-1541-2012, 2012.

Mao, J., Ren, X., Brune, W. H., Van Duin, D. M., Cohen, R. C., Park, J. H., Goldstein, A. H., Paulot, F., Beaver, M. R., Crounse, J. D., Wennberg, P. O., DiGangi, J. P., Henry, S. B., Keutsch, F. N., Park, C., Schade, G. W., Wolfe, G. M., and Thornton, J. A.: Insights into hydroxyl measurements and atmospheric oxidation in a California forest, Atmos. Chem. Phys., 12, 8009–8020, https://doi.org/10.5194/acp-12-8009-2012, 2012.

Martin, J. M. L.: Ab initio total atomization energies of small molecules - towards the basis set limit, Chem. Phys. Lett., 259, https://doi.org/10.1016/0009-2614(96)00898-6, 1996.

MCM: Master Chemical Mechanism, http://mcm.leeds.ac.uk/MCM/, 2017.

Nölscher, A. C., Williams, J., Sinha, V., Custer, T., Song, W., Johnson, A. M., Axinte, R., Bozem, H., Fischer, H., Pouvesle, N., Phillips, G., Crowley, J. N., Rantala, P., Rinne, J., Kulmala, M., Gonzales, D., Valverde-Canossa, J., Vogel, A., Hoffmann, T., Ouwersloot, H. G., Vila-Guerau de Arellano, J., and Lelieveld, J.: Summertime total OH reactivity measurements from boreal forest during HUMPPA-COPEC 2010, Atmos. Chem. Phys., 12, 8257–8270, https://doi.org/10.5194/acp-12-8257-2012, 2012.

Novelli, A., Hens, K., Tatum Ernest, C., Kubistin, D., Regelin, E., Elste, T., Plass-Dülmer, C., Martinez, M., Lelieveld, J., and Harder, H.: Characterisation of an inlet pre-injector laser-induced fluorescence instrument for the measurement of atmospheric hydroxyl radicals, Atmos. Meas. Tech., 7, 3413–3430, https://doi.org/10.5194/amt-7-3413-2014, 2014.

Paulson, S. E., Chung, M., Sen, A. D., and Orzechowska, G.: Measurement of OH radical formation from the reaction of ozone with several biogenic alkenes, J. Geophys. Res., 103, 25 533–25 539, https://doi.org/10.1029/98JD01951, 1998.

Peeters, J., Nguyen, T. L., and Vereecken, L.: HO_X radical regeneration in the oxidation of isoprene, Phys. Chem. Chem. Phys., 11, 5935–5939, https://doi.org/10.1039/b908511d, 2009.

Peeters, J., Müller, J.-F., Stavrakou, T., and Nguyen, V. S.: Hydroxyl radical recycling in isoprene oxidation driven by hydrogen bonding and hydrogen tunneling: The upgraded LIM1 mechanism, J. Phys. Chem. A, 118, 8625–8643, https://doi.org/10.1021/jp5033146, 2014.

Praske, E., Crounse, J. D., Bates, K. H., Kurten, T., Kjaergaard, H. G., and Wennberg, P. O.: Atmospheric fate of methyl vinyl ketone: Peroxy radical reactions with NO and HO_2, J. Phys. Chem. A, 119, 4562–4572, https://doi.org/10.1021/jp5107058, 2015.

Purvis, G. D. and Bartlett, R. J.: A full coupled-cluster singles and doubles model: The inclusion of disconnected triples, J. Chem. Phys., 76, 1910–1918, https://doi.org/10.1063/1.443164, 1982.

Rickly, P. and Stevens, P. S.: Measurements of a potential interference with laser-induced fluorescence measurements of ambient OH from the ozonolysis of biogenic alkenes, Atmos. Meas. Tech., 11, 1–16, https://doi.org/10.5194/amt-11-1-2018, 2018.

Rohrer, F., Bohn, B., Brauers, T., Brüning, D., Johnen, F.-J., Wahner, A., and Kleffmann, J.: Characterisation of the photolytic HONO-source in the atmosphere simulation chamber SAPHIR, Atmos. Chem. Phys., 5, 2189–2201, https://doi.org/10.5194/acp-5-2189-2005, 2005.

Sanchez, J., Tanner, D. J., Chen, D., Huey, L. G., and Ng, N. L.: A new technique for the direct detection of HO_2 radicals using bromide chemical ionization mass spectrometry (Br-CIMS): initial characterization, Atmos. Meas. Tech., 9, 3851–3861, https://doi.org/10.5194/amt-9-3851-2016, 2016.

Schlosser, E., Brauers, T., Dorn, H.-P., Fuchs, H., Häseler, R., Hofzumahaus, A., Holland, F., Wahner, A., Kanaya, Y., Kajii, Y., Miyamoto, K., Nishida, S., Watanabe, K., Yoshino, A., Kubistin, D., Martinez, M., Rudolf, M., Harder, H., Berresheim, H., Elste, T., Plass-Dülmer, C., Stange, G., and Schurath, U.: Technical Note: Formal blind intercomparison of OH measurements: results from the international campaign HOxComp, Atmos. Chem. Phys., 9, 7923–7948, https://doi.org/10.5194/acp-9-7923-2009, 2009.

St. Clair, J. M., Rivera, J. C., Crounse, J. D., Knap, H. C., Bates, K. H., Teng, A. P., Jørgensen, S., Kjaergaard, H. G., Keutsch, F. N., and Wennberg, P. O.: Kinetics and products of the reaction of the first-generation isoprene hydroxy hydroperoxide (ISOPOOH) with OH, J. Phys. Chem. A, 120, 1441–1451, https://doi.org/10.1021/acs.jpca.5b06532, 2015.

Tan, D., Faloona, I., Simpas, J. B., Brune, W., Shepson, P. B., Couch, T. L., Summer, A. L., Carroll, M. A., Thornberry, T., Apel, E., Riemer, D., and Stockwell, W.: HO_X budget in a deciduous forest: results from the PROPHET summer 1998 campaign, J. Geophys. Res., 106, 24 407–24 427, https://doi.org/10.1029/2001JD900016, 2001.

Tuazon, E. C. and Atkinson, R.: A product study of the gas-phase reaction of methyl vinyl ketone with the OH radical in the presence of NO_X, Int. J. Chem. Kin., 21, 1141–1152, https://doi.org/10.1002/kin.550211207, 1989.

Vereecken, L. and Peeters, J.: The 1,5-H-shift in 1-butoxy: A case study in the rigorous implementation of transition state theory for a multirotamer system, J. Chem. Phys., 119, 5159–5170, https://doi.org/10.1063/1.1597479, 2003.

Vereecken, L. and Peeters, J.: Decomposition of substituted alkoxy radicals-part I: a generalized structure-activity relationship for reaction barrier heights, Phys. Chem. Chem. Phys., 11, 9062–9074, https://doi.org/10.1039/B909712K, 2009.

Veres, P. R., Roberts, J. M., Wild, R. J., Edwards, P. M., Brown, S. S., Bates, T. S., Quinn, P. K., Johnson, J. E., Zamora, R. J., and de Gouw, J.: Peroxynitric acid (HO_2NO_2) measurements during the UBWOS 2013 and 2014 studies using iodide ion chemical ionization mass spectrometry, Atmos. Chem. Phys., 15, 8101–8114, https://doi.org/10.5194/acp-15-8101-2015, 2015.

Wennberg, P. O., Bates, K. H., Crounse, J. D., Dodson, L. G., McVay, R. C., Mertens, L. A., Nguyen, T. B., Praske, E., Schwantes, R. H., Smarte, M. D., St Clair, J. M., Teng, A. P., Zhang, X., and Seinfeld, J. H.: Gas-Phase reactions of isoprene and its major oxidation products, Chem. Rev., https://doi.org/10.1021/acs.chemrev.7b00439, 2018.

Whalley, L. K., Edwards, P. M., Furneaux, K. L., Goddard, A., Ingham, T., Evans, M. J., Stone, D., Hopkins, J. R., Jones, C. E., Karunaharan, A., Lee, J. D., Lewis, A. C., Monks, P. S., Moller, S. J., and Heard, D. E.: Quantifying the magnitude of a missing hydroxyl radical source in a tropical rainforest, Atmos. Chem. Phys., 11, 7223–7233, https://doi.org/10.5194/acp-11-7223-2011, 2011.

Whalley, L. K., Blitz, M. A., Desservettaz, M., Seakins, P. W., and Heard, D. E.: Reporting the sensitivity of laser-induced fluorescence instruments used for HO_2 detection to an interference from RO_2 radicals and introducing a novel approach that enables HO_2 and certain RO_2 types to be selectively measured, Atmos. Meas. Tech., 6, 3425–3440, https://doi.org/10.5194/amt-6-3425-2013, 2013.

Winiberg, F. A. F., Dillon, T. J., Orr, S. C., Gro ß, C. B. M., Bejan, I., Brumby, C. A., Evans, M. J., Smith, S. C., Heard, D. E., and Seakins, P. W.: Direct measurements of OH and other product yields from the HO_2 + $CH_3C(O)O_2$ reaction, Atmos. Chem. Phys., 16, 4023–4042, https://doi.org/10.5194/acp-16-4023-2016, 2016.

Wolfe, G. M., Crounse, J. D., Parrish, J. D., St. Clair, J. M., Beaver, M. R., Paulot, F., Yoon, T., Wennberg, P. O., and Keutsch, F. N.: Photolysis, OH reactivity and ozone reactivity of a proxy for isoprene-derived hydroperoxyenals, Phys. Chem. Chem. Phys., 14, 7276–7286, https://doi.org/10.1039/C2CP40388A, 2012.

Zhao, Y. and Truhlar, D. G.: The M06 suite of density functionals for main group thermochemistry, thermochemical kinetics, noncovalent interactions, excited states, and transition elements: two new functionals and systematic testing of four M06-class functionals and 12 other functionals, Theor.Chem. Account., 120, 215–241, https://doi.org/10.1007/s00214-007-0310-x, 2008.

Zheng, J. and Truhlar, D. G.: Quantum thermochemistry: Multistructural method with torsional anharmonicity based on a coupled torsional potential, J. Chem. Theory Comput., 9, 1356–1367, https://doi.org/10.1021/ct3010722, 2013.

Table 1. Changes of reactions and additional reactions applied to the MCM.

	reaction	reaction rate constant	reference
	MCM*:		
R1:	OH+MVK$\rightarrow$HMVKAO$_2$	$0.24 \times 2.6 \times 10^{-12} \exp(610\mathrm{K/T})\,\mathrm{cm^3 s^{-1}}$	Praske et al. (2015)
R2:	OH+MVK$\rightarrow$HMVKBO$_2$	$0.76 \times 2.6 \times 10^{-12} \exp(610\mathrm{K/T})\,\mathrm{cm^3 s^{-1}}$	Praske et al. (2015)
	HOCH$_2$CHO+OH$\rightarrow$products	$8 \times 10^{-12}\,\mathrm{cm^3 s^{-1}}$	Karunanandan et al. (2007)
	MVK+O$_3$ $\rightarrow$OH+products	$0.16 \times 8.5 \times 10^{-16} \exp(-1520\mathrm{K/T})$	Aschmann et al. (1996); Paulson et al. (1998)
	M1 (includes MCM*):		
R3:	HMVKBO$_2$+HO$_2$$\rightarrow$HMVKBOOH	0.34×0.625 KRO2HO2[a]	Praske et al. (2015)
R4:	HMVKBO$_2$+HO$_2$$\rightarrow$HMVKBO+OH	0.48×0.625 KRO2HO2[a]	Praske et al. (2015)
R5:	HMVKBO$_2$+HO$_2$$\rightarrow$BIACETOH+OH+HO$_2$	0.18×0.625 KRO2HO2[a]	Praske et al. (2015)
	M2 (includes M1 and MCM*):		
R7:	HMVKAO$_2$ $\rightarrow$HO$_2$+BIACETOOH	$0.003\ \mathrm{s^{-1}}$[b]	this work
R8:	HMVKBO$_2$ (+X)[c] $\rightarrow$HO$_2$+HOCH$_2$CHO +HCHO+CO	$(0.006 \pm 0.004)\ \mathrm{s^{-1}}$	this work
	HOCH$_2$CO$_3$ + NO$_2$ $\rightarrow$PHAN	0	this work

[a] value from MCM: 0.625 KRO2HO2$= 2.91 \times 10^{-13} \exp(1300\mathrm{K/T})\,\mathrm{cm^3 s^{-1}}$ (MCM, 2017)

[b] from theoretical calculation (see Table 2)

[c] a reaction partner could not be determined from these experiments

Table 2. H-migration and HO_2 elimination in $\mathrm{hydroxy{-}MVK{-}peroxy}$ radicals. Barrier height E_b, reaction energy E_{react} and the rate coefficient k at a temperature of 300 K are listed. Arrhenius expressions for a temperature range between 200 and 400 K are available in the Supporting Information.

Reactant	Reaction class	Product	E_b kcal mol^{-1}	E_{react} kcal mol^{-1}	k (300K) s^{-1}
$\mathbf{HMVKAO_2}$	$-$OH 1,5-H-shift	$CH_3{-}C(=O){-}CH(O^\bullet){-}CH_2OOH$	21.6	20.4	5.0×10^{-4}
	$\alpha-$OH 1,4-H-shift	$CH_3{-}C(=O){-}C^\bullet(OH){-}CH_2OOH$	24.7	-6.2	3.3×10^{-3}
	$-CH_3$ 1,6-H-shift	$C^\bullet H_2{-}C(=O){-}CH(OH){-}CH_2OOH$	23.1	10.2	5.9×10^{-4}
$\mathbf{HMVKBO_2}$	$-$OH 1,5-H-shift	$CH_3{-}C(=O){-}CH(OOH){-}CH_2O^\bullet$	22.5	20.6	8.8×10^{-5} [a]
	$\alpha-$OH 1,4-H-shift	$CH_3{-}C(=O){-}CH(OOH){-}C^\bullet HOH$	25.1	6.5	3.2×10^{-5}
	$-CH_3$ 1,6-H-shift	$C^\bullet H_2{-}C(=O){-}CH(OOH){-}CH_2OH$	27.4	10.0	3.8×10^{-5}
	HO_2 elimination	$CH_3{-}C(=O){-}CH{=}CHOH + HO_2$	30.0	-1.5	6.1×10^{-10}

[a] estimated at $0.01\,\mathrm{s}^{-1}$ by Peeters et al. (2009)

Table 3. Yields of organic products from photooxidation of MVK by OH from this work and from literature. Errors of values from this work take into account the accuracy of measurements and precision of the calculation. HCHO is not only produced in the first oxidation step of MVK but also produced in the subsequent oxidation of glycolaldehyde and methylglyoxal. Therefore, the yield can increase over the course of the experiment.

species	yield	$\frac{\text{loss}(RO_2+HO_2)}{\text{loss}(RO_2+NO)}$	reference
HCHO	0.24 ± 0.08^a	2:1[c]	this work
	0.46 ± 0.04^b	2:1[c]	this work
	0.73 ± 0.15	1:9	this work
	0.54 ± 0.04	0:1	Tuazon and Atkinson (1989)
	0.28	0:1	Grosjean et al. (1993)
MGLYOX	0.05 ± 0.02	2:1[c]	this work
	0.04 ± 0.01	1:0	Praske et al. (2015)
	0.19 ± 0.03	1:9	this work
	0.24 ± 0.001	0:1	Galloway et al. (2011)
	0.25 ± 0.08	0:1	Tuazon and Atkinson (1989)
	0.32	0:1	Grosjean et al. (1993)
$HOCH_2CHO$	0.37 ± 0.09	2:1[c]	this work
	0.38 ± 0.05	1:0	Praske et al. (2015)
	0.65 ± 0.14	1:9	this work
	0.74 ± 0.06	0:1	Praske et al. (2015)
	0.67 ± 0.04	0:1	Galloway et al. (2011)
	0.64 ± 0.16	0:1	Tuazon and Atkinson (1989)
	0.60	0:1	Grosjean et al. (1993)

[a] approximately after 1 hour of oxidation

[b] after 3 hours of oxidation

[c] RO_2+RO_2 contribution to the total RO_2 loss: $<20\,\%$

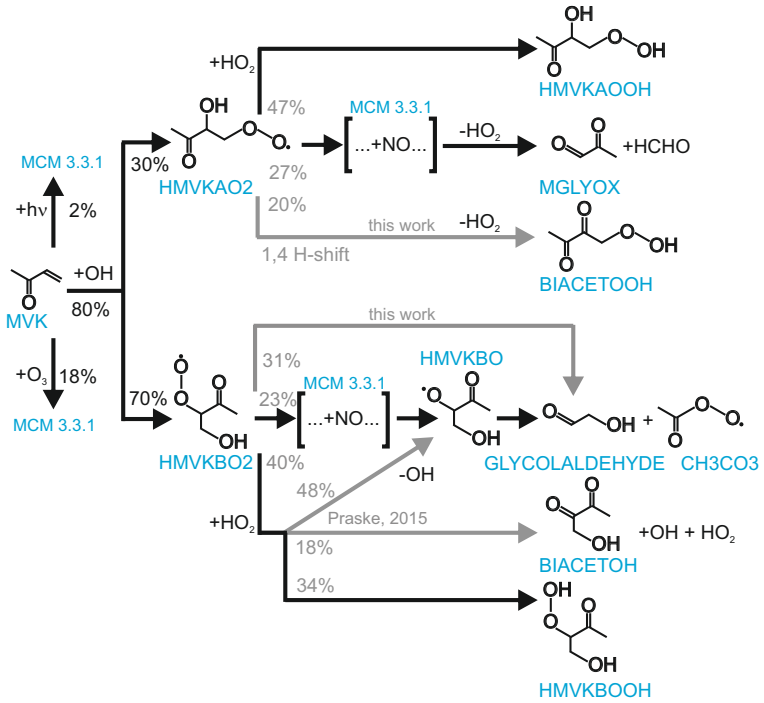

Figure 1. Simplified OH oxidation scheme for MVK. Names of compounds are assigned similar to MCM. Modifications to the MCM mechanism (M2) applied in model sensitivity runs M1 and M2 (Table 1) are shown as grey arrows. Reaction yields are calculated for conditions of the experiment with low NO (high ozone concentrations) on 23 May 2017. Grey numbers refer to model run M2.

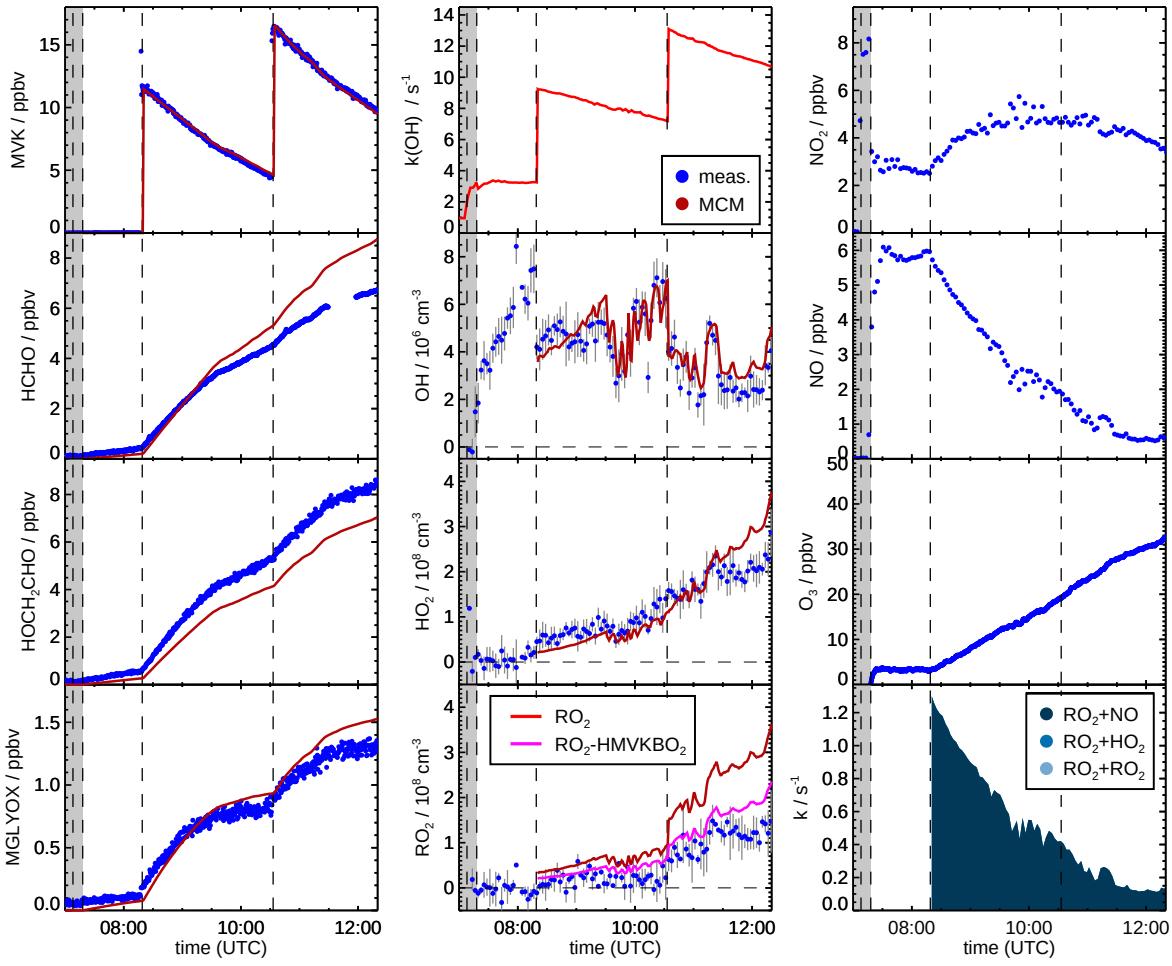

Figure 2. Time series of radicals, inorganic and organic species during the MVK photooxidation for the high NO experiment (20 August 2014) together with results from model calculations applying MCM. Dark shaded areas indicate the time before opening the chamber roof and vertical dashed line times when trace gases were injected into the chamber. OH reactivity was not measured during this experiment. NO, NO_2 and O_3 are constrained to measurements in the model. RO_2 loss rates (most lowest right panel) are calculated from modelled HO_2, RO_2 and NO concentrations. However, contributions from the reactions with RO_2 and HO_2 or RO_2 are too small to be visible. Modelled acetic acid concentrations are small compared to modelled glycolaldehyde concentrations (measured together in the PTR-TOF-MS).

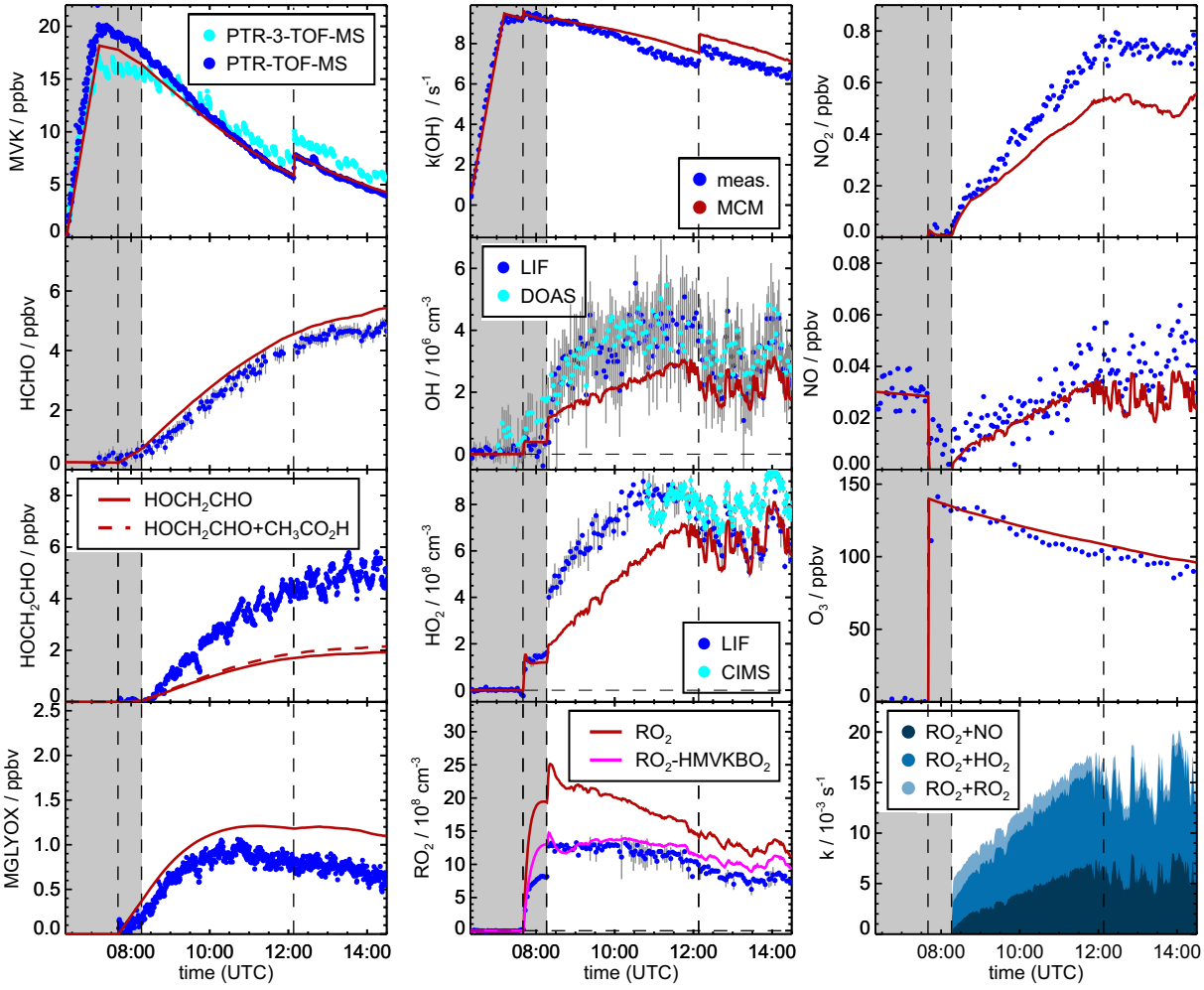

Figure 3. Time series of radicals, inorganic and organic species during the MVK photooxidation at low NO (23 May 2017) together with results from model calculations applying MCM. Dark shaded areas indicate the time before opening the chamber roof and vertical dashed line times when trace gases were injected into the chamber. RO_2 loss rates (most lowest right panel) are calculated from modelled HO_2, RO_2 and NO concentrations.

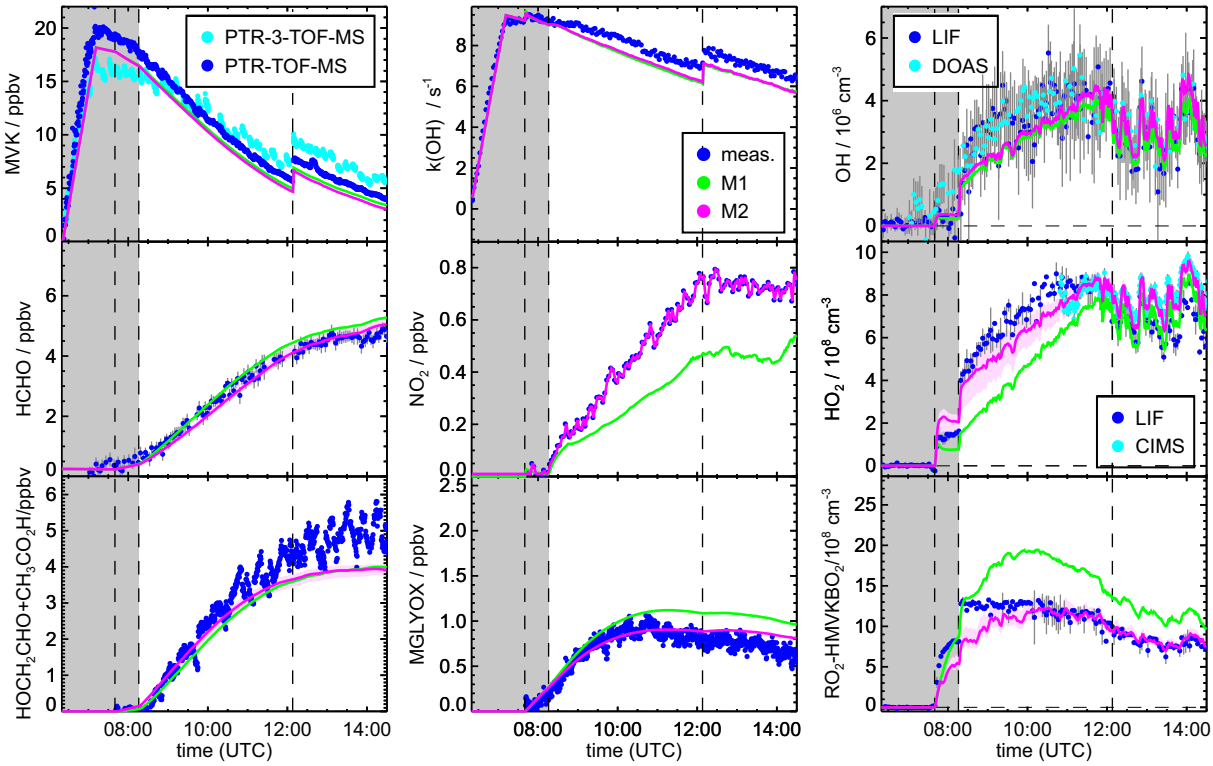

Figure 4. Time series of radicals, inorganic and organic species during the MVK photooxidation at low NO (experiment on 23 May 2017). Dark shaded areas indicate the time before opening the chamber roof and vertical dashed line times when trace gases were injected into the chamber. Model sensitivity runs M1 and M2 include modifications listed in Table 1.

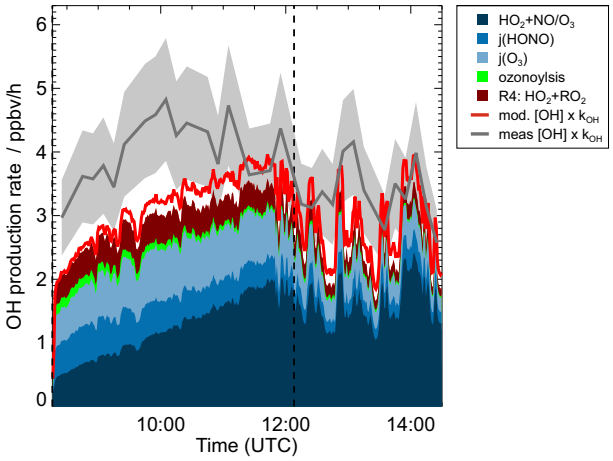

Figure 5. OH budget during the experiment at low NO concentration (23 May 2017) for the period, when MVK photooxidation took place. The vertical dashed line indicates when MVK was reinjected into the chamber. Red and blue coloured areas add contributions to the OH production calculated from the model results (M2 sensitivity run in Fig. 4). The contribution RO_2+HO_2 refers to the OH production from Reaction R4. In addition to modelled OH production contributions, total OH production calculated from the product of OH concentration and OH reactivity (k_{OH}) is shown. These quantities are either taken from the model results (M2) or from measurements. The coloured grey area gives the uncertainty of the total OH production calculation, if measured OH concentrations and measured OH reactivity are used.

Supporting Information to "Investigation of the oxidation of methyl vinyl ketone (MVK) by OH radicals in the atmosphere simulation chamber SAPHIR"

Hendrik Fuchs[1], Sascha Albrecht[1], Ismail–Hakki Acir[1, a], Birger Bohn[1], Martin Breitenlechner[2], Hans-Peter Dorn[1], Georgios I. Gkatzelis[1], Andreas Hofzumahaus[1], Frank Holland[1], Martin Kaminski[1, b], Frank N. Keutsch[2], Anna Novelli[1], David Reimer[1], Franz Rohrer[1], Ralf Tillmann[1], Luc Vereecken[1], Robert Wegener[1], Alexander Zaytsev[2], Astrid Kiendler-Scharr[1], and Andreas Wahner[1]

[1]Institute of Energy and Climate Research, IEK-8: Troposphere, Forschungszentrum Jülich GmbH, Jülich, Germany
[2]School of Engineering and Applied Sciences and Department of Chemistry and Chemical Biology, Harvard University, Cambridge, MA, USA
[a]now at: Institute of Nutrition and Food Sciences, Food Chemistry, University of Bonn, Germany
[b]now at: Bundesamt für Verbraucherschutz, Abteilung 5 – Methodenstandardisierung, Germany

Correspondence to: Hendrik Fuchs
(h.fuchs@fz-juelich.de)

1 Additional Figures

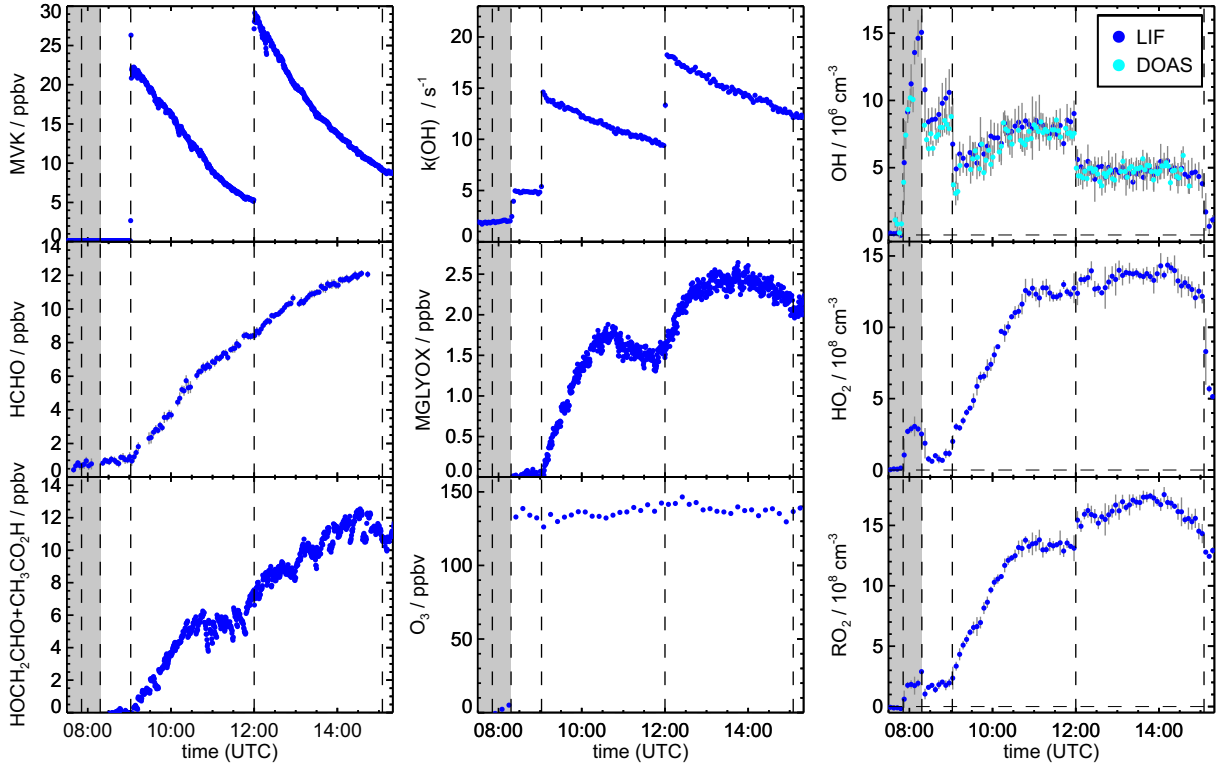

Figure 1. Time series of radicals, inorganic and organic species during the MVK photooxidation for the high NO experiment (17 May 2017). Dark shaded areas indicate the time before opening the chamber roof and vertical dashed line times when trace gases were injected into the chamber. Model calculations were not performed due to the lack of reliable NO_x measurements in this experiment. Approximately 8 ppbv NO_2 was injected at the beginning of the experiment.

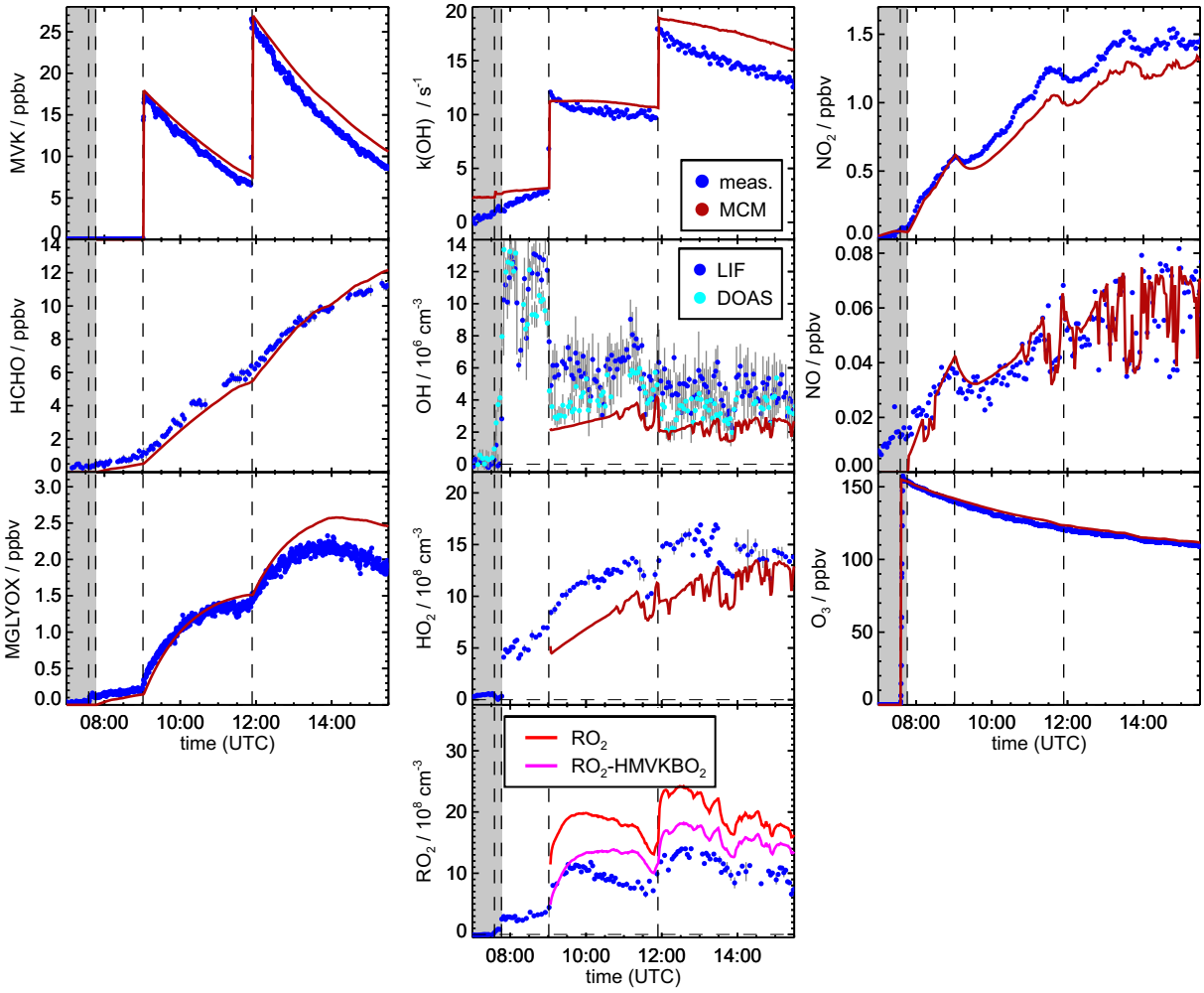

Figure 2. Time series of radicals, inorganic and organic species during the MVK photooxidation for the low NO experiment (23 June 2016) together with results from model calculations applying MCM. Dark shaded areas indicate the time before opening the chamber roof and vertical dashed line times when trace gases were injected into the chamber. Glycolaldehyde could not be derived from PTR-TOF-MS measurements for this experiment because no calibration was available.

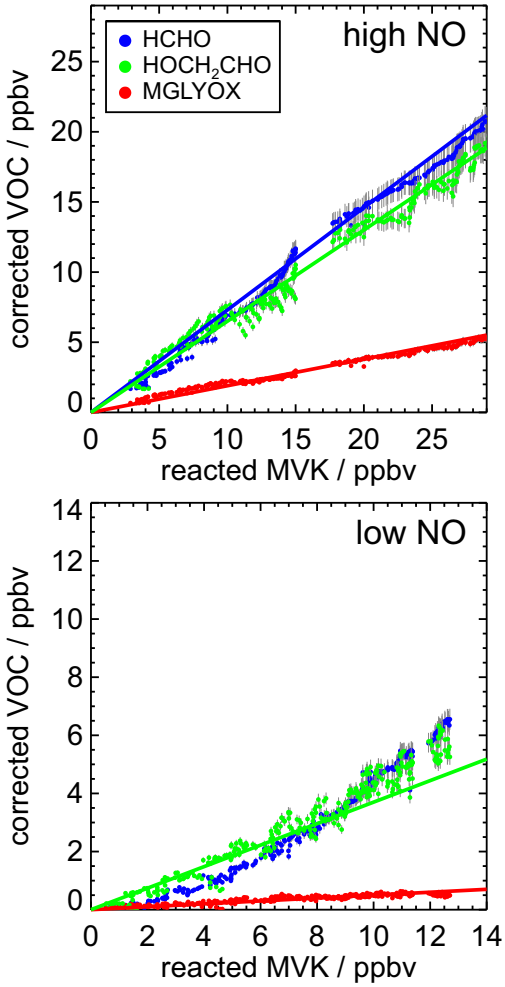

Figure 3. Corrected product concentrations versus the MVK that reacted away. Corrections are applied to account for production not connected to the oxidation of MVK (small chamber source) and additional loss processes (reaction with OH, photolysis). The slope gives the product yield of the organic compound in the MVK reaction with OH

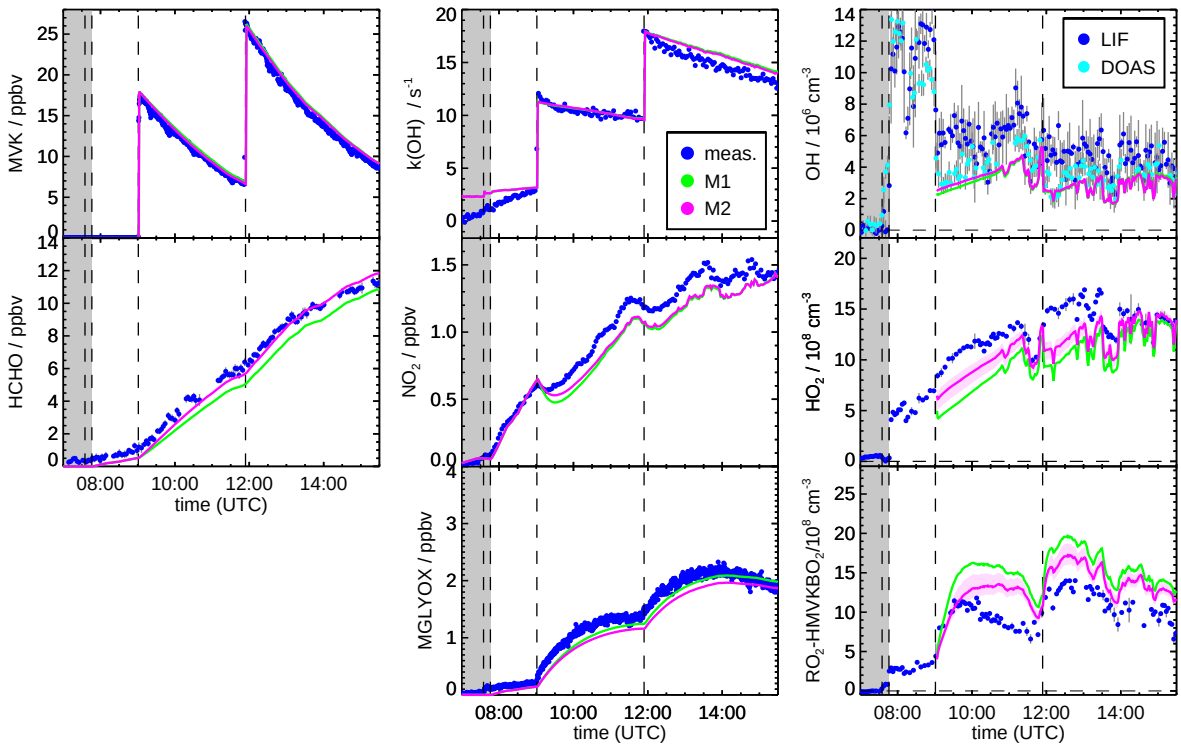

Figure 4. Time series of radicals, inorganic and organic species during the MVK photooxidation at low NO (experiment on 23 June 2016). Dark shaded areas indicate the time before opening the chamber roof and vertical dashed line times when trace gases were injected into the chamber. Model sensitivity runs include additional reaction pathways listed in Table 2 in the main paper.

2 Theoretical analysis of unimolecular reactions of the primary peroxy radicals

2.1 Theoretical methodology

The geometries of the reactants and transition states are optimized at the M06-2X/cc-pVTZ level of theory (Dunning, 1989; Zhao and Truhlar, 2008), exhaustively searching the entire conformer space afforded by the internal rotors. The lowest-lying structures, i.e those contributing 0.1 % to the population at 300 K, are then re-optimized at the M06-2X/aug-cc-pVTZ level of theory, and their harmonic vibrational wavenumbers are calculated and scaled by 0.971 (Alecu et al., 2010; Bao et al., 2017). Finally, the relative energies of the barrier heights are refined by CCSD(T)/aug-cc-pVxZ (x=D,T) single point energy calculations (Purvis and Bartlett, 1982) on the most stable conformer for each critical point, and extrapolated to the complete basis set using the aug-Schwartz4(DT) method described by (Martin, 1996). These CCSD(T)/CBS(DT)//M06-2X/aug-cc-pVTZ energies and rovibrational characteristics (see Table 1) are selected for theoretical kinetic calculations.

For the chemically most critical transition state, i.e. the 1,5-H-shift of the hydroxy-H-atom in the $\mathrm{HMVKBO_2}$ radical, we have performed additional calculations using the B3LYP and M05-2X DFT functionals with various basis sets, as well as CBS-QB3, G3X, and G3SX calculations (Becke, 1992; Curtiss et al., 2001; Lee et al., 1988; Montgomery et al., 1999; Zhao et al., 2006). All quantum chemical calculations are performed using the Gaussian-09 program suite (Frisch et al., 2010).

The high-pressure rate coefficients for each of the elementary processes is calculated using multi-conformer canonical transition state theory, MC-CTST (Vereecken and Peeters, 2003; Zheng and Truhlar, 2013), as implemented in our in-house software. The rate is predicted based on a rigid rotor harmonic oscillator paradigm using M06 2X/aug-cc-pVTZ rovibrational characteristics and CCSD(T) barrier heights, where the population includes all conformers that contribute more than 0.1 %. The temperature range considered is 200 to 400 K. Tunnelling is included by asymmetric Eckart tunnelling (Johnston and Heicklen, 1962) with unscaled imaginary frequency, where the conformer-specific reactant and product for the lowest TS are discovered by IRC calculations. The tunnelling correction for the lowest TS is then used for all TS. For one reaction channel, we have also performed WKB tunnelling corrections (Garrett and Truhlar, 1979) based on the M06-2X/aug-cc-pVTZ minimum energy path.

2.2 Theoretical results

Table 1 lists barrier heights for the various reaction pathways studied in this work , with the preferred values shown in Fig. 5. For the 1,5-H-migration in $\mathrm{HMVKBO_2}$, we find that our calculations using a wide range of methodologies yield significantly higher energy barriers than the earlier predictions by Peeters et al. (2009). Partly, this is due to the methodologies used, where the B3LYP functional in particular is known to underestimate H-migration barrier heights, and yield TS geometries that are not ideal for single-point energy calculations. Another reason for the systematic underprediction in the earlier work is that the conformer space of the reactant was not examined exhaustively. Several lower-lying conformers were identified since, leading to a higher effective barrier height and hence lower rate coefficients for all reaction channels. The M05-2X functional seems to overpredict barrier heights somewhat, whereas the M06-2X functional leads to good agreement with higher-level single-

point energy calculations. Extrapolation to the complete basis set limit appears to have only a limited influence, though the computational cost prohibited us from applying basis sets above aug-cc-pVTZ.

The rate coefficient predictions are listed in Table 1 and Table 2. Compared to the earlier predictions by Peeters et al. (2009), we find rate coefficients that are about two orders of magnitude slower; this is mainly related to the higher energy barriers found at the levels of theory applied in this work, as discussed above. Tunnelling has a large contribution for the $\alpha-\mathrm{OH}$ 1,4-H-shift and $-\mathrm{CH_3}$ 1,6-H-shift, with rate enhancements between 10^2 and 10^4; as expected, $\mathrm{HO_2}$ elimination is not affected much by tunnelling (factor 4 at 300 K) due to its high reduced mass and concomitant low imaginary wavenumber of $\approx 1060i\,\mathrm{cm^{-1}}$. Tunnelling has the lowest impact on the $-\mathrm{OH}$ 1,5-H-migrations, with enhancements of a factor 2 to 3 only, with similar values obtained when using Eckart and WKB tunnelling corrections. This is related directly to the high endoenergicity of the reaction, which leads to a broad energy profile (imaginary wavenumber $\approx 1200i\,\mathrm{cm^{-1}}$) with a limited energy range accessible for tunnelling (reverse barrier only $\approx 2.5\,\mathrm{kcalmol^{-1}}$). Despite having the lowest energy barrier of the processes discussed here, its rate coefficient thus remains rather low. The highest rate coefficient is predicted for the 1,4-H-migration of the $\alpha-\mathrm{OH}$ hydrogen atom in $\mathrm{HMVKAO_2}$. This channel is entropically slightly more favourable than a 1,5-H-shift, with less degrees of freedom for internal rotation converted to more rigid vibrations in the cyclic transition state. This channel also has the highest tunnelling factor, 2×10^4 at 300 K, using asymmetric Eckart tunnelling.

The two fastest reactions, both H-migrations in the $\mathrm{HMVKAO_2}$ radicals lead to a product radical that is stabilized by vinoxy resonance; delocalization of the unpaired electron only becomes active after the migrating H-atom is transferred to the peroxy group. It is conceivable that an Eckart potential energy barrier shape is not appropriate for these reactions. For example, allyl resonance has been shown to produce a non-Eckart energy profiles, with an minimum energy profile that cannot be reproduced accurately by the Eckart barrier shape (Nguyen et al., 2010; Peeters et al., 2009, 2014). To probe the reliability of the Eckart tunnelling, a zero-curvature tunnelling (ZCT) correction using the WKB methodology was implemented, based explicitly on the shape of the minimum energy path. In both cases, a significantly lower tunnelling correction was found, about an order of magnitude below the Eckart correction at 300 K (see Table 1). The ZCT values are expected to be a lower bound to the tunnelling correction, as corner-cutting will increase tunnelling. The effective rate coefficient is expected to be bracketed by the two tunnelling predictions. As our final rate coefficient prediction, we then employ the geometric average of the two tunnelling corrections, but with a large uncertainty of a factor 5. As none of the reactions studied theoretically in this work are contributing significantly to the oxidation of MVK, we choose not to perform additional calculations to reduce the uncertainty interval further.

Table 1. H-migration and HO_2 elimination in $\mathrm{hydroxy-MVK-peroxy}$ radicals. Barrier height E_b and the rate coefficient k at a temperature of 300 K are listed. aVxZ is used as abbreviation for aug-cc-pVxZ (x = D,T); CBS(DT) refers to extrapolation to the complete basis set using the aug-Schwartz4(DT) method.

Reactant	Reaction class	Level of theory	E_b kcal mol^{-1}	$k(300)$ K s^{-1}
HMVKAO₂	−OH 1,5-H-shift	CCSD(T)/aVTZ//M06-2X/aVTZ	22.0	2.9×10^{-4}
$CH_3-C(=O)-CH(OH)-CH_2OO^\bullet$		CCSD(T)/CB S(DT)//M06-2X/aVTZ	21.6	5.0×10^{-4}
	α−OH 1,4-H-shift	CCSD(T)/aVTZ//M06-2X/aVTZ	24.7	1.3×10^{-2}
		CCSD(T)/CBS(DT)//M06-2X/aVTZ	24.7	1.5×10^{-2}
				7.7×10^{-4} [a]
	$-CH_3$ 1,6-H-shift	CCSD(T)/aVTZ//M06-2X/aVTZ	23.1	1.5×10^{-3}
		CCSD(T)/CBS(DT)//M06-2X/aVTZ	23.1	1.4×10^{-3}
				2.5×10^{-4} [a]
HMVKBO₂	−OH 1,5-H-shift	B3LYP/6-31+G(d,p)	17.7[b]	
$CH_3-C(=O)-CH(OO^\bullet)-CH_2OH$		CBS-QB3	21.3[b]	
		M05-2X/6-31+G(d,p)	24.3	
		M05-2X/aVDZ	24.0	
		M06-2X/cc-pVTZ	22.3	
		M06-2X/aug-cc-pVTZ	22.2	
		CBS-QB3//M05-2X/6-311G(d,p)	23.0	
		CBS-Q//QCISD/6-311G(d,p)	20.6[b]	
		CBS-APNO	20.0 [b]	7×10^{-3} [b,c]
		CCSD(T)/aVDZ//M05-2X/aVDZ	24.2	
		CCSD(T)/CBS(DT)//M05-2X/6-311G(d,p)	22.4	
		G3X//B3LYP/6-31G(2df,p)	24.7	
		G3SX//B3LYP/6-31G(2df,p)	23.8	
		CCSD(T)/aVTZ//M06-2X/aVTZ	22.7	6.0×10^{-5}
		CCSD(T)/CBS(DT)//M06-2X/aVTZ	22.5	8.8×10^{-5}
	α−OH 1,4-H-shift	CCSD(T)/aVTZ//M06-2X/aVTZ	25.2	2.7×10^{-5}
		CCSD(T)/CBS(DT)//M06-2X/aVTZ	25.1	3.2×10^{-5}
	$-CH_3$ 1,6-H-shift	CCSD(T)/aVTZ//M06-2X/aVTZ	27.4	3.6×10^{-5}
		CCSD(T)/CBS(DT)//M06-2X/aVTZ	27.4	3.8×10^{-5}
	HO_2 elimination	CCSD(T)/aVTZ//M06-2X/aVTZ	29.7	9.5×10^{-10}
		CCSD(T)/CBS(DT)//M06-2X/aVTZ	30.0	6.1×10^{-10}

[a] Based on WKB zero-curvature tunnelling

[b] Peeters et al. (2009)

[c] reported as $0.01\,\mathrm{s}^{-1}$ by Peeters et al. (2009)

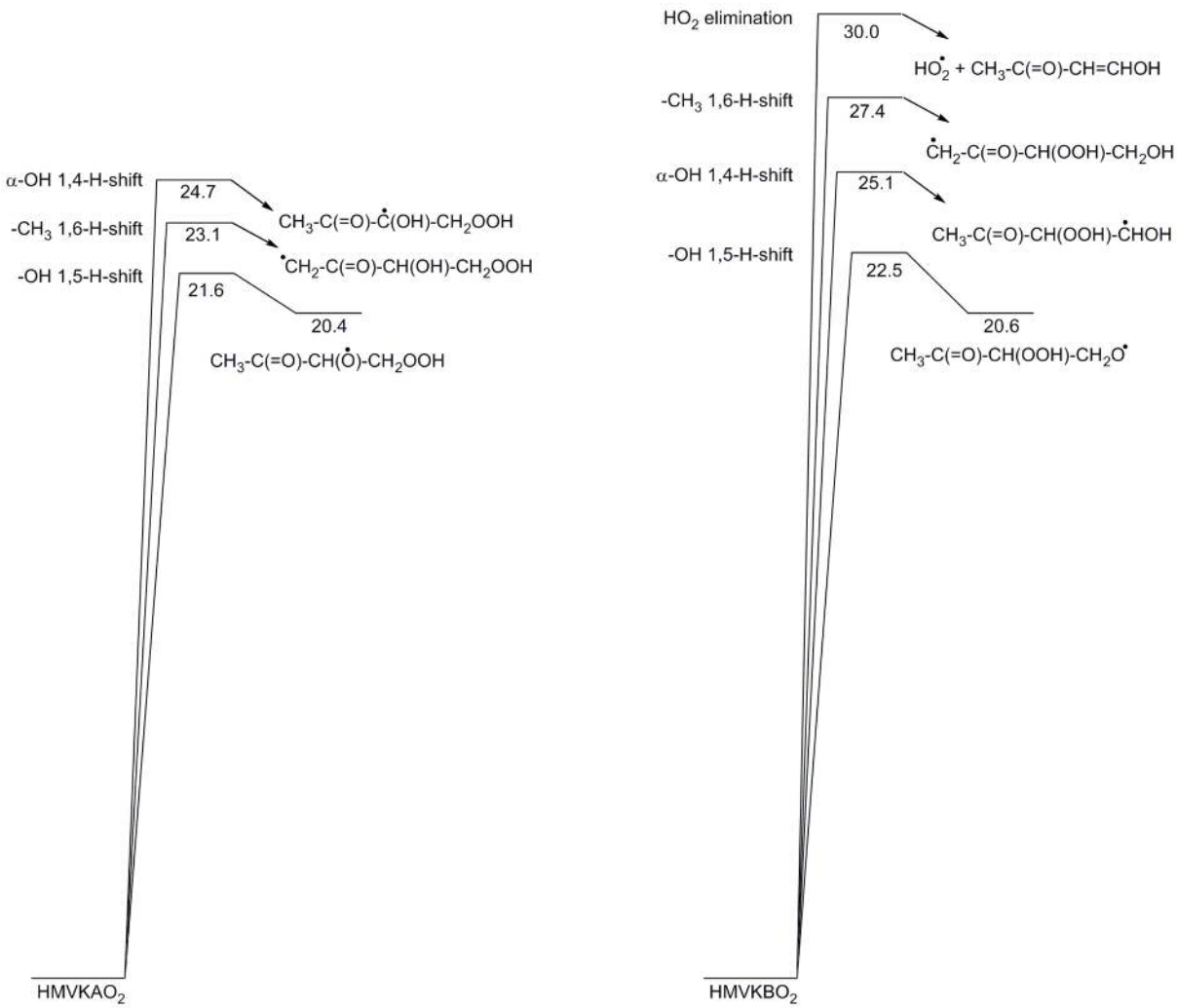

Figure 5. ZPE-corrected potential energy surface at the CCSD(T)/CBS(DT)//M06-2X/aug-cc-pVTZ level of theory, showing the energetics of the $\mathrm{HMVKAO_2}$ and $\mathrm{HMVKBO_2}$ reactions.

Table 2. Temperature dependence of the rate coefficients between 200 and 400 K as a Kooij expression: $k(T) = AT^n \exp(-E_a/T)$. The rates are based on the CCSD(T)/CBS(DT)//M06-2X/aug-cc-pVTZ quantum chemical data.

Reactant	Reaction class	A	n	E_a
		$\mathrm{cm^3 molecule^{-1} s^{-1}}$		K
HMVKAO₂	$-$OH 1,5-H-shift	1.25×10^{11}	-0.03	9897
$CH_3-C(=O)-CH(OH)-CH_2OO^\bullet$	$\alpha-$OH 1,4-H-shift	4.12×10^{-67}	24.46	-2295
	$-CH_3$ 1,6-H-shift	8.97×10^{-29}	12.54	4308
	all unimolecular	7.4×10^{-109}	39.35	-5769
HMVKBO₂	$-$OH 1,5-H-shift	7.13×10^{11}	-0.24	10571
$CH_3-C(=O)-CH(OO^\bullet)-CH_2OH$	$\alpha-$OH 1,4-H-shift	3.11×10^{-81}	29.64	-1790
	$-CH_3$ 1,6-H-shift	2.05×10^{-57}	21.74	1083
	HO_2 elimination	2.15×10^{-45}	18.86	7811
	all unimolecular	6.71×10^{-112}	41.14	-3722

[a] Geometric average across the Eckart and WKB tunneling corrections

References

Alecu, I. M., Zheng, J., Zhao, Y., and Truhlar, D. G.: Computational thermochemistry: Scale factor databases and scale factors for vibrational frequencies obtained from electronic model chemistries, J. Chem. Theory Comput., 6, 2872–2887, https://doi.org/10.1021/ct100326h, 2010.

Bao, J. L., Zheng, J., Alecu, I. M., Lynch, B. J., Zhao, Y., and Truhlar, D. G.: Database of frequency scale factors for electronic model chemistries (version 3 beta 2), [online] Available from: http://comp.chem.umn.edu/freqscale/index.html, 2017.

Becke, A. D.: Density-functional thermochemistry. II. The effect of the Perdew–Wang generalized-gradient correlation correction, J. Phys. Chem., 97, 9173–9177, https://doi.org/10.1063/1.463343, 1992.

Curtiss, L. A., Redfern, P. C., Raghavachari, K., and Pople, J. A.: Gaussian-3X (G3X) theory: Use of improved geometries, zero-point energies, and Hartree–Fock basis sets, J. phys. Chem., 114, 108–117, https://doi.org/10.1063/1.1321305, 2001.

Dunning, T. H.: Gaussian basis sets for use in correlated molecular calculations. I. The atoms boron through neon and hydrogen, J. Chem. Phys., 90, 1007–1023, https://doi.org/10.1063/1.456153, 1989.

Frisch, M. J., Trucks, G. W., Schlegel, H. B., Scuseria, G. E., Robb, M. A., Cheeseman, J. R., Scalmani, G., Barone, V., Mennucci, B., Petersson, G. A., Nakatsuji, H., Caricato, M., Li, X., Hratchian, H. P., Izmaylov, A. F., Bloino, J., Zheng, G., Sonnenberg, J. L., Hada, M., Ehara, M., Toyota, K., Fukuda, R., Hasegawa, J., Ishida, M., Nakajima, T., Honda, Y., Kitao, O., Nakai, H., Vreven, T., A., M. J. J., Peralta, J. E., Ogliaro, F., Bearpark, M., Heyd, J. J., Brothers, E., Kudin, K. N., Staroverov, V. N., Keith, T., Kobayashi, R., Normand, J., Normand, J., Raghavachari, K., Rendell, A., Burant, J. C., Iyengar, S. S., Tomasi, J., Cossi, M., Rega, N., Millam, J. M., Klene, M., Knox, J. E., Cross, J. B., Bakken, V., Adamo, C., Jaramillo, J., Gomperts, R., Stratmann, R. E., Yazyev, O., Austin, A. J., Cammi, R., Pomelli, C., Ochterski, J. W., Martin, R. L., Morokuma, K., Zakrzewski, V. G., Voth, G. A., Salvador, P., Dannenberg, J. J., Dapprich, S., Daniels, A. D., Farkas, O., Foresman, J. B., Ortiz, J. V., Cioslowski, J., Fox, D. J., and Pople, J. A.: Gaussian 09, Revision B.01, Gaussian Inc., Wallington CT., 2010.

Garrett, B. C. and Truhlar, D. G.: Criterion of minimum state density in the transition-state theory of bimolecular reactions, J. Chem. Phys., 70, 1593–1598, https://doi.org/10.1063/1.437698, 1979.

Johnston, H. S. and Heicklen, J.: Tunneling corrections for unsymmetrical Eckart potential energy barriers, J. Phys. Chem., 66, 532–533, https://doi.org/10.1021/j100809a040, 1962.

Lee, C., Yang, W., and Parr, R. G.: Development of the Colle-Salvetti correlation-energy formula into a functional of the electron density, Phys. Rev. B, 37, 785–789, https://doi.org/10.1103/PhysRevB.37.785, 1988.

Martin, J. M. L.: Ab initio total atomization energies of small molecules - towards the basis set limit, Chem. Phys. Lett., 259, https://doi.org/10.1016/0009-2614(96)00898-6, 1996.

Montgomery, J. A., Frisch, M. J., Ochterski, J. W., and Petersson, G. A.: A complete basis set model chemistry. VI. Use of density functional geometries and frequencies, J. Phys. Chem., 110, 2822–2827, https://doi.org/10.1063/1.477924, 1999.

Nguyen, T. L., Vereecken, L., and Peeters, J.: HO_X regeneration in the oxidation of isoprene III: Theoretical study of the key isomerisation of the z-δ-hydroxy-peroxy isoprene radicals, Chem. Phys. Chem., 11, 3996–4001, https://doi.org/10.1002/cphc.201000480, 2010.

Peeters, J., Nguyen, T. L., and Vereecken, L.: HO_X radical regeneration in the oxidation of isoprene, Phys. Chem. Chem. Phys., 11, 5935–5939, https://doi.org/10.1039/b908511d, 2009.

Peeters, J., Müller, J.-F., Stavrakou, T., and Nguyen, V. S.: Hydroxyl radical recycling in isoprene oxidation driven by hydrogen bonding and hydrogen tunneling: The upgraded LIM1 mechanism, J. Phys. Chem. A, 118, 8625–8643, https://doi.org/10.1021/jp5033146, 2014.

Purvis, G. D. and Bartlett, R. J.: A full coupled-cluster singles and doubles model: The inclusion of disconnected triples, J. Chem. Phys., 76, 1910–1918, https://doi.org/10.1063/1.443164, 1982.

Vereecken, L. and Peeters, J.: The 1,5-H-shift in 1-butoxy: A case study in the rigorous implementation of transition state theory for a multirotamer system, J. Chem. Phys., 119, 5159–5170, https://doi.org/10.1063/1.1597479, 2003.

Zhao, Y. and Truhlar, D. G.: The M06 suite of density functionals for main group thermochemistry, thermochemical kinetics, noncovalent interactions, excited states, and transition elements: two new functionals and systematic testing of four M06-class functionals and 12 other functionals, Theor.Chem. Account., 120, 215–241, https://doi.org/10.1007/s00214-007-0310-x, 2008.

Zhao, Y., Schultz, N. E., and Truhlar, D. G.: Design of density functionals by combining the method of constraint satisfaction with parametrization for thermochemistry, Thermochemical kinetics, and noncovalent interactions, J. Chem. Theory Comput., 2, 364–382, https://doi.org/10.1021/ct0502763, 2006.

Zheng, J. and Truhlar, D. G.: Quantum thermochemistry: Multistructural method with torsional anharmonicity based on a coupled torsional potential, J. Chem. Theory Comput., 9, 1356–1367, https://doi.org/10.1021/ct3010722, 2013.

Quantum chemical data

a. Population analysis at the M06-2X/cc-pVTZ level of theory

Relative energies in kcal mol^{-1}
Population contribution in %

HMVKAO2

Conformer	Erel	%
HMVKAO2.mppt	0.34	23.2
HMVKAO2.mpmt	0.00	19.4
HMVKAO2.hptp	0.68	13.9
HMVKAO2.mmpt	1.08	8.33
HMVKAO2.mtmt	0.92	8.3
HMVKAO2.hmtp	1.71	3.72
HMVKAO2.hmmm	1.16	3.69
HMVKAO2.mmtt	1.44	3.41
HMVKAO2.mmmt	1.57	3.21
HMVKAO2.mmpm	1.50	2.98
HMVKAO2.mmtm	1.92	2.55
HMVKAO2.hpmm	1.35	1.86
HMVKAO2.http	2.42	1.43
HMVKAO2.mttm	2.91	1.13
HMVKAO2.htmm	2.64	1.05
HMVKAO2.mttt	2.39	1
HMVKAO2.mptt	3.01	0.394
HMVKAO2.tmtm	4.17	0.127
HMVKAO2.htmp	4.16	0.0736
HMVKAO2.hpmt	3.66	0.0597
HMVKAO2.hpmp	3.50	0.0553
HMVKAO2.httm	4.88	0.0445
HMVKAO2.htmt	4.38	0.0366
HMVKAO2.tppp	4.82	0.0153
HMVKAO2.hmmt	4.87	0.0114
HMVKAO2.pmpt	5.19	0.00546
HMVKAO2.pppt	5.65	0.00484
HMVKAO2.ptpt	6.12	0.00369
HMVKAO2.pmpp	6.11	0.00227
HMVKAO2.hppt	6.23	0.0019
HMVKAO2.mmtp	6.11	0.00189
HMVKAO2.hppp	6.20	0.00178
HMVKAO2.mptp	6.18	0.00177
HMVKAO2.ttpp	6.40	0.00177
HMVKAO2.tmpp	6.53	0.00124
HMVKAO2.ttpt	7.10	0.000732
HMVKAO2.htpp	7.30	0.000598
HMVKAO2.mttp	7.02	0.000573
HMVKAO2.pmpm	6.85	0.000273
HMVKAO2.mppp	7.52	0.000266
HMVKAO2.hppm	7.51	0.000231
HMVKAO2.ptpm	8.17	0.000134
HMVKAO2.cpmp	8.88	5.95e-05
HMVKAO2.mtmp	8.78	2.12e-05
HMVKAO2.mpmp	8.39	1.97e-05
HMVKAO2.mtpp	8.99	1.39e-05

HMVKBO2

Conformer	Erel	%
HMVKBO2.hmmt	0.00	52.5
HMVKBO2.pppp	1.38	6.02
HMVKBO2.ptmp	0.97	5.81
HMVKBO2.ptmm	1.38	4.12
HMVKBO2.pppt	1.39	3.99
HMVKBO2.ptmt	0.85	3.98
HMVKBO2.pmmp	1.28	3.87
HMVKBO2.pttp	1.46	3.6
HMVKBO2.hmmm	1.36	2.72
HMVKBO2.htpm	1.56	2.65
HMVKBO2.pppm	2.07	2.43
HMVKBO2.ptpp	1.55	2.2
HMVKBO2.pptt	2.32	1.38
HMVKBO2.pttm	2.02	1.09
HMVKBO2.ltmt	1.57	0.931
HMVKBO2.htpt	1.97	0.671
HMVKBO2.pptp	2.88	0.658
HMVKBO2.ppmp	3.01	0.328
HMVKBO2.ppmt	3.21	0.177
HMVKBO2.ppmm	3.68	0.126
HMVKBO2.ltmp	3.14	0.125
HMVKBO2.ltmm	3.29	0.112
HMVKBO2.tppp	4.07	0.0611
HMVKBO2.pttt	3.98	0.0578
HMVKBO2.lppp	4.12	0.0529
HMVKBO2.tppm	4.07	0.0446
HMVKBO2.lppm	4.40	0.0426
HMVKBO2.lppt	4.21	0.0331
HMVKBO2.tmtp	4.67	0.0219
HMVKBO2.hmpm	5.92	0.0211
HMVKBO2.tmtm	4.74	0.0163
HMVKBO2.tmpm	5.21	0.0127
HMVKBO2.ttpm	4.95	0.0115
HMVKBO2.cmtp	5.39	0.00984
HMVKBO2.pmtp	5.50	0.00842
HMVKBO2.tmtt	5.43	0.00784
HMVKBO2.tptp	5.65	0.007
HMVKBO2.lttm	5.06	0.00699
HMVKBO2.lttp	5.17	0.00604
HMVKBO2.hmpt	5.60	0.00585
HMVKBO2.tmpp	5.70	0.0042
HMVKBO2.cmtm	5.52	0.00418
HMVKBO2.cmtt	5.54	0.00349
HMVKBO2.lmtt	5.48	0.00321
HMVKBO2.lmpt	5.82	0.0031
HMVKBO2.lptp	6.19	0.00168
HMVKBO2.tpmp	6.61	0.000895
HMVKBO2.lpmt	7.21	0.000188

TS.HMVKAO2.14HshiftCH2OH

Conformer	Erel	%
TS.HMVKAO2.14HshiftCH2OH.dtSl	0.00	94.9
TS.HMVKAO2.14HshiftCH2OH.utSl	1.79	4.93
TS.HMVKAO2.14HshiftCH2OH.umSc	4.38	0.119
TS.HMVKAO2.14HshiftCH2OH.dmSc	6.47	0.00315
TS.HMVKAO2.14HshiftCH2OH.umSl	7.81	0.000285
TS.HMVKAO2.14HshiftCH2OH.dmSl	8.06	0.000178
TS.HMVKAO2.14HshiftCH2OH.dtSc	8.33	0.000139

TS.HMVKAO2.14HshiftCH2OH.utSc 8.65 0.000139
TS.HMVKAO2.14HshiftCH2OH.upSc 9.08 5.71e-05

TS.HMVKAO2.15HshiftOH

Conformer	Erel	%
TS.HMVKAO2.15HshiftOH.md	0.05	50.1
TS.HMVKAO2.15HshiftOH.mu	0.00	49.9
TS.HMVKAO2.15HshiftOH.pd	5.66	0.00606

TS.HMVKAO2.16HshiftCH3

Conformer	Erel	%
TS.HMVKAO2.16HshiftCH3.a.Sp	0.00	97.9
TS.HMVKAO2.16HshiftCH3.b.Sp	2.45	1.76
TS.HMVKAO2.16HshiftCH3.a.Rm	3.52	0.237
TS.HMVKAO2.16HshiftCH3.a.Rt	4.53	0.0631
TS.HMVKAO2.16HshiftCH3.b.Rm	4.27	0.0517
TS.HMVKAO2.16HshiftCH3.b.Rt	6.17	0.00335
TS.HMVKAO2.16HshiftCH3.a.Sm	7.07	0.0011
TS.HMVKAO2.16HshiftCH3.b.Sm	9.61	1.33e-05

TS.HMVKBO2.14HshiftCH2OH

Conformer	Erel	%
TS.HMVKBO2.14HshiftCH2OH.umRlp	0.00	99.4
TS.HMVKBO2.14HshiftCH2OH.mmSht	3.58	0.482
TS.HMVKBO2.14HshiftCH2OH.umSlp	5.24	0.0493
TS.HMVKBO2.14HshiftCH2OH.mtShp	5.27	0.0324
TS.HMVKBO2.14HshiftCH2OH.mmRmp	5.50	0.0235
TS.HMVKBO2.14HshiftCH2OH.mmRlp	5.77	0.0217
TS.HMVKBO2.14HshiftCH2OH.mmRhm	5.65	0.0205
TS.HMVKBO2.14HshiftCH2OH.mtRhm	6.20	0.00761
TS.HMVKBO2.14HshiftCH2OH.utRhm	7.11	0.00238
TS.HMVKBO2.14HshiftCH2OH.mtShm	8.00	0.000734
TS.HMVKBO2.14HshiftCH2OH.umScm	8.10	0.000502
TS.HMVKBO2.14HshiftCH2OH.utScm	8.05	0.000494
TS.HMVKBO2.14HshiftCH2OH.mmScm	9.25	0.000384
TS.HMVKBO2.14HshiftCH2OH.mpSlt	10.27	2.29e-05
TS.HMVKBO2.14HshiftCH2OH.mtRct	9.96	2.03e-05
TS.HMVKBO2.14HshiftCH2OH.mpRhm	10.65	1.32e-05
TS.HMVKBO2.14HshiftCH2OH.utRct	10.53	7.49e-06

TS.HMVKBO2.15HshiftOH

Conformer	Erel	%
TS.HMVKBO2.15HshiftOH.t	0.00	56.5
TS.HMVKBO2.15HshiftOH.bis.t	0.46	43.4
TS.HMVKBO2.15HshiftOH.bis.c	4.10	0.15

TS.HMVKBO2.15HshiftCH3

Conformer	Erel	%
TS.HMVKBO2.15HshiftCH3.bis.pm	0.00	24.5
TS.HMVKBO2.15HshiftCH3.mp	0.34	20.2
TS.HMVKBO2.15HshiftCH3.tm	0.36	12.2
TS.HMVKBO2.15HshiftCH3.bis.mp	0.78	11.3
TS.HMVKBO2.15HshiftCH3.bis.pp	0.82	10.4
TS.HMVKBO2.15HshiftCH3.bis.pt	1.02	6.47
TS.HMVKBO2.15HshiftCH3.bis.tm	0.82	6.38
TS.HMVKBO2.15HshiftCH3.pm	0.96	5.97
TS.HMVKBO2.15HshiftCH3.mt	2.34	0.717
TS.HMVKBO2.15HshiftCH3.pp	2.40	0.626

TS.HMVKBO2.15HshiftCH3.bis.mm	2.63	0.614
TS.HMVKBO2.15HshiftCH3.bis.mt	2.74	0.466
TS.HMVKBO2.15HshiftCH3.mm	3.00	0.208
TS.HMVKBO2.15HshiftCH3.tp	4.81	0.0165
TS.HMVKBO2.15HshiftCH3.tt	5.65	0.00444

TS.HMVKBO2.HO2elim

Conformer	Erel	%
TS.HMVKBO2.HO2elim.cZm	0.00	95.1
TS.HMVKBO2.HO2elim.mEc	2.23	3.24
TS.HMVKBO2.HO2elim.cEc	3.29	0.723
TS.HMVKBO2.HO2elim.mEt	3.81	0.362
TS.HMVKBO2.HO2elim.mZt	4.12	0.19
TS.HMVKBO2.HO2elim.cEt	4.30	0.181
TS.HMVKBO2.HO2elim.pEt	4.50	0.101
TS.HMVKBO2.HO2elim.pZl	4.88	0.0572
TS.HMVKBO2.HO2elim.pZt	5.15	0.0356
TS.HMVKBO2.HO2elim.mZh	7.44	0.000766
TS.HMVKBO2.HO2elim.mZc	7.86	0.000462

b. Selected energetic and rovibrational data on M06-2X/aug-cc-pVTZ geometries

```
HMVKAO2.mpmt
------------
E(CCSD(T)/Aug-CC-pVDZ) (Hartree): -456.36512897
E(CCSD/Aug-CC-pVDZ) (Hartree): -456.31464640
     T1 diagnostic:  0.022666
E(MP2/Aug-CC-pVDZ) (Hartree): -456.25443317
E(MP3/Aug-CC-pVDZ) (Hartree): -456.29038221
E(PMP2/Aug-CC-pVDZ) (Hartree): -456.25740556
E(PMP3/Aug-CC-pVDZ) (Hartree): -456.29218027
E(PUHF/Aug-CC-pVDZ) (Hartree): -454.93913768
E(UHF/Aug-CC-pVDZ) (Hartree): -454.93431610
E(CCSD(T)/Aug-CC-pVTZ) (Hartree): -456.75629660
E(CCSD/Aug-CC-pVTZ) (Hartree): -456.68407033
     T1 diagnostic:  0.021789
E(MP2/Aug-CC-pVTZ) (Hartree): -456.64334697
E(MP3/Aug-CC-pVTZ) (Hartree): -456.66793458
E(PMP2/Aug-CC-pVTZ) (Hartree): -456.64653130
E(PMP3/Aug-CC-pVTZ) (Hartree): -456.66981848
E(PUHF/Aug-CC-pVTZ) (Hartree): -455.04635905
E(UHF/Aug-CC-pVTZ) (Hartree): -455.04118977
E(UM062X/Aug-CC-pVTZ) (Hartree): -457.39156917
Electronic state : 2-A
Cartesian coordinates (Angs):
     O      -1.094970     -1.312715      -0.935448
     O      -1.841554     -0.447335      -0.322886
     C      -1.230065     -0.002509       0.901537
     C       0.032742      0.803278       0.636344
     C       1.152820     -0.008357      -0.018623
     C       1.645135     -1.240473       0.684559
     H      -1.980220      0.635139       1.362652
     H      -1.035318     -0.876978       1.522377
     O      -0.266653      1.932801      -0.117518
     H       0.416194      1.093642       1.625733
     H       0.301111      1.900456      -0.902046
     O       1.631720      0.401010      -1.045504
     H       2.661406     -1.455052       0.366931
     H       1.603372     -1.124521       1.767264
     H       1.001325     -2.074415       0.405041
Rotational constants (GHz):    2.5687900    1.9095300    1.5178200
Vibrational harmonic frequencies (cm-1): (Scaled by 0.9710)
       66.0531                93.3947               108.0521
      148.4992               219.8635               234.7154
      329.5622               406.3559               432.1195
      452.3623               523.9337               596.3041
      702.1359               769.9792               897.3103
      912.7623               963.8776              1019.8574
     1058.5634              1143.6388              1184.2557
     1204.1422              1258.8232              1268.9397
     1322.9307              1350.5397              1357.4521
     1399.3340              1427.6173              1437.4639
     1441.8474              1790.7276              2910.6599
     2987.7133              3008.6247              3055.8498
     3075.9330              3087.8866              3635.1552
Zero-point correction (Hartree): 0.115633

HMVKAO2.hmmm
------------
E(UM062X/Aug-CC-pVTZ) (Hartree): -457.38937903
Electronic state : 2-A
Cartesian coordinates (Angs):
     O      -1.937322      0.479021      -0.948134
     O      -1.432342     -0.701723      -0.751454
     C      -1.029459     -0.894725       0.624528
     C       0.131024      0.021538       0.981549
     C       1.274788     -0.216706      -0.019865
     C       1.691597      0.932166      -0.886584
     H      -1.893796     -0.697577       1.256253
     H      -0.723319     -1.935917       0.672723
     O      -0.241271      1.366752       1.115166
     H       0.506687     -0.311824       1.951697
     H      -0.911090      1.572476       0.452642
     O       1.772065     -1.311961      -0.071687
     H       2.502471      0.621653      -1.537597
     H       0.835456      1.263416      -1.478979
     H       1.986861      1.777429      -0.265645
Rotational constants (GHz):    2.7989200    1.6528800    1.5300100
Vibrational harmonic frequencies (cm-1): (Scaled by 0.9710)
       44.3212                49.6524               150.6729
      178.3463               207.0611               257.3070
      332.0887               399.5535               424.3418
      484.2938               509.5258               532.2280
      677.8098               755.8077               849.4299
      945.7859               958.9797              1005.3203
     1038.2026              1138.4951              1203.0695
     1220.2100              1233.0585              1260.3784
     1314.9898              1343.8977              1351.6106
```

```
     1380.0436                1418.5389                1427.3745
     1432.2132                1794.9309                2977.1398
     2994.1644                3019.4504                3041.2628
     3093.6439                3097.0517                3701.3854
Zero-point correction (Hartree): 0.115536

HMVKAO2.hmmt
------------
E(UM062X/Aug-CC-pVTZ) (Hartree): -457.38309537
Electronic state : 2-A
Cartesian coordinates (Angs):
     O       2.436332      0.067965       0.784395
     O       1.390100     -0.681042       0.601019
     C       0.957413     -0.697036      -0.773050
     C      -0.230137      0.233500      -0.938782
     C      -1.341734     -0.216472       0.021769
     C      -1.610676      0.633321       1.228201
     H       1.794119     -0.378143      -1.389220
     H       0.657294     -1.720906      -0.985679
     O       0.222075      1.547232      -0.722541
     H      -0.611216      0.088007      -1.954665
     H      -0.449608      2.176615      -0.994268
     O      -1.927902     -1.239882      -0.219428
     H      -2.332254      0.134458       1.867296
     H      -0.675338      0.818451       1.757035
     H      -1.997035      1.607455       0.923124
Rotational constants (GHz):    2.9984100    1.4860700    1.4078800
Vibrational harmonic frequencies (cm-1): (Scaled by 0.9710)
       41.6720                  62.2229                  78.1180
      152.3784                 185.1956                 247.0477
      257.0986                 313.2798                 433.9886
      490.2720                 507.7232                 533.0408
      655.6971                 767.4048                 861.9043
      953.3239                 954.1866                1000.3775
     1042.3627                1140.7029                1171.5548
     1199.6747                1227.4004                1270.5995
     1313.4194                1344.5411                1349.8786
     1358.5040                1416.4038                1422.6419
     1428.1287                1796.2399                2967.5207
     2979.9307                3020.0025                3040.9201
     3089.1008                3095.9500                3775.0823
Zero-point correction (Hartree): 0.114836

HMVKAO2.hmtp
------------
E(UM062X/Aug-CC-pVTZ) (Hartree): -457.38822723
Electronic state : 2-A
Cartesian coordinates (Angs):
     O       2.689267     -0.141984      -0.768238
     O       2.235471     -0.003363       0.441306
     C       0.920311     -0.584796       0.581250
     C      -0.077453      0.232779      -0.215723
     C      -1.468041     -0.387781      -0.106411
     C      -2.636174      0.552191      -0.120812
     H       0.953936     -1.614788       0.238335
     H       0.707677     -0.531944       1.647059
     O      -0.132845      1.571269       0.220522
     H       0.204850      0.178166      -1.274819
     H       0.723804      1.983445       0.075796
     O      -1.579245     -1.585526      -0.038075
     H      -3.558222     -0.019550      -0.148424
     H      -2.600275      1.185039       0.766028
     H      -2.564809      1.222109      -0.977914
Rotational constants (GHz):    4.0708900    1.2399700    1.0458300
Vibrational harmonic frequencies (cm-1): (Scaled by 0.9710)
       33.1847                  61.5060                 114.4529
      162.7090                 185.0760                 263.9730
      300.5009                 336.2959                 405.8084
      457.8591                 511.5307                 568.7287
      599.3044                 793.8402                 886.3408
      914.4605                 967.1365                1006.7507
     1095.1418                1145.4205                1179.5804
     1190.9687                1213.9713                1257.7062
     1293.6214                1350.9393                1357.0994
     1390.8257                1420.8311                1426.0005
     1434.8168                1792.0838                2942.9012
     2987.1132                3026.4237                3048.5223
     3095.9960                3098.1367                3754.3004
Zero-point correction (Hartree): 0.115133

HMVKAO2.hpmm
------------
E(UM062X/Aug-CC-pVTZ) (Hartree): -457.38912749
Electronic state : 2-A
Cartesian coordinates (Angs):
     O       1.070887     -0.172680       1.441916
     O       1.912846     -0.371452       0.478247
     C       1.287710     -0.418494      -0.832484
     C       0.003316      0.385640      -0.880161
     C      -1.139945     -0.359259      -0.175454
     C      -2.060063      0.440764       0.699298
```

```
     H       2.042801     -0.009065      -1.498897
     H       1.089488     -1.464560      -1.061345
     O       0.176201      1.716971      -0.473664
     H      -0.290569      0.421520      -1.933015
     H       0.444119      1.721515       0.451223
     O      -1.286545     -1.534508      -0.393279
     H      -2.880346     -0.190035       1.026687
     H      -1.509923      0.810724       1.565163
     H      -2.428790      1.311359       0.157231
Rotational constants (GHz):    2.8090900    1.7425700    1.5973700
Vibrational harmonic frequencies (cm-1): (Scaled by 0.9710)
       55.3243                  93.6720                 112.4145
      167.5204                 213.5378                 254.6567
      321.6953                 398.5843                 415.4629
      463.4280                 512.8632                 560.2389
      716.6765                 764.9209                 853.2719
      906.7812                 957.6689                1002.6551
     1050.5814                1123.0351                1189.1198
     1209.2447                1238.6997                1268.4701
     1292.6619                1351.2038                1361.6327
     1374.5378                1419.7543                1434.8696
     1441.1957                1792.1344                2985.4445
     2986.8555                3017.5826                3049.7165
     3078.8609                3095.4665                3736.1443
Zero-point correction (Hartree): 0.115594

HMVKAO2.hpmp
------------
E(UM062X/Aug-CC-pVTZ) (Hartree): -457.38552622
Electronic state : 2-A
Cartesian coordinates (Angs):
     O       1.059916     -1.078945       1.111721
     O       1.893560     -0.429269       0.360708
     C       1.288262     -0.028536      -0.884049
     C      -0.005551      0.739309      -0.662202
     C      -1.149157     -0.213793      -0.291927
     C      -1.913281      0.060526       0.965879
     H       2.049716      0.590442      -1.356737
     H       1.092226     -0.915910      -1.485133
     O       0.111159      1.747414       0.311050
     H      -0.290009      1.151837      -1.637835
     H       0.824110      2.348586       0.081311
     O      -1.405935     -1.107461      -1.056323
     H      -2.671586     -0.704590       1.098082
     H      -1.225801      0.081545       1.810464
     H      -2.369896      1.049140       0.906394
Rotational constants (GHz):    2.7161900    1.7574900    1.6038000
Vibrational harmonic frequencies (cm-1): (Scaled by 0.9710)
       66.0101                 101.0653                 117.4223
      173.0801                 184.6929                 221.3036
      246.5522                 306.4058                 415.9394
      468.4214                 511.0148                 548.6454
      714.9243                 756.6897                 873.2843
      915.0342                 961.4854                1017.7253
     1046.4212                1138.2614                1164.0215
     1207.1803                1221.4494                1253.2902
     1304.6069                1351.4107                1356.3746
     1383.4674                1419.8776                1428.5781
     1443.7143                1795.9519                2940.7250
     2987.8783                3004.8792                3052.7252
     3062.7606                3097.4692                3765.8756
Zero-point correction (Hartree): 0.115027

HMVKAO2.hpmt
------------
E(UM062X/Aug-CC-pVTZ) (Hartree): -457.38501930
Electronic state : 2-A
Cartesian coordinates (Angs):
     O      -1.037225     -1.240566      -0.944952
     O      -1.875425     -0.462590      -0.336476
     C      -1.306495      0.102169       0.862666
     C      -0.000372      0.817976       0.583209
     C       1.131540     -0.186907       0.311012
     C       1.845849     -0.110581      -1.006992
     H      -2.064260      0.799602       1.210344
     H      -1.146444     -0.699378       1.582094
     O      -0.230169      1.747866      -0.447059
     H       0.274379      1.312042       1.522459
     H       0.519914      2.340822      -0.528612
     O       1.433032     -0.951761       1.189803
     H       2.519214     -0.957164      -1.097153
     H       1.126977     -0.090444      -1.823813
     H       2.425384      0.814989      -1.055212
Rotational constants (GHz):    2.6665500    1.7800900    1.6071900
Vibrational harmonic frequencies (cm-1): (Scaled by 0.9710)
       47.0286                 106.0288                 119.0716
      174.4696                 191.6539                 214.1697
      238.8637                 298.4593                 415.0036
      478.4024                 512.8252                 542.1990
      705.3374                 753.2893                 876.1455
      917.5224                 963.1422                1010.7247
```

```
     1054.9147                1137.3928                1169.1519
     1202.5621                1229.8541                1267.2414
     1314.5091                1345.4941                1359.7238
     1369.4588                1421.6331                1431.9671
     1437.7506                1795.0989                2951.3054
     2973.4202                3017.6621                3047.0486
     3082.0968                3097.7616                3779.6146
Zero-point correction (Hartree): 0.115081

HMVKAO2.hptp
------------
E(UM062X/Aug-CC-pVTZ) (Hartree): -457.38999356
Electronic state : 2-A
Cartesian coordinates (Angs):
     O       2.699607      0.512275      -0.036585
     O       2.210113     -0.684949      -0.144115
     C       0.879355     -0.779969       0.408919
     C      -0.078411      0.148458      -0.314103
     C      -1.521643     -0.313024      -0.083523
     C      -2.556930      0.757192       0.087451
     H       0.591189     -1.817234       0.266537
     H       0.938316     -0.528310       1.467751
     O       0.045036      1.490240       0.084297
     H       0.097733      0.040478      -1.394058
     H       0.981541      1.718469       0.063581
     O      -1.775231     -1.490456      -0.077619
     H      -3.540531      0.301642       0.138511
     H      -2.343354      1.323748       0.993759
     H      -2.495319      1.468390      -0.736368
Rotational constants (GHz):    4.2678100    1.2729400    1.0187700
Vibrational harmonic frequencies (cm-1): (Scaled by 0.9710)
       38.9724                  53.4639                 150.1838
      163.8450                 205.0663                 281.8801
      310.9090                 395.0146                 442.9044
      453.2489                 519.5213                 555.0789
      601.7913                 796.5157                 886.0312
      951.2771                 961.9388                1003.8463
     1069.5111                1153.0967                1193.4934
     1202.6976                1217.5372                1260.5183
     1307.8089                1350.9797                1352.1497
     1391.1871                1420.0396                1425.0613
     1439.3784                1792.9337                2918.1379
     2988.5289                3010.3327                3049.6105
     3094.2506                3099.5669                3713.9030
Zero-point correction (Hartree): 0.115486

HMVKAO2.htmm
------------
E(UM062X/Aug-CC-pVTZ) (Hartree): -457.38653665
Electronic state : 2-A
Cartesian coordinates (Angs):
     O       2.739667     -0.501148       0.645118
     O       1.487379     -0.177987       0.544921
     C       1.061438     -0.068166      -0.832814
     C      -0.320307      0.549531      -0.775552
     C      -1.298264     -0.431433      -0.106692
     C      -2.067269      0.047283       1.088378
     H       1.770834      0.575101      -1.348711
     H       1.035974     -1.065885      -1.265300
     O      -0.302071      1.829644      -0.194543
     H      -0.673514      0.670971      -1.801138
     H       0.201690      1.799237       0.625009
     O      -1.408505     -1.536307      -0.571137
     H      -2.758459     -0.726245       1.407234
     H      -1.369517      0.277856       1.896404
     H      -2.592356      0.972059       0.851711
Rotational constants (GHz):    2.9987400    1.4181000    1.2484800
Vibrational harmonic frequencies (cm-1): (Scaled by 0.9710)
       38.7405                  53.7813                 110.4226
      175.7166                 185.8578                 250.5812
      319.1218                 330.4689                 400.8328
      465.7606                 507.9985                 529.7145
      679.3516                 736.2681                 895.4801
      929.2844                 960.3914                1028.4491
     1042.7013                1122.9171                1187.6321
     1214.9293                1248.2141                1260.3485
     1293.2981                1340.5126                1351.8391
     1370.2210                1420.6334                1430.4574
     1442.6362                1796.4649                2979.0797
     3007.2382                3018.8053                3042.7534
     3083.7883                3097.3238                3740.2881
Zero-point correction (Hartree): 0.115176

HMVKAO2.htmp
------------
E(UM062X/Aug-CC-pVTZ) (Hartree): -457.38441394
Electronic state : 2-A
Cartesian coordinates (Angs):
     O       2.721512     -0.585591       0.569285
     O       1.462073     -0.280977       0.522404
     C       1.067055      0.124200      -0.802731
```

```
     C      -0.346301      0.663454      -0.706114
     C      -1.264377     -0.436870      -0.158634
     C      -1.938856     -0.197437       1.155835
     H       1.774066      0.880735      -1.143447
     H       1.100314     -0.749551      -1.451644
     O      -0.441093      1.804800       0.112712
     H      -0.690759      0.865103      -1.725873
     H       0.124918      2.501165      -0.229306
     O      -1.385337     -1.444419      -0.805559
     H      -2.534644     -1.065626       1.418431
     H      -1.179431     -0.000743       1.913648
     H      -2.556821      0.698332       1.097318
Rotational constants (GHz):    2.9134900    1.4499700    1.2755500
Vibrational harmonic frequencies (cm-1): (Scaled by 0.9710)
       44.4456                52.6062                102.5225
      161.9025               175.1203                231.0717
      255.8608               316.6670                390.6067
      476.7800               498.6264                532.1321
      681.8647               753.0173                888.8975
      936.1481               963.8890               1023.2228
     1052.1217              1133.7905               1161.1244
     1209.0530              1224.5081               1260.4553
     1309.7224              1346.7688               1350.9645
     1378.1331              1419.0953               1423.3386
     1443.2917              1798.2646               2960.0752
     2986.0737              2998.6409               3048.3240
     3061.8767              3099.1163               3767.1540
Zero-point correction (Hartree): 0.114770

HMVKAO2.htmt
------------
E(UM062X/Aug-CC-pVTZ) (Hartree): -457.38381153
Electronic state : 2-A
Cartesian coordinates (Angs):
     O       2.701373     -0.656466       0.469981
     O       1.454874     -0.300516       0.478134
     C       1.056499      0.243363      -0.797035
     C      -0.366605      0.735364      -0.650406
     C      -1.248065     -0.433165      -0.179926
     C      -1.768594     -0.398828       1.226334
     H       1.732197      1.060620      -1.039683
     H       1.115319     -0.553397      -1.535871
     O      -0.355156      1.840455       0.222587
     H      -0.714710      1.006524      -1.651548
     H      -1.191249      2.308736       0.171664
     O      -1.464178     -1.330739      -0.951850
     H      -2.280190     -1.331079       1.443518
     H      -0.940123     -0.233202       1.915036
     H      -2.455957      0.439529       1.352268
Rotational constants (GHz):    2.8243500    1.4707200    1.2985900
Vibrational harmonic frequencies (cm-1): (Scaled by 0.9710)
       52.1938                62.7039                107.5678
      157.4896               165.9704                225.3072
      248.2663               308.4853                386.4867
      474.5078               504.3817                530.8604
      668.9022               758.2235                896.5823
      932.5623               963.8940               1021.4739
     1044.7157              1131.7217               1190.7293
     1204.1415              1231.0694               1261.0120
     1301.7642              1342.6621               1352.9531
     1370.8932              1417.2942               1428.4291
     1437.7623              1796.9992               2971.8308
     2981.0543              3014.9580               3043.2169
     3078.9689              3096.8454               3777.5855
Zero-point correction (Hartree): 0.114829

HMVKAO2.httm
------------
E(UM062X/Aug-CC-pVTZ) (Hartree): -457.38266297
Electronic state : 2-A
Cartesian coordinates (Angs):
     O       3.219527     -0.288710       0.231858
     O       2.152491      0.163439      -0.350869
     C       0.964239     -0.436054       0.197581
     C      -0.222826      0.314435      -0.361520
     C      -1.521877     -0.446386      -0.058657
     C      -2.761562      0.382039       0.121080
     H       0.935249     -1.484162      -0.089481
     H       1.020378     -0.357190       1.285109
     O      -0.271128      1.661713       0.045799
     H      -0.136010      0.337627      -1.452756
     H      -0.050674      1.729702       0.979118
     O      -1.519919     -1.649571      -0.005717
     H      -3.628007     -0.270885       0.150772
     H      -2.691033      0.951059       1.048904
     H      -2.845521      1.114684      -0.681145
Rotational constants (GHz):    4.3537400    1.1208100    0.9288800
Vibrational harmonic frequencies (cm-1): (Scaled by 0.9710)
       19.0722                50.0898                 84.4035
      152.2733               158.1273                212.7663
      261.8703               312.2695                391.9313
```

```
      398.3336                516.4385                551.5671
      608.6673                790.1938                883.2225
      939.5702                984.8704               1033.5761
     1044.6022               1156.1051               1169.0321
     1190.4175               1254.8563               1267.2915
     1284.5482               1348.2583               1355.5589
     1377.1209               1417.4589               1428.4307
     1452.3995               1792.1516               2970.4463
     2986.0995               2991.6522               3046.5927
     3072.1493               3096.6880               3750.5292
Zero-point correction (Hartree): 0.114499

HMVKAO2.http
------------
E(UM062X/Aug-CC-pVTZ) (Hartree): -457.38707391
Electronic state : 2-A
Cartesian coordinates (Angs):
     O       3.194829     -0.281486      0.314191
     O       2.131532      0.141518     -0.297241
     C       0.934262     -0.494408      0.198889
     C      -0.219022      0.268103     -0.416096
     C      -1.539285     -0.420504     -0.069197
     C      -2.696588      0.458513      0.297133
     H       0.935982     -1.537154     -0.108351
     H       0.936476     -0.409161      1.284570
     O      -0.257439      1.606023      0.022483
     H      -0.128234      0.219653     -1.509184
     H       0.565605      2.038055     -0.224116
     O      -1.605195     -1.621778     -0.123115
     H      -3.580925     -0.153413      0.442468
     H      -2.456403      1.015304      1.203005
     H      -2.858518      1.202273     -0.483306
Rotational constants (GHz):    4.3828500    1.1309400    0.9418900
Vibrational harmonic frequencies (cm-1): (Scaled by 0.9710)
       23.5481                 56.1398                101.3017
      146.1245                167.1784                265.1543
      308.7196                343.2977                397.4449
      420.2489                511.1563                551.9320
      601.5554                788.8277                888.2451
      945.3259                975.8449               1021.8631
     1077.2863               1152.8319               1179.2898
     1193.0603               1216.5560               1256.3249
     1291.8255               1352.4573               1358.1275
     1387.5093               1419.6446               1425.2936
     1445.6919               1794.0651               2933.0239
     2987.2803               3013.2904               3047.7659
     3083.2144               3099.3731               3753.0309
Zero-point correction (Hartree): 0.114919

HMVKAO2.mmmt
------------
E(UM062X/Aug-CC-pVTZ) (Hartree): -457.38884339
Electronic state : 2-A
Cartesian coordinates (Angs):
     O      -2.456112     -0.245068     -0.784754
     O      -1.366082     -0.833298     -0.390233
     C      -0.947786     -0.406692      0.918375
     C       0.220457      0.559815      0.786758
     C       1.305353     -0.002494     -0.132746
     C       1.826302     -1.381718      0.150072
     H      -1.791016      0.082406      1.398825
     H      -0.660752     -1.310683      1.455014
     O      -0.218583      1.797020      0.331383
     H       0.671196      0.653785      1.785604
     H       0.294461      2.004830     -0.463148
     O       1.696346      0.674040     -1.048704
     H       2.780116     -1.521966     -0.349335
     H       1.925472     -1.557448      1.220930
     H       1.110024     -2.105936     -0.244178
Rotational constants (GHz):    2.9169000    1.5753800    1.3408700
Vibrational harmonic frequencies (cm-1): (Scaled by 0.9710)
       18.8404                 74.9240                 87.6395
      158.1056                188.4142                260.3961
      336.8073                402.6684                430.5932
      469.7190                511.2312                578.8863
      676.5003                770.3057                872.9785
      949.1313                965.8152               1015.7850
     1042.1477               1146.1248               1174.8874
     1201.1619               1240.0734               1287.8877
     1319.1635               1344.6046               1353.7789
     1387.3394               1419.9918               1435.6573
     1440.3832               1795.9622               2912.3961
     2977.9095               3009.4804               3043.2612
     3080.8192               3091.0123               3644.0730
Zero-point correction (Hartree): 0.115238

HMVKAO2.mmpm
------------
E(UM062X/Aug-CC-pVTZ) (Hartree): -457.38911290
Electronic state : 2-A
Cartesian coordinates (Angs):
```

```
     O       2.068339      0.577820      -0.577347
     O       1.927989     -0.438918       0.221202
     C       0.775860     -1.222851      -0.124517
     C      -0.515412     -0.692072       0.511517
     C      -0.866244      0.701149      -0.014617
     C      -0.262737      1.903472       0.646867
     H       0.681535     -1.236357      -1.208878
     H       0.970225     -2.221929       0.257788
     O      -1.524004     -1.601567       0.180929
     H      -0.397280     -0.648354       1.597459
     H      -2.047407     -1.186089      -0.520463
     O      -1.668411      0.779647      -0.912419
     H      -0.112083      2.690533      -0.086971
     H      -0.983270      2.255499       1.389260
     H       0.668165      1.672647       1.157391
Rotational constants (GHz):    2.6359600    1.8528400    1.2856600
Vibrational harmonic frequencies (cm-1): (Scaled by 0.9710)
       38.1236                67.0561                94.2133
      162.1301               210.6093               285.9233
      314.5478               349.1289               429.4013
      461.1153               549.8518               597.6666
      634.2725               756.4624               931.3650
      962.4828               994.0660              1019.0486
     1077.8145              1115.5951              1172.4412
     1198.5848              1254.7533              1269.3855
     1305.9176              1341.6692              1354.7727
     1398.8560              1431.1245              1436.6890
     1442.3620              1786.1864              2978.4616
     2981.9621              3015.9064              3055.7621
     3084.0487              3097.1041              3639.4080
Zero-point correction (Hartree): 0.115659

HMVKAO2.mmpt
------------
E(UM062X/Aug-CC-pVTZ) (Hartree): -457.38954508
Electronic state : 2-A
Cartesian coordinates (Angs):
     O       2.533484      0.419224      -0.416863
     O       1.880747     -0.380553       0.370813
     C       0.782242     -1.042780      -0.283808
     C      -0.533653     -0.693923       0.415262
     C      -1.045974      0.694930       0.037005
     C      -0.168921      1.880684       0.302244
     H       0.791553     -0.759197      -1.334095
     H       0.946468     -2.113515      -0.177538
     O      -1.468982     -1.668053       0.070066
     H      -0.351218     -0.693791       1.497601
     H      -2.231592     -1.198774      -0.300362
     O      -2.137741      0.783278      -0.469301
     H      -0.767245      2.786531       0.279407
     H       0.355981      1.780636       1.251060
     H       0.593828      1.933478      -0.478020
Rotational constants (GHz):    3.0248900    1.5914300    1.1301200
Vibrational harmonic frequencies (cm-1): (Scaled by 0.9710)
       47.2227                81.7230               111.8291
      176.3485               212.9832               291.7050
      306.0841               357.5337               435.4580
      475.1429               524.9477               578.5752
      636.8265               747.0483               928.0651
      965.4282               973.5848              1023.3643
     1088.3998              1137.7454              1180.1716
     1189.8514              1261.9081              1278.5302
     1293.0466              1349.6656              1361.4048
     1397.8028              1426.4253              1436.1664
     1448.3632              1784.2316              2935.4829
     2980.5208              3011.3493              3046.3715
     3076.7360              3092.9530              3631.0164
Zero-point correction (Hartree): 0.115626

HMVKAO2.mmtm
------------
E(UM062X/Aug-CC-pVTZ) (Hartree): -457.38932208
Electronic state : 2-A
Cartesian coordinates (Angs):
     O      -2.588263      0.630343      -0.635974
     O      -2.235831     -0.076676       0.392311
     C      -0.871638      0.200058       0.764915
     C       0.081702     -0.378876      -0.269571
     C       1.494266      0.158953      -0.069042
     C       1.700706      1.646863      -0.098639
     H      -0.778171      1.280818       0.856919
     H      -0.734733     -0.292725       1.725260
     O       0.065178     -1.769791      -0.221795
     H      -0.256946     -0.020200      -1.251541
     H       0.981753     -2.056794      -0.099272
     O       2.396164     -0.623351       0.097473
     H       1.557471      2.040339       0.909986
     H       2.718752      1.864652      -0.408459
     H       0.983671      2.137712      -0.754991
Rotational constants (GHz):    3.5968600    1.3035900    1.0560700
Vibrational harmonic frequencies (cm-1): (Scaled by 0.9710)
```

```
       51.1625                71.8067                120.6617
      154.8383               196.1412                262.0396
      325.3506               389.0274                411.4303
      456.7741               547.2398                561.4819
      629.1568               820.1374                900.2869
      931.2981               967.4570               1006.7449
     1089.0421              1141.3179               1188.0387
     1211.0296              1236.9668               1279.2870
     1311.7761              1351.4861               1362.5997
     1393.7405              1427.5288               1429.1911
     1441.7931              1788.4735               2932.5124
     2979.0855              3011.2719               3045.6536
     3077.3424              3088.6399               3646.5822
Zero-point correction (Hartree): 0.115519

HMVKAO2.mppt
------------
E(CCSD(T)/Aug-CC-pVDZ) (Hartree): -456.36447322
E(CCSD/Aug-CC-pVDZ) (Hartree): -456.31424675
     T1 diagnostic:  0.022692
E(MP2/Aug-CC-pVDZ) (Hartree): -456.25346708
E(MP3/Aug-CC-pVDZ) (Hartree): -456.28996447
E(PMP2/Aug-CC-pVDZ) (Hartree): -456.25635073
E(PMP3/Aug-CC-pVDZ) (Hartree): -456.29171757
E(PUHF/Aug-CC-pVDZ) (Hartree): -454.94047181
E(UHF/Aug-CC-pVDZ) (Hartree): -454.93576234
E(CCSD(T)/Aug-CC-pVTZ) (Hartree): -456.75578191
E(CCSD/Aug-CC-pVTZ) (Hartree): -456.68380725
     T1 diagnostic:  0.021786
E(MP2/Aug-CC-pVTZ) (Hartree): -456.64247456
E(MP3/Aug-CC-pVTZ) (Hartree): -456.66766572
E(PMP2/Aug-CC-pVTZ) (Hartree): -456.64556846
E(PMP3/Aug-CC-pVTZ) (Hartree): -456.66950140
E(PUHF/Aug-CC-pVTZ) (Hartree): -455.04765520
E(UHF/Aug-CC-pVTZ) (Hartree): -455.04259446
E(UM062X/Aug-CC-pVTZ) (Hartree): -457.39079856
Electronic state : 2-A
Cartesian coordinates (Angs):
     O      -2.479236      0.197130      -0.617633
     O      -1.836708      0.286801       0.508534
     C      -0.884596     -0.780459       0.655683
     C       0.269752     -0.660900      -0.342642
     C       1.170590      0.537294      -0.053252
     C       0.576553      1.913568      -0.096861
     H      -0.532419     -0.713799       1.683858
     H      -1.394939     -1.726306       0.489516
     O       0.999855     -1.846522      -0.277705
     H      -0.166209     -0.523355      -1.339123
     H       1.911742     -1.597793      -0.064533
     O       2.332366      0.332388       0.202292
     H       1.372194      2.648671      -0.172810
     H      -0.128484      2.011438      -0.921142
     H       0.014111      2.085756       0.822761
Rotational constants (GHz):    3.0574000    1.5833300    1.1646600
Vibrational harmonic frequencies (cm-1): (Scaled by 0.9710)
       45.9000                73.9665               141.8265
      159.7013               201.3066               287.2900
      308.9659               353.8382               431.4591
      457.1968               551.6724               592.1856
      634.0541               745.4390               925.2148
      957.2824               973.8735              1022.3296
     1093.1384              1136.5243              1189.0421
     1195.2579              1246.2433              1275.9191
     1294.5337              1351.1883              1360.9925
     1399.3596              1422.9120              1436.0124
     1447.9794              1782.3110              2953.1140
     2983.4728              3013.6931              3047.7724
     3077.7398              3091.9292              3630.6979
Zero-point correction (Hartree): 0.115652

HMVKAO2.mptt
------------
E(UM062X/Aug-CC-pVTZ) (Hartree): -457.38762419
Electronic state : 2-A
Cartesian coordinates (Angs):
     O      -3.144348     -0.488120      -0.272461
     O      -2.127133      0.057597       0.317698
     C      -0.893057     -0.330687      -0.315086
     C       0.224059      0.402889       0.403039
     C       1.586505     -0.158762       0.001837
     C       1.841048     -1.626968       0.191780
     H      -0.810644     -1.413404      -0.224296
     H      -0.943005     -0.035090      -1.362175
     O       0.154896      1.768709       0.146112
     H       0.111497      0.211371       1.479980
     H       1.021647      2.034511      -0.194117
     O       2.412790      0.594642      -0.446872
     H       2.909591     -1.800777       0.278495
     H       1.316088     -2.015525       1.063179
     H       1.473875     -2.162536      -0.686293
Rotational constants (GHz):    3.9321700    1.1593600    0.9482900
```

```
Vibrational harmonic frequencies (cm-1): (Scaled by 0.9710)
       54.9632                76.9741                96.3934
      156.8415               162.1109               256.3337
      335.1344               367.8861               407.2047
      444.2978               467.8995               589.6304
      631.8637               820.4356               897.0323
      952.7943               971.5637              1033.0031
     1078.9590              1145.1832              1181.4230
     1223.9606              1238.3767              1256.6885
     1314.3277              1350.6375              1364.0348
     1395.2613              1426.9265              1435.1303
     1444.4384              1791.4260              2919.3429
     2979.5858              2999.3969              3045.8763
     3061.5053              3090.4310              3644.4143
Zero-point correction (Hartree): 0.115222

HMVKAO2.mtmt
------------
E(UM062X/Aug-CC-pVTZ) (Hartree): -457.39003314
Electronic state : 2-A
Cartesian coordinates (Angs):
     O      -2.707871     -0.523962      -0.501435
     O      -1.465855     -0.151371      -0.520940
     C      -1.027157      0.285862       0.780955
     C       0.423568      0.707970       0.655123
     C       1.260279     -0.354197      -0.061256
     C       1.176509     -1.767572       0.436125
     H      -1.643247      1.130710       1.080873
     H      -1.160366     -0.545366       1.472864
     O       0.524466      1.935852       0.007600
     H       0.822941      0.777680       1.677235
     H       1.146766      1.816629      -0.724720
     O       1.951516     -0.018254      -0.987895
     H       2.010470     -2.343407       0.046846
     H       1.163929     -1.801914       1.525399
     H       0.242269     -2.204831       0.077175
Rotational constants (GHz):    2.8513500    1.5466700    1.2359000
Vibrational harmonic frequencies (cm-1): (Scaled by 0.9710)
       50.4405                80.2300               120.4407
      159.9724               170.6262               262.6058
      341.1771               387.3799               407.5405
      435.8850               487.8237               600.4469
      689.1991               764.2914               902.7885
      933.9365               959.7116              1037.9678
     1054.9706              1142.3648              1181.8151
     1203.8190              1256.6117              1262.0736
     1331.4079              1351.3732              1357.5931
     1391.7556              1424.5184              1439.3132
     1444.4454              1796.9812              2916.3570
     2978.3086              3005.6891              3042.8044
     3067.3373              3091.1395              3645.8175
Zero-point correction (Hartree): 0.115384

HMVKAO2.mttm
------------
E(UM062X/Aug-CC-pVTZ) (Hartree): -457.38673248
Electronic state : 2-A
Cartesian coordinates (Angs):
     O      -3.144129     -0.502243      -0.322911
     O      -2.128337     -0.030725       0.330159
     C      -0.895000     -0.307117      -0.360201
     C       0.216531      0.353676       0.440943
     C       1.573758     -0.141430      -0.056466
     C       1.993232     -1.542935       0.280632
     H      -0.795885     -1.390094      -0.423165
     H      -0.959427      0.128384      -1.356310
     O       0.130415      1.740880       0.342431
     H       0.107103      0.050416       1.489222
     H       0.891818      2.032726      -0.179391
     O       2.279066      0.622653      -0.665568
     H       2.761257     -1.876111      -0.411092
     H       2.412973     -1.526665       1.288892
     H       1.154921     -2.236339       0.289517
Rotational constants (GHz):    3.8806600    1.1428900    0.9614600
Vibrational harmonic frequencies (cm-1): (Scaled by 0.9710)
       52.2819                57.6277                74.2192
      102.2574               167.4903               253.2880
      321.0248               376.0466               395.0560
      436.0323               489.9314               610.5484
      614.8621               833.0515               894.2333
      945.7864               974.6595              1030.8643
     1075.6596              1136.5001              1174.7851
     1213.0947              1244.7064              1259.1878
     1304.2716              1355.5133              1365.4888
     1391.0496              1426.7108              1433.5427
     1443.8018              1791.2480              2950.3555
     2982.3242              3001.1129              3050.2723
     3062.8517              3093.4871              3649.4865
Zero-point correction (Hartree): 0.115046

HMVKAO2.tmtm
```

```
------------
E(UM062X/Aug-CC-pVTZ) (Hartree): -457.38379567
Electronic state : 2-A
Cartesian coordinates (Angs):
     O      -2.666954     -0.102077      0.857345
     O      -2.274104     -0.017583     -0.376299
     C      -0.958721     -0.578199     -0.543268
     C       0.077851      0.273951      0.159714
     C       1.454004     -0.395731      0.094149
     C       2.641221      0.498390      0.316980
     H      -0.957023     -1.592004     -0.152803
     H      -0.797879     -0.597724     -1.621660
     O       0.109501      1.606086     -0.299998
     H      -0.194575      0.332863      1.217811
     H       0.133733      1.619336     -1.261244
     O       1.551260     -1.579487     -0.109703
     H       3.527303     -0.110256      0.467540
     H       2.778478      1.143227     -0.551776
     H       2.466215      1.158581      1.165922
Rotational constants (GHz):    3.9592800    1.2274900    1.0474300
Vibrational harmonic frequencies (cm-1): (Scaled by 0.9710)
       33.4619                59.7255               113.0360
      134.9421               188.9764               244.2672
      265.6634               303.4995               378.7914
      467.1706               512.8112               572.3056
      605.9303               800.4753               884.0376
      918.2081               975.5425              1019.0587
     1055.3383              1146.8642              1180.4708
     1186.9668              1241.7074              1276.1955
     1296.4107              1352.8056              1362.9387
     1374.0704              1418.7859              1428.9692
     1441.4032              1789.5760              2982.9262
     2986.7212              3009.0926              3047.2028
     3082.6137              3096.1299              3746.6155
Zero-point correction (Hartree): 0.114921

HMVKAO2.tppp
------------
E(UM062X/Aug-CC-pVTZ) (Hartree): -457.38340412
Electronic state : 2-A
Cartesian coordinates (Angs):
     O      -2.554109     -0.057422      0.892221
     O      -1.973085     -0.647658     -0.107147
     C      -1.076508      0.251333     -0.785972
     C       0.130674      0.564326      0.088331
     C       1.190318     -0.535292      0.009956
     C       2.551975     -0.188004      0.538301
     H      -0.791613     -0.265963     -1.698109
     H      -1.628278      1.163712     -1.006347
     O       0.744095      1.780082     -0.284017
     H      -0.210825      0.598416      1.130411
     H       0.205097      2.515991      0.016354
     O       0.908420     -1.613721     -0.441945
     H       3.154607     -1.087911      0.610457
     H       3.020477      0.527825     -0.137235
     H       2.469217      0.303509      1.507886
Rotational constants (GHz):    3.3000500    1.3937300    1.1388600
Vibrational harmonic frequencies (cm-1): (Scaled by 0.9710)
       44.2196                63.3972               118.3372
      145.1153               202.1860               278.1230
      287.1753               329.4333               385.0060
      447.5637               514.7723               586.8065
      612.4401               736.6090               911.8375
      953.4319               977.9932              1025.0465
     1069.0636              1134.5136              1176.2887
     1189.2965              1211.7459              1264.9204
     1300.7930              1350.5097              1370.3267
     1394.5539              1423.9446              1430.3500
     1434.1345              1802.6620              2944.7735
     2986.5210              3012.3735              3048.9798
     3085.9154              3095.5167              3766.7338
Zero-point correction (Hartree): 0.115230

HMVKBO2.hmmm
------------
E(UM062X/Aug-CC-pVTZ) (Hartree): -457.38601666
Electronic state : 2-A
Cartesian coordinates (Angs):
     C      -0.295418     -0.120935     -0.248545
     H      -0.490830     -0.161200     -1.323563
     C       1.196278      0.116204     -0.031796
     C      -1.167808      0.954802      0.390267
     O      -0.609874     -1.413645      0.305360
     O       1.594738      1.242253      0.137986
     C       2.103906     -1.076294     -0.070026
     H       1.880463     -1.692818     -0.941269
     H       1.917746     -1.696427      0.807906
     H       3.137692     -0.746005     -0.082562
     O      -1.042387      2.169040     -0.299866
     H      -2.205925      0.634769      0.316643
     H      -0.904645      1.052851      1.447916
```

```
     H      -0.132920      2.468388      -0.189225
     O      -1.720393     -1.885426      -0.177886
Rotational constants (GHz):    2.2424400    2.0326600    1.1226800
Vibrational harmonic frequencies (cm-1): (Scaled by 0.9710)
       41.8211                  86.1842                 143.7879
      153.2770                 205.7749                 241.4123
      285.0609                 370.9473                 441.0036
      463.5506                 512.4466                 562.2539
      614.9058                 762.9668                 923.7757
      947.3793                1009.6484                1056.5799
     1077.7947                1100.7797                1167.4701
     1205.8266                1244.4364                1259.2896
     1321.6536                1350.1286                1360.2928
     1391.1680                1420.2299                1429.7315
     1468.9250                1786.7622                2959.9654
     2983.2563                2990.8611                3043.0634
     3044.3387                3097.4613                3721.6557
Zero-point correction (Hartree): 0.115546

HMVKBO2.hmmt
------------
E(CCSD(T)/Aug-CC-pVDZ) (Hartree): -456.36228035
E(CCSD/Aug-CC-pVDZ) (Hartree): -456.31196852
     T1 diagnostic:  0.022819
E(MP2/Aug-CC-pVDZ) (Hartree): -456.25052340
E(MP3/Aug-CC-pVDZ) (Hartree): -456.28759527
E(PMP2/Aug-CC-pVDZ) (Hartree): -456.25339001
E(PMP3/Aug-CC-pVDZ) (Hartree): -456.28934166
E(PUHF/Aug-CC-pVDZ) (Hartree): -454.93781106
E(UHF/Aug-CC-pVDZ) (Hartree): -454.93312479
E(CCSD(T)/Aug-CC-pVTZ) (Hartree): -456.75274738
E(CCSD/Aug-CC-pVTZ) (Hartree): -456.68071667
     T1 diagnostic:  0.021933
E(MP2/Aug-CC-pVTZ) (Hartree): -456.63873437
E(MP3/Aug-CC-pVTZ) (Hartree): -456.66445591
E(PMP2/Aug-CC-pVTZ) (Hartree): -456.64181153
E(PMP3/Aug-CC-pVTZ) (Hartree): -456.66628735
E(PUHF/Aug-CC-pVTZ) (Hartree): -455.04444045
E(UHF/Aug-CC-pVTZ) (Hartree): -455.03940173
E(UM062X/Aug-CC-pVTZ) (Hartree): -457.38774592
Electronic state : 2-A
Cartesian coordinates (Angs):
     C       0.168693     -0.338645       0.542811
     H       0.360975     -0.216773       1.611565
     C      -0.489529      0.940519       0.022094
     C       1.475992     -0.664231      -0.175101
     O      -0.744416     -1.445959       0.462108
     O       0.193985      1.772848      -0.519474
     C      -1.961836      1.114568       0.253029
     H      -2.234430      0.784923       1.255645
     H      -2.507838      0.486219      -0.451389
     H      -2.229110      2.155266       0.098726
     O       2.473257      0.254985       0.183371
     H       1.806863     -1.653116       0.139046
     H       1.295747     -0.682355      -1.252650
     H       2.210769      1.111088      -0.173205
     O      -1.155687     -1.619189      -0.761596
Rotational constants (GHz):    2.5812600    1.9422000    1.2647800
Vibrational harmonic frequencies (cm-1): (Scaled by 0.9710)
       54.8136                 107.9351                 145.0558
      150.4859                 188.8972                 254.3537
      272.1788                 384.2404                 430.9141
      471.0983                 507.3485                 578.8845
      664.9822                 755.6207                 920.2916
      957.3054                 985.7546                1033.3337
     1076.4458                1105.8887                1168.0677
     1202.6481                1205.0512                1289.8933
     1328.0027                1348.4916                1355.8334
     1390.9839                1422.9861                1431.3208
     1470.1653                1788.6138                2976.1864
     2985.8059                3001.7244                3041.9637
     3049.5521                3095.8439                3721.0237
Zero-point correction (Hartree): 0.115715

HMVKBO2.htpm
------------
E(UM062X/Aug-CC-pVTZ) (Hartree): -457.38560665
Electronic state : 2-A
Cartesian coordinates (Angs):
     C      -0.275109     -0.109746      -0.528328
     H      -0.399952     -0.490528      -1.546293
     C       1.211314     -0.142509      -0.182253
     C      -0.871287      1.283166      -0.413569
     O      -0.942266     -1.042076       0.349854
     O       1.869319      0.852689      -0.355233
     C       1.780734     -1.428402       0.335177
     H       1.458985     -2.265591      -0.284680
     H       1.386182     -1.610637       1.336022
     H       2.863504     -1.359672       0.366106
     O      -0.583336      1.891866       0.818869
     H      -0.507891      1.876765      -1.255370
```

```
     H      -1.953552      1.193118      -0.493222
     H       0.341637      2.156634       0.808521
     O      -2.126569     -1.341872      -0.088145
Rotational constants (GHz):    2.4594600    1.9322500    1.2338200
Vibrational harmonic frequencies (cm-1): (Scaled by 0.9710)
       47.6130                82.9656                133.6649
      166.0596               209.1338                215.3120
      303.6500               385.5156                428.6993
      454.8453               502.8540                560.3778
      684.9740               796.1875                850.5170
      928.0016               964.2144               1023.8657
     1066.3216              1113.7771               1174.4969
     1206.0177              1249.6644               1284.1323
     1311.1610              1358.2685               1361.5554
     1378.6846              1420.7760               1429.8616
     1451.6729              1790.1856               2977.8438
     2982.3002              2988.3199               3043.5675
     3046.4503              3096.4365               3747.7734
Zero-point correction (Hartree): 0.115475

HMVKBO2.htpt
------------
E(UM062X/Aug-CC-pVTZ) (Hartree): -457.38498868
Electronic state : 2-A
Cartesian coordinates (Angs):
     C      -0.171767      0.165805       0.811420
     H       0.068122      0.186162       1.878527
     C       0.893460     -0.672283       0.098911
     C      -1.583189     -0.372196       0.625790
     O      -0.079354      1.542545       0.405251
     O       0.601198     -1.763722      -0.318896
     C       2.279332     -0.102224       0.002396
     H       2.532115      0.470517       0.893913
     H       2.315447      0.581064      -0.846252
     H       2.987617     -0.910137      -0.155453
     O      -1.972216     -0.465036      -0.714856
     H      -1.630121     -1.340199       1.133847
     H      -2.278560      0.307714       1.116393
     H      -1.415644     -1.126532      -1.138910
     O       0.064623      1.650813      -0.885645
Rotational constants (GHz):    2.6133200    2.0378500    1.4509700
Vibrational harmonic frequencies (cm-1): (Scaled by 0.9710)
       59.9358                93.2346                120.3062
      175.3317               204.4379                218.0102
      317.3178               330.7297                441.4846
      473.3125               520.8014                577.3602
      686.6530               800.8391                868.3274
      934.6709               971.1242               1021.0531
     1041.4595              1125.4804               1160.3434
     1201.6176              1210.9168               1302.9794
     1331.7900              1357.8512               1360.1541
     1391.4469              1425.9508               1434.6136
     1448.6704              1792.1918               2963.1050
     2987.1661              2989.7979               3035.6634
     3055.3390              3091.6888               3739.4762
Zero-point correction (Hartree): 0.115580

HMVKBO2.ltmm
------------
E(UM062X/Aug-CC-pVTZ) (Hartree): -457.38275007
Electronic state : 2-A
Cartesian coordinates (Angs):
     C      -0.269109     -0.146356      -0.529960
     H      -0.389395     -0.448199      -1.572907
     C       1.087726     -0.605771      -0.005250
     C      -0.453455      1.357343      -0.387441
     O      -1.285093     -0.821704       0.238438
     O       1.176661     -1.457377       0.833906
     C       2.277097      0.096883      -0.601614
     H       2.347484      1.088259      -0.149427
     H       2.167601      0.225106      -1.678768
     H       3.176979     -0.466802      -0.375799
     O      -0.092650      1.804752       0.897798
     H       0.196410      1.870111      -1.095085
     H      -1.489478      1.599818      -0.634808
     H      -0.678965      1.407467       1.549005
     O      -2.446943     -0.711715      -0.332219
Rotational constants (GHz):    2.7045200    1.7251000    1.2996300
Vibrational harmonic frequencies (cm-1): (Scaled by 0.9710)
       57.3966                91.4060                113.8358
      170.7709               193.3369                209.9038
      316.1493               361.6076                374.3667
      462.3873               477.4024                574.2544
      679.5297               812.0626                853.6056
      935.6415               953.2807               1038.9404
     1056.2030              1108.0326               1157.2511
     1192.8550              1247.2049               1250.0158
     1312.8826              1346.8165               1362.6181
     1376.0668              1426.7965               1438.3994
     1464.9343              1816.0856               2977.3779
     2983.4431              2999.8109               3042.4519
```

```
     3042.7286                3091.8938                3745.9751
Zero-point correction (Hartree): 0.115236

HMVKBO2.ltmp
------------
E(UM062X/Aug-CC-pVTZ) (Hartree): -457.38307280
Electronic state : 2-A
Cartesian coordinates (Angs):
     C      -0.270934      0.219250      -0.596878
     H      -0.484882     -0.017106      -1.641676
     C       0.487232     -0.945161       0.051044
     C       0.505774      1.519853      -0.473379
     O      -1.516567      0.431270       0.074432
     O       0.009667     -1.573862       0.950891
     C       1.862492     -1.199592      -0.504526
     H       2.538419     -0.448601      -0.090323
     H       1.878962     -1.107151      -1.590587
     H       2.196610     -2.187304      -0.202041
     O       1.000711      1.711980       0.830849
     H       1.368942      1.488245      -1.136311
     H      -0.137349      2.344591      -0.790673
     H       0.263629      1.747241       1.448417
     O      -2.385275     -0.492640      -0.212968
Rotational constants (GHz):    2.3897800    1.9802600    1.3450600
Vibrational harmonic frequencies (cm-1): (Scaled by 0.9710)
       65.1638                  95.2324                 110.8721
      154.6955                 162.5004                 255.8422
      306.0399                 349.2375                 384.5720
      433.1074                 492.8386                 599.2923
      663.0260                 793.7187                 866.5581
      941.9997                 955.4868                1031.1973
     1062.6538                1114.3263                1159.1461
     1205.0048                1241.3257                1252.4847
     1309.5465                1344.9532                1355.3348
     1380.7233                1426.2816                1438.2127
     1461.5598                1820.2171                2974.2037
     2977.1634                3001.3954                3042.1990
     3042.9910                3091.6192                3744.7470
Zero-point correction (Hartree): 0.115216

HMVKBO2.ltmt
------------
E(UM062X/Aug-CC-pVTZ) (Hartree): -457.38557278
Electronic state : 2-A
Cartesian coordinates (Angs):
     C       0.169954     -0.047912       0.825026
     H      -0.063288     -0.120015       1.889070
     C      -1.028048     -0.549641       0.008751
     C       0.520989      1.390634       0.454511
     O       1.287183     -0.932823       0.658548
     O      -0.934365     -1.502191      -0.710401
     C      -2.286135      0.259766       0.166721
     H      -2.159686      1.188863      -0.392305
     H      -2.467007      0.514852       1.211159
     H      -3.126159     -0.295689      -0.238869
     O       0.406625      1.644314      -0.922386
     H      -0.178108      2.058425       0.957102
     H       1.525302      1.605510       0.829999
     H       1.001568      1.038186      -1.378298
     O       1.891410     -0.747703      -0.476750
Rotational constants (GHz):    2.6420400    1.9810700    1.4753200
Vibrational harmonic frequencies (cm-1): (Scaled by 0.9710)
       70.7910                 112.8546                 144.0210
      149.7968                 208.8947                 248.4337
      329.9750                 351.7887                 434.1508
      500.7448                 533.8174                 570.1607
      694.6942                 798.8306                 868.9105
      941.2740                 970.9506                1018.9021
     1034.0424                1118.1087                1154.7921
     1198.4145                1227.0856                1246.0614
     1341.8251                1344.8153                1362.3830
     1393.3283                1426.7489                1438.1171
     1459.3515                1819.1844                2970.5536
     2978.4292                3010.2307                3032.7122
     3044.4124                3091.0465                3721.2178
Zero-point correction (Hartree): 0.115813

HMVKBO2.pmmp
------------
E(UM062X/Aug-CC-pVTZ) (Hartree): -457.38605168
Electronic state : 2-A
Cartesian coordinates (Angs):
     C      -0.073869     -0.446687      -0.202854
     H      -0.057929     -0.673670      -1.270866
     C       0.179497      1.052735      -0.018916
     C      -1.401288     -0.887950       0.407452
     O       0.974231     -1.208608       0.423441
     O      -0.768431      1.797722       0.037018
     C       1.597899      1.528172       0.063512
     H       2.165790      1.158338      -0.790736
     H       2.071660      1.112634       0.953949
```

```
     H       1.611019      2.612649       0.099588
     O      -2.477712     -0.401967      -0.348915
     H      -1.446491     -1.975464       0.386771
     H      -1.453029     -0.560839       1.450322
     H      -2.449420      0.560556      -0.299286
     O       1.990033     -1.401125      -0.364659
Rotational constants (GHz):    2.6560700    1.8096900    1.1499900
Vibrational harmonic frequencies (cm-1): (Scaled by 0.9710)
       29.3370                92.1224               137.4153
      187.4753               214.7167               245.0729
      293.7142               370.1615               423.1506
      471.4444               519.0918               583.6509
      612.5507               739.7493               920.8275
      948.6184              1026.0429              1039.0144
     1085.6430              1105.1152              1177.4556
     1203.9053              1244.1436              1270.4952
     1305.1716              1352.0703              1358.1149
     1396.0066              1421.3734              1430.6372
     1472.1997              1780.4187              2960.8289
     2984.3219              3004.9277              3040.6368
     3044.8809              3099.0686              3712.5695
Zero-point correction (Hartree): 0.115678

HMVKBO2.ppmm
------------
E(UM062X/Aug-CC-pVTZ) (Hartree): -457.38187741
Electronic state : 2-A
Cartesian coordinates (Angs):
     C       0.097276     -0.067479      -0.346786
     H       0.340036     -0.085975      -1.410359
     C      -1.407836     -0.224091      -0.168338
     C       0.823366     -1.188121       0.396316
     O       0.520501      1.206636       0.165521
     O      -1.930820     -1.199964      -0.639622
     C      -2.146891      0.824387       0.608695
     H      -2.051220      1.788618       0.108169
     H      -1.697213      0.942886       1.595539
     H      -3.190543      0.539000       0.693014
     O       2.217114     -1.052871       0.353571
     H       0.544220     -1.162190       1.450565
     H       0.473543     -2.132279      -0.029051
     H       2.508035     -0.903852      -0.550590
     O       1.552912      1.664402      -0.479047
Rotational constants (GHz):    2.9281300    1.5704400    1.1531500
Vibrational harmonic frequencies (cm-1): (Scaled by 0.9710)
       34.7856                85.6573               127.4500
      171.2138               178.3183               214.2633
      236.7573               311.2924               386.9152
      449.0142               478.8825               547.0694
      586.3216               842.7041               868.2483
      946.1716               984.5389              1039.9110
     1078.1989              1115.8314              1165.5931
     1216.6648              1248.2188              1274.4499
     1308.9865              1325.6860              1357.2191
     1385.3495              1419.4563              1429.1750
     1464.1188              1796.1878              2972.5498
     2982.3487              3007.1971              3027.8095
     3042.8095              3096.9468              3754.2843
Zero-point correction (Hartree): 0.114867

HMVKBO2.ppmp
------------
E(UM062X/Aug-CC-pVTZ) (Hartree): -457.38305263
Electronic state : 2-A
Cartesian coordinates (Angs):
     C       0.276412     -0.005210      -0.301158
     H       0.487136      0.079292      -1.368019
     C      -1.085935     -0.682748      -0.130555
     C       1.359138     -0.800129       0.414484
     O       0.283971      1.321998       0.250801
     O      -1.233335     -1.766873      -0.630847
     C      -2.143160      0.017827       0.668947
     H      -2.438840      0.935469       0.158798
     H      -1.743008      0.316392       1.638959
     H      -2.996600     -0.641770       0.787719
     O       2.649939     -0.312474       0.147852
     H       1.210455     -0.711510       1.491437
     H       1.239456     -1.848335       0.135132
     H       2.907420     -0.554989      -0.744926
     O      -0.338668      2.163226      -0.518982
Rotational constants (GHz):    2.5086700    1.7359400    1.1607800
Vibrational harmonic frequencies (cm-1): (Scaled by 0.9710)
       38.8721                95.2404               113.0322
      175.9211               189.9353               236.5696
      264.5373               291.5241               346.3134
      462.7306               520.5808               574.3105
      579.5246               799.9983               850.2093
      952.6980               990.9950              1043.6508
     1073.1789              1106.2352              1179.6281
     1219.6558              1239.0379              1254.3435
     1303.5145              1352.7399              1354.7301
```

```
     1378.7326                1421.2466                1430.2613
     1458.0333                1795.3886                2981.4968
     2985.5546                3013.2393                3036.2376
     3042.2121                3097.8618                3766.7791
Zero-point correction (Hartree): 0.115003

HMVKBO2.ppmt
------------
E(UM062X/Aug-CC-pVTZ) (Hartree): -457.38262265
Electronic state : 2-A
Cartesian coordinates (Angs):
     C      -0.225815     -0.115045      0.472810
     H      -0.385538     -0.402480      1.515320
     C       1.162333     -0.622168      0.064912
     C      -1.333634     -0.678229     -0.404522
     O      -0.272365      1.325929      0.515148
     O       1.279001     -1.782171     -0.232602
     C       2.318824      0.333939      0.114285
     H       2.302871      0.903734      1.043655
     H       2.230729      1.054873     -0.698712
     H       3.242926     -0.226894      0.017215
     O      -2.613469     -0.372861      0.097112
     H      -1.259218     -0.220592     -1.389447
     H      -1.165238     -1.750148     -0.506947
     H      -2.832498     -0.974145      0.812300
     O      -0.101202      1.842187     -0.664445
Rotational constants (GHz):    2.8615600    1.7063400    1.1894100
Vibrational harmonic frequencies (cm-1): (Scaled by 0.9710)
       30.6995                  76.8091                 127.8559
      183.2377                 195.9827                 211.9420
      260.8098                 306.9296                 348.0882
      441.6987                 496.8116                 577.9107
      655.9839                 784.0356                 859.6897
      950.5229                 990.8198                1019.4969
     1060.4766                1097.3815                1163.0105
     1190.7140                1229.6263                1259.2339
     1340.1784                1350.6213                1353.0369
     1369.0224                1422.4405                1430.5732
     1459.5652                1793.1857                2985.8957
     2992.0049                3005.2398                3049.2809
     3058.1770                3096.0724                3773.8960
Zero-point correction (Hartree): 0.114962

HMVKBO2.pppm
------------
E(UM062X/Aug-CC-pVTZ) (Hartree): -457.38448356
Electronic state : 2-A
Cartesian coordinates (Angs):
     C       0.085530     -0.062836     -0.322456
     H       0.316099     -0.121091     -1.388410
     C      -1.410292     -0.301944     -0.119614
     C       0.932472     -1.069671      0.445281
     O       0.382354      1.284945      0.113256
     O      -1.835119     -1.411321     -0.305140
     C      -2.275716      0.856590      0.281833
     H      -2.166751      1.671449     -0.434673
     H      -1.948934      1.246349      1.246552
     H      -3.308227      0.526672      0.334194
     O       2.261372     -1.120786      0.001267
     H       0.867699     -0.833696      1.513885
     H       0.493029     -2.051247      0.280826
     H       2.622707     -0.228532     -0.007772
     O       1.582944      1.654320     -0.216241
Rotational constants (GHz):    3.0053900    1.5981800    1.1042900
Vibrational harmonic frequencies (cm-1): (Scaled by 0.9710)
       24.3305                  49.4088                 138.2027
      187.2052                 200.2285                 221.0619
      332.0613                 395.2853                 396.8329
      416.5813                 449.8376                 544.3039
      592.3846                 836.3206                 846.1745
      944.7846                1001.9338                1049.1484
     1066.2250                1101.2570                1186.8150
     1204.1434                1240.6986                1261.8346
     1305.8180                1346.1158                1358.2028
     1388.8844                1420.7169                1431.2297
     1461.0865                1800.3194                2943.3956
     2983.8046                3004.1170                3044.0688
     3054.9615                3098.1627                3733.2039
Zero-point correction (Hartree): 0.115108

HMVKBO2.pppp
------------
E(UM062X/Aug-CC-pVTZ) (Hartree): -457.38544420
Electronic state : 2-A
Cartesian coordinates (Angs):
     C       0.261460     -0.055277     -0.333960
     H       0.463923      0.020518     -1.401860
     C      -1.141421     -0.625106     -0.120922
     C       1.306271     -0.918781      0.353522
     O       0.399179      1.263434      0.232450
     O      -1.373717     -1.712171     -0.580035
```

```
     C      -2.134995      0.176435       0.666144
     H      -2.358418      1.104679       0.138764
     H      -1.708103      0.459569       1.629440
     H      -3.038134     -0.409651       0.801663
     O       2.612043     -0.496609       0.054215
     H       1.119794     -0.921573       1.433104
     H       1.192607     -1.934947      -0.016128
     H       2.754896      0.377998       0.426094
     O      -0.159310      2.175318      -0.506604
Rotational constants (GHz):    2.5316200    1.7502900    1.1591400
Vibrational harmonic frequencies (cm-1): (Scaled by 0.9710)
       33.1502                101.3747                122.0450
      171.3028                186.7654                250.6214
      277.7278                336.2307                351.5365
      454.8613                521.0974                572.1374
      578.8619                794.2581                850.5543
      952.6400                994.3599               1048.9013
     1077.5756               1098.4816               1190.4935
     1216.6849               1232.2015               1251.8481
     1300.5122               1350.4082               1354.5593
     1375.7838               1421.6538               1430.2523
     1459.2989               1796.8678               2949.4225
     2981.7498               3030.9733               3042.4802
     3063.4235               3098.3650               3759.5137
Zero-point correction (Hartree): 0.115154

HMVKBO2.pppt
------------
E(UM062X/Aug-CC-pVTZ) (Hartree): -457.38559643
Electronic state : 2-A
Cartesian coordinates (Angs):
     C      -0.201634     -0.145643       0.502130
     H      -0.323498     -0.387436       1.560199
     C       1.204248     -0.562109       0.063598
     C      -1.294530     -0.817259      -0.311220
     O      -0.355592      1.292503       0.470732
     O       1.378327     -1.694314      -0.302033
     C       2.307653      0.452056       0.162748
     H       2.257485      0.979166       1.115854
     H       2.185135      1.199967      -0.621126
     H       3.261998     -0.051807       0.047080
     O      -2.572701     -0.515322       0.193207
     H      -1.187685     -0.530061      -1.359475
     H      -1.151974     -1.891728      -0.234975
     H      -2.776891      0.405010       0.007573
     O      -0.244908      1.756459      -0.739239
Rotational constants (GHz):    2.9395000    1.6979800    1.2038200
Vibrational harmonic frequencies (cm-1): (Scaled by 0.9710)
       34.1663                 84.5920                132.5795
      175.2633                184.8622                256.3641
      287.5115                332.9495                355.5396
      447.6494                490.3882                578.4060
      657.7165                776.6129                857.9300
      952.3378                989.9856               1020.7370
     1078.0167               1093.6517               1171.9210
     1187.5010               1226.5372               1257.7610
     1337.5590               1353.9156               1355.5643
     1370.0442               1423.8223               1433.6211
     1457.5495               1797.6352               2985.0581
     2987.6623               3008.0366               3048.2969
     3072.3986               3096.0977               3761.7874
Zero-point correction (Hartree): 0.115246

HMVKBO2.pptp
------------
E(UM062X/Aug-CC-pVTZ) (Hartree): -457.38319855
Electronic state : 2-A
Cartesian coordinates (Angs):
     C       0.269735     -0.008816      -0.281047
     H       0.471285      0.114474      -1.345707
     C      -1.084888     -0.706839      -0.110473
     C       1.378711     -0.798241       0.375601
     O       0.263680      1.302567       0.312649
     O      -1.180337     -1.846608      -0.483195
     C      -2.216234      0.060624       0.505783
     H      -2.453677      0.926045      -0.114142
     H      -1.917699      0.449885       1.479944
     H      -3.078771     -0.591305       0.597504
     O       2.603050     -0.251667      -0.059467
     H       1.269878     -0.727200       1.463221
     H       1.260768     -1.840553       0.074696
     H       3.327672     -0.681338       0.399348
     O      -0.306818      2.179411      -0.456743
Rotational constants (GHz):    2.5415400    1.7689900    1.1430300
Vibrational harmonic frequencies (cm-1): (Scaled by 0.9710)
       27.9185                 97.9612                116.5699
      181.9591                197.7506                210.6049
      270.6874                287.7640                348.1112
      443.6351                517.1663                567.2144
      584.7587                795.8430                866.7977
      947.6971                996.4104               1053.4444
```

```
     1090.3072                1108.6697                1189.6189
     1211.1619                1244.5519                1254.0372
     1262.0759                1309.8692                1353.8205
     1416.3269                1421.9616                1429.9800
     1471.6997                1795.2592                2948.9335
     2983.3987                3012.7190                3023.1671
     3043.7955                3098.8050                3784.2259
Zero-point correction (Hartree): 0.114886

HMVKBO2.pptt
------------
E(UM062X/Aug-CC-pVTZ) (Hartree): -457.38385697
Electronic state : 2-A
Cartesian coordinates (Angs):
     C       0.227521     -0.099929      -0.475074
     H       0.373600     -0.319987      -1.535478
     C      -1.153923     -0.616431      -0.058753
     C       1.351591     -0.707601       0.328407
     O       0.267689      1.343270      -0.423402
     O      -1.259147     -1.738211       0.361061
     C      -2.327559      0.300353      -0.257124
     H      -2.262690      0.804063      -1.221699
     H      -2.312736      1.076242       0.508665
     H      -3.243547     -0.276732      -0.179653
     O       2.560381     -0.355475      -0.311676
     H       1.300330     -0.319774       1.348737
     H       1.195765     -1.786765       0.351998
     H       3.300424     -0.645285       0.225064
     O       0.063962      1.776652       0.783721
Rotational constants (GHz):    2.9057200    1.6946600    1.2100900
Vibrational harmonic frequencies (cm-1): (Scaled by 0.9710)
       41.9529                  87.0286                 129.4222
      170.2735                 190.9055                 213.9529
      256.4142                 308.1670                 352.5393
      454.6422                 484.5264                 577.2760
      661.9600                 779.9339                 871.6284
      951.1732                1004.5754                1035.3765
     1074.6016                1097.0879                1169.9718
     1204.6371                1212.8751                1252.0693
     1279.2774                1344.0204                1355.0891
     1413.9729                1423.7619                1433.0009
     1474.7444                1798.8531                2976.8026
     2986.1378                3000.8442                3028.3669
     3049.8639                3095.8275                3787.5883
Zero-point correction (Hartree): 0.115037

HMVKBO2.ptmm
------------
E(UM062X/Aug-CC-pVTZ) (Hartree): -457.38541874
Electronic state : 2-A
Cartesian coordinates (Angs):
     C      -0.207111     -0.081349      -0.632725
     H      -0.324968     -0.325954      -1.688003
     C       1.264917     -0.197614      -0.246708
     C      -0.721224      1.321462      -0.343717
     O      -0.971672     -1.041224       0.135531
     O       2.062314      0.378729      -0.938130
     C       1.630587     -0.980298       0.976943
     H       1.300930     -2.014478       0.875074
     H       1.104427     -0.559688       1.835290
     H       2.704599     -0.932635       1.126004
     O      -0.578423      1.648401       1.020163
     H      -0.114460      2.022249      -0.914095
     H      -1.759394      1.392500      -0.673362
     H      -1.253846      1.188036       1.525392
     O      -2.194757     -1.128811      -0.293696
Rotational constants (GHz):    2.6449000    1.6748400    1.3717600
Vibrational harmonic frequencies (cm-1): (Scaled by 0.9710)
       56.0002                  68.9391                 115.6606
      163.1310                 197.0979                 214.3560
      282.1476                 344.2629                 389.1909
      428.8006                 502.2004                 567.6253
      676.5713                 788.4973                 862.2212
      924.0932                 979.7005                1031.6174
     1045.2235                1099.0648                1178.5429
     1210.4048                1246.2574                1258.3690
     1300.9182                1351.7209                1359.0597
     1366.6487                1420.4869                1429.4954
     1456.3396                1802.4164                2982.4722
     2988.8938                3029.1413                3045.4470
     3055.5251                3097.3201                3759.3561
Zero-point correction (Hartree): 0.115141

HMVKBO2.ptmp
------------
E(UM062X/Aug-CC-pVTZ) (Hartree): -457.38616208
Electronic state : 2-A
Cartesian coordinates (Angs):
     C       0.200181      0.262901      -0.667408
     H      -0.014395      0.434566      -1.721658
     C      -0.647214     -0.918442      -0.182856
```

```
     C       1.675206     -0.018547      -0.439751
     O      -0.087990      1.477394       0.051790
     O      -0.617148     -1.918165      -0.849367
     C      -1.417283     -0.784337       1.094848
     H      -2.184234     -0.016645       0.990640
     H      -0.741332     -0.463281       1.888539
     H      -1.869405     -1.740140       1.339519
     O       1.951595     -0.247996       0.924169
     H       1.929671     -0.927794      -0.980463
     H       2.268578      0.808189      -0.837427
     H       1.885087      0.583573       1.401265
     O      -1.263870      1.947777      -0.240269
Rotational constants (GHz):    2.1504900    2.0699500    1.4157600
Vibrational harmonic frequencies (cm-1): (Scaled by 0.9710)
       60.3906                105.0131                112.2804
      158.9012                172.3129                247.9999
      282.1159                342.4722                368.5942
      487.2192                501.2833                553.3674
      664.8032                778.1565                875.6863
      924.3854                982.3656               1025.7450
     1046.7165               1105.4728               1181.6672
     1217.3587               1250.1195               1263.2864
     1291.2312               1350.2354               1355.9515
     1370.7613               1421.3988               1431.0105
     1457.4311               1801.6516               2977.8896
     2984.1615               3031.5200               3048.4822
     3055.4916               3097.6252               3759.2044
Zero-point correction (Hartree): 0.115297

HMVKBO2.ptmt
------------
E(UM062X/Aug-CC-pVTZ) (Hartree): -457.38651897
Electronic state : 2-A
Cartesian coordinates (Angs):
     C      -0.116533      0.131926      -0.854754
     H       0.083683      0.291361      -1.913404
     C       1.231199     -0.038425      -0.140910
     C      -0.871311      1.321327      -0.275544
     O      -0.893411     -1.088531      -0.834921
     O       2.095271      0.751377      -0.409413
     C       1.382883     -1.145382       0.856663
     H       1.199112     -2.109077       0.380633
     H       0.634143     -1.027639       1.641247
     H       2.382250     -1.111053       1.278336
     O      -0.889773      1.340379       1.129825
     H      -0.342845      2.216959      -0.597061
     H      -1.879594      1.336184      -0.699019
     H      -1.418355      0.591243       1.421048
     O      -1.614064     -1.228806       0.236445
Rotational constants (GHz):    2.5880700    1.8948500    1.5155800
Vibrational harmonic frequencies (cm-1): (Scaled by 0.9710)
       65.2674                 91.5164                135.3830
      168.0937                206.6647                245.0121
      298.5172                382.5474                418.6313
      483.7740                491.7933                577.0722
      696.5067                794.7127                836.7653
      945.4678                985.1181                998.9883
     1028.1956               1115.4329               1186.7456
     1213.9712               1229.1401               1243.3893
     1338.7468               1351.6332               1355.5719
     1386.3746               1420.5855               1430.9494
     1448.3091               1802.7665               2970.0614
     2983.7571               3035.8041               3046.5786
     3048.9355               3097.4236               3745.3665
Zero-point correction (Hartree): 0.115672

HMVKBO2.ptpp
------------
E(UM062X/Aug-CC-pVTZ) (Hartree): -457.38573015
Electronic state : 2-A
Cartesian coordinates (Angs):
     C      -0.019616     -0.417300      -0.534748
     H       0.346524     -0.565198      -1.553350
     C       0.120357      1.068906      -0.186089
     C      -1.457573     -0.890457      -0.400404
     O       0.811475     -1.221267       0.326352
     O      -0.805901      1.799152      -0.436405
     C       1.398777      1.540525       0.434325
     H       2.249663      1.235741      -0.175234
     H       1.524661      1.060163       1.405963
     H       1.365895      2.619419       0.546353
     O      -2.035848     -0.526188       0.827777
     H      -2.021912     -0.494254      -1.246723
     H      -1.469569     -1.977891      -0.454371
     H      -2.238646      0.413685       0.792340
     O       2.029239     -1.314410      -0.116910
Rotational constants (GHz):    2.4709700    1.9727300    1.2665900
Vibrational harmonic frequencies (cm-1): (Scaled by 0.9710)
       33.3405                 97.7831                112.7793
      183.8623                188.2793                257.4453
      307.6236                389.9054                414.5123
```

```
      452.7363                497.0320                555.4023
      672.1927                792.7407                851.0493
      932.4196                966.7542               1024.2907
     1060.1629               1121.5695               1185.6749
     1205.9792               1254.0582               1287.3592
     1293.7897               1355.5532               1360.7531
     1381.0659               1421.1339               1427.7896
     1449.2558               1783.9538               2983.8085
     2985.4759               3001.9224               3045.1487
     3045.1918               3098.8830               3747.8877
Zero-point correction (Hartree): 0.115496

HMVKBO2.pttm
------------
E(UM062X/Aug-CC-pVTZ) (Hartree): -457.38457772
Electronic state : 2-A
Cartesian coordinates (Angs):
     C      -0.261432     -0.095853      -0.610895
     H      -0.423200     -0.351396      -1.657271
     C       1.216950     -0.274615      -0.267496
     C      -0.682340      1.334014      -0.349547
     O      -1.044600     -1.006897       0.192629
     O       2.020668      0.231708      -1.005310
     C       1.573487     -1.028825       0.975277
     H       1.209058     -2.054253       0.907041
     H       1.067120     -0.565828       1.823311
     H       2.650528     -1.013536       1.108954
     O      -0.333125      1.634669       0.986693
     H      -0.147372      1.968062      -1.060712
     H      -1.758414      1.416377      -0.517968
     H      -0.603869      2.530052       1.198114
     O      -2.277174     -1.051706      -0.209700
Rotational constants (GHz):    2.6356000    1.6976700    1.3813700
Vibrational harmonic frequencies (cm-1): (Scaled by 0.9710)
       66.3023                 82.6482                120.1623
      167.8721                178.9902                199.7035
      216.5603                303.0397                383.6611
      427.0117                503.6255                567.8711
      661.9545                800.9025                874.3112
      933.9567                984.1521               1039.4178
     1073.4055               1109.1335               1161.0414
     1212.3320               1235.5293               1253.6985
     1299.1084               1311.3344               1356.7202
     1398.4878               1420.7526               1429.9668
     1467.8101               1801.0880               2968.1492
     2983.2765               3015.5040               3033.0184
     3046.8383               3096.9583               3789.4607
Zero-point correction (Hartree): 0.114907

HMVKBO2.pttp
------------
E(UM062X/Aug-CC-pVTZ) (Hartree): -457.38522117
Electronic state : 2-A
Cartesian coordinates (Angs):
     C      -0.040028     -0.395706      -0.634049
     H       0.238531     -0.505859      -1.681171
     C       0.184703      1.064891      -0.221122
     C      -1.488721     -0.769671      -0.420453
     O       0.761618     -1.311590       0.134039
     O      -0.269061      1.912170      -0.943284
     C       0.904178      1.344037       1.061341
     H       1.942741      1.021704       0.980786
     H       0.444119      0.762369       1.860866
     H       0.854985      2.407392       1.273218
     O      -1.812895     -0.459242       0.919744
     H      -2.082638     -0.184414      -1.126157
     H      -1.619443     -1.834603      -0.629256
     H      -2.737631     -0.654309       1.083214
     O       2.020156     -1.200537      -0.169974
Rotational constants (GHz):    2.2423500    2.0264800    1.4304800
Vibrational harmonic frequencies (cm-1): (Scaled by 0.9710)
       70.0097                108.7506                114.6693
      167.4057                175.7500                207.1586
      254.2924                289.0592                353.3932
      487.5893                496.8874                553.8032
      653.6210                784.8339                884.9331
      936.1688                983.0298               1021.3123
     1092.8179               1117.3398               1172.3681
     1209.6483               1237.8308               1251.5239
     1296.3613               1303.7654               1351.9150
     1408.6215               1424.0275               1429.9098
     1465.0896               1800.2201               2963.9023
     2984.1362               3010.2189               3034.0693
     3049.0904               3097.0753               3787.1405
Zero-point correction (Hartree): 0.115034

TS.HMVKAO2.14HshiftCH2OH.dtSl
-----------------------------
E(UM062X/Aug-CC-pVTZ) (Hartree): -457.34602051
Electronic state : 2-A
Cartesian coordinates (Angs):
```

```
     O       1.884171      0.188745      -1.055055
     O       1.852812      0.548972       0.277798
     C       1.123920     -0.489998       0.893118
     C      -0.104567     -0.650375      -0.015422
     H       0.648553     -0.322220      -1.015917
     H       0.900320     -0.181208       1.914315
     H       1.672279     -1.432968       0.878928
     O      -0.593223     -1.907358      -0.057665
     H      -1.546562     -1.831176      -0.241213
     C      -1.193966      0.393339      -0.015825
     O      -2.327034      0.006330      -0.200933
     C      -0.830192      1.834260       0.159317
     H      -0.071840      2.116848      -0.570816
     H      -0.386807      1.988826       1.143882
     H      -1.720905      2.445021       0.050537
Rotational constants (GHz):    2.9661000    1.7353800    1.3023300
Vibrational harmonic frequencies (cm-1): (Scaled by 0.9710)
    i2103.8767                  92.9891                 125.7682
      182.2763                 218.3234                 281.4142
      325.3019                 373.9734                 405.0106
      483.8817                 564.7528                 618.2414
      652.0706                 684.0746                 740.0971
      933.8709                 963.0414                 973.5332
     1044.2322                1046.0252                1060.0143
     1159.8413                1202.2727                1211.6371
     1279.5388                1348.7362                1369.2613
     1383.3540                1418.8511                1432.7145
     1456.8753                1698.4056                1748.0782
     2985.4161                2986.0010                3046.7891
     3048.4940                3095.5150                3564.4345
Zero-point correction (Hartree): 0.110753

TS.HMVKAO2.15HshiftOH.md
------------------------
E(CCSD(T)/Aug-CC-pVDZ) (Hartree): -456.32252047
E(CCSD/Aug-CC-pVDZ) (Hartree): -456.26584391
     T1 diagnostic:  0.035376
E(MP2/Aug-CC-pVDZ) (Hartree): -456.20231883
E(MP3/Aug-CC-pVDZ) (Hartree): -456.23515652
E(PMP2/Aug-CC-pVDZ) (Hartree): -456.20749097
E(PMP3/Aug-CC-pVDZ) (Hartree): -456.23842643
E(PUHF/Aug-CC-pVDZ) (Hartree): -454.86974318
E(UHF/Aug-CC-pVDZ) (Hartree): -454.86206821
E(CCSD(T)/Aug-CC-pVTZ) (Hartree): -456.71475739
E(CCSD/Aug-CC-pVTZ) (Hartree): -456.63566900
     T1 diagnostic:  0.033944
E(MP2/Aug-CC-pVTZ) (Hartree): -456.59254836
E(MP3/Aug-CC-pVTZ) (Hartree): -456.61373848
E(PMP2/Aug-CC-pVTZ) (Hartree): -456.59792785
E(PMP3/Aug-CC-pVTZ) (Hartree): -456.61710646
E(PUHF/Aug-CC-pVTZ) (Hartree): -454.97777406
E(UHF/Aug-CC-pVTZ) (Hartree): -454.96980049
E(UM062X/Aug-CC-pVTZ) (Hartree): -457.35092637
Electronic state : 2-A
Cartesian coordinates (Angs):
     O      -2.194552      0.560661      -0.341599
     O      -1.376592     -0.347004      -0.972750
     C      -0.859745     -1.192702      -0.020123
     C       0.156353     -0.295562       0.879044
     O      -0.490127      0.804216       1.266050
     H      -1.527908      0.901480       0.464448
     H      -1.631658     -1.554724       0.656101
     H      -0.292442     -1.977730      -0.512487
     H       0.403470     -0.986455       1.698519
     C       1.400321     -0.065880       0.005497
     O       2.169709     -0.977478      -0.149342
     C       1.549924      1.290269      -0.610553
     H       2.431720      1.312457      -1.242577
     H       0.652566      1.526328      -1.185575
     H       1.615637      2.038732       0.179502
Rotational constants (GHz):    3.3642900    1.5528300    1.4423400
Vibrational harmonic frequencies (cm-1): (Scaled by 0.9710)
    i1254.5188                  58.4025                  86.4330
      167.5849                 191.7071                 268.2428
      386.3769                 422.2017                 485.1879
      523.9390                 555.6501                 641.2558
      680.5528                 700.9230                 774.9743
      883.7553                 951.0160                 965.6347
      986.8015                1024.1314                1082.1581
     1165.3930                1204.0555                1217.2889
     1241.6209                1268.4149                1315.2966
     1352.4414                1416.7158                1425.6615
     1438.7196                1770.9353                1796.8264
     2910.7482                2980.9627                3009.3562
     3041.9162                3098.5096                3101.2741
Zero-point correction (Hartree): 0.109317

TS.HMVKAO2.15HshiftOH.mu
------------------------
IRC pathway available
E(CCSD(T)/Aug-CC-pVDZ) (Hartree): -456.32262687
```

```
E(CCSD/Aug-CC-pVDZ) (Hartree): -456.26547103
     T1 diagnostic:  0.040391
E(MP2/Aug-CC-pVDZ) (Hartree): -456.20041131
E(MP3/Aug-CC-pVDZ) (Hartree): -456.23338339
E(PMP2/Aug-CC-pVDZ) (Hartree): -456.20547813
E(PMP3/Aug-CC-pVDZ) (Hartree): -456.23662340
E(PUHF/Aug-CC-pVDZ) (Hartree): -454.86836382
E(UHF/Aug-CC-pVDZ) (Hartree): -454.86083426
E(CCSD(T)/Aug-CC-pVTZ) (Hartree): -456.71525572
E(CCSD/Aug-CC-pVTZ) (Hartree): -456.63558622
     T1 diagnostic:  0.038365
E(MP2/Aug-CC-pVTZ) (Hartree): -456.59115793
E(MP3/Aug-CC-pVTZ) (Hartree): -456.61244759
E(PMP2/Aug-CC-pVTZ) (Hartree): -456.59645225
E(PMP3/Aug-CC-pVTZ) (Hartree): -456.61579632
E(PUHF/Aug-CC-pVTZ) (Hartree): -454.97676820
E(UHF/Aug-CC-pVTZ) (Hartree): -454.96891190
E(UM062X/Aug-CC-pVTZ) (Hartree): -457.35136408
Electronic state : 2-A
Cartesian coordinates (Angs):
     O       2.421102      0.568993      0.284794
     O       2.058305     -0.742989      0.096903
     C       0.738987     -0.882780      0.466299
     C      -0.101163     -0.076133     -0.647893
     O       0.381045      1.161292     -0.735574
     H       1.597110      1.080473     -0.230205
     H       0.469663     -1.934205      0.417473
     H       0.549910     -0.426079      1.438454
     H      -0.039670     -0.667377     -1.569183
     C      -1.544636     -0.169451     -0.080214
     O      -2.155652     -1.188275     -0.231977
     C      -2.051004      1.044497      0.635661
     H      -3.015634      0.831354      1.084670
     H      -1.326843      1.364928      1.384805
     H      -2.126043      1.861949     -0.082311
Rotational constants (GHz):    4.0840000    1.3513100    1.1612800
Vibrational harmonic frequencies (cm-1): (Scaled by 0.9710)
    i1175.4275                66.3794                100.6276
     156.0419                 183.5656                269.9151
     370.4835                 399.0959                512.9335
     513.7438                 554.8283                578.3265
     693.6849                 700.4782                772.6359
     883.6102                 939.9847                975.7201
     993.5901                1048.7162               1114.4712
    1173.5535                1180.5114               1203.4188
    1268.1748                1280.3517               1321.2393
    1349.7902                1414.1226               1420.1917
    1433.8348                1775.0689               1804.2545
    2950.6215                2986.2198               2993.7107
    3046.9900                3094.5837               3101.0906
Zero-point correction (Hartree): 0.109396

TS.HMVKAO2.16HshiftCH3.a.Sp
---------------------------
IRC pathway available
E(CCSD(T)/Aug-CC-pVDZ) (Hartree): -456.32282572
E(CCSD/Aug-CC-pVDZ) (Hartree): -456.26825438
     T1 diagnostic:  0.024330
E(MP2/Aug-CC-pVDZ) (Hartree): -456.21180407
E(MP3/Aug-CC-pVDZ) (Hartree): -456.24375974
E(PMP2/Aug-CC-pVDZ) (Hartree): -456.22202486
E(PMP3/Aug-CC-pVDZ) (Hartree): -456.25029721
E(PUHF/Aug-CC-pVDZ) (Hartree): -454.88015200
E(UHF/Aug-CC-pVDZ) (Hartree): -454.86685827
E(CCSD(T)/Aug-CC-pVTZ) (Hartree): -456.71395585
E(CCSD/Aug-CC-pVTZ) (Hartree): -456.63705508
     T1 diagnostic:  0.023234
E(MP2/Aug-CC-pVTZ) (Hartree): -456.60076598
E(MP3/Aug-CC-pVTZ) (Hartree): -456.62086538
E(PMP2/Aug-CC-pVTZ) (Hartree): -456.61127981
E(PMP3/Aug-CC-pVTZ) (Hartree): -456.62756435
E(PUHF/Aug-CC-pVTZ) (Hartree): -454.98634600
E(UHF/Aug-CC-pVTZ) (Hartree): -454.97268688
E(UM062X/Aug-CC-pVTZ) (Hartree): -457.34948846
Electronic state : 2-A
Cartesian coordinates (Angs):
     O      -2.034844      0.381901     -0.558831
     H      -1.343551      1.192867     -0.092088
     C      -0.284735      1.733053      0.588736
     O      -1.788701     -0.734668      0.198473
     C       0.757086      0.826163      0.089710
     C      -0.558452     -1.313862     -0.196905
     C       0.658119     -0.644102      0.479413
     H      -0.666170      1.541014      1.586562
     H      -0.189588      2.769722      0.290608
     H      -0.599297     -2.352546      0.125735
     H      -0.453846     -1.263187     -1.280849
     O       1.643684      1.179359     -0.657519
     O       1.802278     -1.333181      0.082637
     H       0.530287     -0.714396      1.564007
     H       2.310719     -0.728276     -0.477777
```

```
Rotational constants (GHz):    2.8338200    1.9070400    1.2979500
Vibrational harmonic frequencies (cm-1): (Scaled by 0.9710)
    i1872.5623                101.2725                 119.9780
      244.3469                295.0858                 324.0826
      354.7458                414.7901                 441.5113
      522.3909                546.6416                 600.5345
      641.4140                665.5430                 759.3995
      892.8739                949.9451                 976.4107
     1009.7079               1051.5321                1069.0764
     1119.1297               1136.9355                1190.5607
     1235.1835               1260.3616                1295.5344
     1334.0887               1402.7679                1408.2471
     1434.8895               1447.7660                1736.9053
     2968.1232               3000.1752                3043.4983
     3066.4384               3146.8376                3638.5821
Zero-point correction (Hartree): 0.109914

TS.HMVKAO2.16HshiftCH3.b.St
---------------------------
E(UM062X/Aug-CC-pVTZ) (Hartree): -457.34542770
Electronic state : 2-A
Cartesian coordinates (Angs):
     O      -2.151359      0.140081      -0.305700
     H      -1.478585      1.018788       0.042125
     C      -0.435404      1.698677       0.646150
     O      -1.264356     -0.821926      -0.716329
     C       0.651286      0.884346       0.102687
     C      -0.550072     -1.313282       0.412009
     C       0.781905     -0.556221       0.599827
     H      -0.710163      1.531518       1.682543
     H      -0.487939      2.718290       0.285309
     H      -1.195990     -1.244055       1.285903
     H      -0.309772     -2.353130       0.198295
     O       1.393254      1.271961      -0.773465
     O       1.812983     -1.197807      -0.081447
     H       1.003171     -0.531457       1.675095
     H       2.168811     -0.559550      -0.717779
Rotational constants (GHz):    2.7254600    2.0162200    1.4085000
Vibrational harmonic frequencies (cm-1): (Scaled by 0.9710)
    i1862.5122                 85.5569                 115.6288
      264.9617                279.5386                 335.7266
      403.8751                413.7656                 446.8780
      501.1056                519.5281                 590.6030
      614.2366                693.3021                 811.5645
      899.6150                928.0395                 984.4128
      989.2139               1039.7892                1054.5468
     1101.7804               1147.2013                1169.3000
     1220.6310               1285.0151                1303.0087
     1337.4599               1393.4307                1410.5817
     1427.1204               1440.5856                1728.6471
     2927.3395               3005.1192                3046.6354
     3068.5662               3148.8787                3631.4786
Zero-point correction (Hartree): 0.109720

TS.HMVKBO2.14HshiftCH2OH.umRlp
------------------------------
IRC pathway available
E(CCSD(T)/Aug-CC-pVDZ) (Hartree): -456.31676020
E(CCSD/Aug-CC-pVDZ) (Hartree): -456.26121932
     T1 diagnostic:  0.024454
E(MP2/Aug-CC-pVDZ) (Hartree): -456.20488418
E(MP3/Aug-CC-pVDZ) (Hartree): -456.23592090
E(PMP2/Aug-CC-pVDZ) (Hartree): -456.21278298
E(PMP3/Aug-CC-pVDZ) (Hartree): -456.24067724
E(PUHF/Aug-CC-pVDZ) (Hartree): -454.86786824
E(UHF/Aug-CC-pVDZ) (Hartree): -454.85692566
E(CCSD(T)/Aug-CC-pVTZ) (Hartree): -456.70766299
E(CCSD/Aug-CC-pVTZ) (Hartree): -456.62976787
     T1 diagnostic:  0.023693
E(MP2/Aug-CC-pVTZ) (Hartree): -456.59335513
E(MP3/Aug-CC-pVTZ) (Hartree): -456.61254242
E(PMP2/Aug-CC-pVTZ) (Hartree): -456.60152856
E(PMP3/Aug-CC-pVTZ) (Hartree): -456.61744357
E(PUHF/Aug-CC-pVTZ) (Hartree): -454.97407001
E(UHF/Aug-CC-pVTZ) (Hartree): -454.96277393
E(UM062X/Aug-CC-pVTZ) (Hartree): -457.34102477
Electronic state : 2-A
Cartesian coordinates (Angs):
     O       0.030855      1.693522      -0.905691
     O       0.278002      1.581015       0.468525
     C      -0.123051      0.261882       0.744546
     C      -1.537333      0.238381       0.139886
     H      -1.087115      0.971146      -0.829715
     O      -2.123173     -0.935785      -0.159351
     H      -1.423473     -1.586982      -0.350916
     H      -2.225324      0.916677       0.643108
     C       0.817364     -0.758675       0.102187
     H      -0.105425      0.122473       1.829707
     O       0.395450     -1.843896      -0.232519
     C       2.247922     -0.354227      -0.051545
     H       2.630568      0.036422       0.891808
```

```
     H       2.298585      0.460911      -0.774239
     H       2.833698     -1.203650      -0.387907
Rotational constants (GHz):    2.5144600    2.1689300    1.3592700
Vibrational harmonic frequencies (cm-1): (Scaled by 0.9710)
    i1720.0102                  70.0149                 151.7520
      176.5398                 237.4238                 240.8273
      302.9182                 431.1423                 461.7598
      485.3768                 547.5701                 625.7265
      684.7628                 701.5996                 774.6627
      906.2657                 947.0595                 958.4325
     1013.2427                1057.1299                1066.7569
     1171.9378                1193.3112                1235.1972
     1250.4523                1314.0060                1334.8429
     1356.5694                1418.0833                1425.5807
     1429.0119                1750.9040                1768.6382
     2982.7178                2985.6879                3033.2588
     3048.3434                3098.4020                3501.0526
Zero-point correction (Hartree): 0.110598

TS.HMVKBO2.15HshiftCH3.mp
-------------------------
E(UM062X/Aug-CC-pVTZ) (Hartree): -457.33644494
Electronic state : 2-A
Cartesian coordinates (Angs):
     O       0.201107      1.711954      -0.627580
     O      -0.275255      1.245265       0.585368
     C      -0.271170     -0.183531       0.540160
     C       1.124183     -0.664273       0.138014
     C       2.140221      0.405979      -0.000860
     H       1.321141      1.311043      -0.591765
     H       2.319121      1.005619       0.887705
     H       3.001357      0.160155      -0.608588
     O       1.324777     -1.824982      -0.120056
     H      -0.493634     -0.487286       1.564562
     C      -1.341109     -0.718921      -0.399036
     O      -2.621355     -0.316697       0.020832
     H      -1.126636     -0.387852      -1.418661
     H      -1.308401     -1.805569      -0.376099
     H      -2.659893      0.644043       0.004656
Rotational constants (GHz):    2.9586100    1.7846500    1.2436200
Vibrational harmonic frequencies (cm-1): (Scaled by 0.9710)
    i1999.0682                  68.7395                 108.2236
      174.7116                 255.6608                 302.2956
      354.4028                 367.8836                 457.7299
      503.5329                 526.9672                 573.1544
      598.8990                 681.7914                 816.9942
      883.2750                 921.8354                 952.0351
      984.4238                1045.3135                1091.4188
     1096.0339                1108.0500                1167.6634
     1194.7102                1231.9245                1311.2107
     1351.9559                1375.3268                1379.1848
     1460.9286                1571.4736                1766.0710
     2974.4332                3014.0022                3036.8963
     3061.6024                3147.2530                3751.9136
Zero-point correction (Hartree): 0.109497

TS.HMVKBO2.15HshiftCH3.bis.pm
-----------------------------
IRC pathway available
E(CCSD(T)/Aug-CC-pVDZ) (Hartree): -456.31237540
E(CCSD/Aug-CC-pVDZ) (Hartree): -456.25856605
     T1 diagnostic:  0.022101
E(MP2/Aug-CC-pVDZ) (Hartree): -456.20268700
E(MP3/Aug-CC-pVDZ) (Hartree): -456.23458198
E(PMP2/Aug-CC-pVDZ) (Hartree): -456.21229527
E(PMP3/Aug-CC-pVDZ) (Hartree): -456.24064295
E(PUHF/Aug-CC-pVDZ) (Hartree): -454.87136962
E(UHF/Aug-CC-pVDZ) (Hartree): -454.85871419
E(CCSD(T)/Aug-CC-pVTZ) (Hartree): -456.70300785
E(CCSD/Aug-CC-pVTZ) (Hartree): -456.62694511
     T1 diagnostic:  0.021103
E(MP2/Aug-CC-pVTZ) (Hartree): -456.59114466
E(MP3/Aug-CC-pVTZ) (Hartree): -456.61113840
E(PMP2/Aug-CC-pVTZ) (Hartree): -456.60107187
E(PMP3/Aug-CC-pVTZ) (Hartree): -456.61737601
E(PUHF/Aug-CC-pVTZ) (Hartree): -454.97746327
E(UHF/Aug-CC-pVTZ) (Hartree): -454.96441293
E(UM062X/Aug-CC-pVTZ) (Hartree): -457.33727492
Electronic state : 2-A
Cartesian coordinates (Angs):
     O       1.541131     -1.501412      -0.253918
     O       0.164209     -1.431274      -0.160893
     C      -0.262151     -0.197213      -0.724566
     C       0.530727      0.955242      -0.098392
     C       1.433896      0.567494       1.007693
     H       1.858203     -0.593629       0.446336
     H       2.248758      1.248362       1.217172
     H       0.943250      0.106213       1.860867
     O       0.442557      2.065876      -0.556308
     H      -0.078277     -0.184962      -1.801829
     C      -1.741850     -0.070472      -0.415196
```

```
     O      -1.973330     -0.032670       0.975626
     H      -2.094497      0.872496      -0.828591
     H      -2.284359     -0.890549      -0.892147
     H      -1.753343     -0.892394       1.344901
Rotational constants (GHz):    2.4049100    2.0563600    1.4501700
Vibrational harmonic frequencies (cm-1): (Scaled by 0.9710)
    i1984.4981                82.6755               109.9682
      159.5793               262.1384               291.0805
      347.9969               376.4799               435.4536
      504.2152               526.0002               577.8632
      626.3082               689.2824               772.4624
      877.3116               925.2918               944.2674
     1016.7547              1036.5645              1069.8357
     1104.6733              1110.0099              1161.8959
     1212.2982              1275.6507              1290.1107
     1353.5253              1371.8910              1376.7065
     1455.3543              1569.0197              1774.7764
     2973.1973              2992.0208              3035.6566
     3051.3003              3146.2402              3759.0546
Zero-point correction (Hartree): 0.109439

TS.HMVKBO2.15HshiftOH.t
-----------------------
IRC pathway available
E(CCSD(T)/Aug-CC-pVDZ) (Hartree): -456.31841429
E(CCSD/Aug-CC-pVDZ) (Hartree): -456.26241001
     T1 diagnostic:  0.035348
E(MP2/Aug-CC-pVDZ) (Hartree): -456.19762041
E(MP3/Aug-CC-pVDZ) (Hartree): -456.23292148
E(PMP2/Aug-CC-pVDZ) (Hartree): -456.20220625
E(PMP3/Aug-CC-pVDZ) (Hartree): -456.23583228
E(PUHF/Aug-CC-pVDZ) (Hartree): -454.87036633
E(UHF/Aug-CC-pVDZ) (Hartree): -454.86348135
E(CCSD(T)/Aug-CC-pVTZ) (Hartree): -456.70991292
E(CCSD/Aug-CC-pVTZ) (Hartree): -456.63172003
     T1 diagnostic:  0.033539
E(MP2/Aug-CC-pVTZ) (Hartree): -456.58735544
E(MP3/Aug-CC-pVTZ) (Hartree): -456.61111167
E(PMP2/Aug-CC-pVTZ) (Hartree): -456.59214593
E(PMP3/Aug-CC-pVTZ) (Hartree): -456.61411650
E(PUHF/Aug-CC-pVTZ) (Hartree): -454.97787761
E(UHF/Aug-CC-pVTZ) (Hartree): -454.97068590
E(UM062X/Aug-CC-pVTZ) (Hartree): -457.34568179
Electronic state : 2-A
Cartesian coordinates (Angs):
     O       0.745605      1.501524      -0.620875
     O       0.525690      1.231735       0.715991
     C       0.116002     -0.084617       0.828991
     C       1.341605     -1.004066       0.389523
     O       1.799705     -0.579280      -0.802316
     H       1.370616      0.652473      -0.913900
     H       2.086464     -0.951690       1.189223
     H       0.870296     -1.994835       0.318864
     H      -0.077107     -0.255372       1.890267
     C      -1.154136     -0.432817       0.030386
     O      -1.349639     -1.570229      -0.296362
     C      -2.129430      0.685590      -0.199325
     H      -3.047786      0.277482      -0.608948
     H      -2.323876      1.205862       0.739379
     H      -1.693744      1.411536      -0.883843
Rotational constants (GHz):    2.8483700    1.9725100    1.4629400
Vibrational harmonic frequencies (cm-1): (Scaled by 0.9710)
    i1158.7670                54.9385               113.6510
      130.0334               204.4073               270.6639
      335.2259               417.8518               467.2986
      518.1767               570.4574               607.4376
      673.7363               775.2853               794.0243
      873.4363               925.9955               964.5587
      972.0458              1038.5901              1062.5708
     1139.6786              1179.2062              1205.6529
     1241.0571              1283.6026              1323.1509
     1349.7309              1422.7638              1431.1558
     1454.4978              1755.7741              1803.3453
     2896.2745              2980.7331              2987.9592
     3009.9441              3055.9995              3099.9579
Zero-point correction (Hartree): 0.108843

TS.HMVKBO2.15HshiftOH.bis.c
---------------------------
E(UM062X/Aug-CC-pVTZ) (Hartree): -457.33974626
Electronic state : 2-A
Cartesian coordinates (Angs):
     O      -2.043193     -1.018306       0.443766
     O      -0.768707     -1.157121      -0.057623
     C      -0.032754     -0.077789       0.359886
     C      -0.626854      1.210855      -0.445540
     O      -1.945881      1.238620      -0.249758
     H      -2.277737     -0.012157       0.127477
     H      -0.108463      2.056806       0.026760
     H      -0.323068      1.078372      -1.491014
     H      -0.196682      0.128820       1.419089
```

```
     C       1.435821     -0.249294      -0.002334
     O       1.802043     -1.178971      -0.663090
     C       2.357317      0.838196       0.483881
     H       3.378627      0.469596       0.470850
     H       2.286070      1.690195      -0.195677
     H       2.085969      1.182787       1.480803
Rotational constants (GHz):    3.4716400    1.5030500    1.1684700
Vibrational harmonic frequencies (cm-1): (Scaled by 0.9710)
    i1013.8197                43.1844                119.0336
      147.8901               193.0349                208.9061
      340.3352               367.1566                469.6613
      481.4378               530.3842                604.0190
      646.9820               671.0444                879.1713
      892.7017               935.8769                967.3829
     1009.5274              1072.7320               1123.7730
     1172.3153              1206.3595               1217.9980
     1226.8518              1275.4401               1344.3337
     1362.9907              1426.5258               1437.6367
     1469.3026              1808.2405               1831.5482
     2895.1876              2961.7268               2979.0601
     3005.3212              3045.3523               3092.2116
Zero-point correction (Hartree): 0.109011

TS.HMVKBO2.15HshiftOH.bis.t
---------------------------
E(CCSD(T)/Aug-CC-pVDZ) (Hartree): -456.31690208
E(CCSD/Aug-CC-pVDZ) (Hartree): -456.26077363
     T1 diagnostic:  0.037099
E(MP2/Aug-CC-pVDZ) (Hartree): -456.19580528
E(MP3/Aug-CC-pVDZ) (Hartree): -456.23028948
E(PMP2/Aug-CC-pVDZ) (Hartree): -456.20066373
E(PMP3/Aug-CC-pVDZ) (Hartree): -456.23344478
E(PUHF/Aug-CC-pVDZ) (Hartree): -454.86814107
E(UHF/Aug-CC-pVDZ) (Hartree): -454.86099526
E(CCSD(T)/Aug-CC-pVTZ) (Hartree): -456.70918662
E(CCSD/Aug-CC-pVTZ) (Hartree): -456.63076391
     T1 diagnostic:  0.035250
E(MP2/Aug-CC-pVTZ) (Hartree): -456.58628082
E(MP3/Aug-CC-pVTZ) (Hartree): -456.60915747
E(PMP2/Aug-CC-pVTZ) (Hartree): -456.59135563
E(PMP3/Aug-CC-pVTZ) (Hartree): -456.61241794
E(PUHF/Aug-CC-pVTZ) (Hartree): -454.97640047
E(UHF/Aug-CC-pVTZ) (Hartree): -454.96893868
E(UM062X/Aug-CC-pVTZ) (Hartree): -457.34522621
Electronic state : 2-A
Cartesian coordinates (Angs):
     O      -1.872571      1.215932      -0.410969
     O      -0.555085      1.153499      -0.021354
     C      -0.038682     -0.056620      -0.434548
     C      -0.771555     -1.187352       0.465574
     O      -2.091096     -0.997269       0.356708
     H      -2.237036      0.248610      -0.044487
     H      -0.419101     -2.113343      -0.006419
     H      -0.384772     -1.082437       1.486730
     H      -0.292586     -0.270700      -1.472514
     C       1.457171     -0.144926      -0.172208
     O       2.046132     -1.103971      -0.593114
     C       2.090804      0.953012       0.627682
     H       3.142305      0.729862       0.776189
     H       1.967556      1.902771       0.106115
     H       1.578167      1.055016       1.585211
Rotational constants (GHz):    3.4397400    1.5178900    1.1907400
Vibrational harmonic frequencies (cm-1): (Scaled by 0.9710)
    i1201.7934                45.2626                147.6267
      158.5306               183.1466                212.5315
      321.2716               411.0014                473.1626
      486.1009               546.3366                568.8128
      665.5663               681.8361                831.6410
      863.2232               917.4099                982.8861
     1012.1289              1069.8365               1123.7764
     1189.4767              1195.1637               1204.1936
     1229.2232              1276.5268               1320.4431
     1357.5302              1419.0248               1426.6049
     1466.8381              1778.1354               1802.4415
     2903.7104              2966.9422               2983.3432
     3027.4038              3044.1597               3099.6627
Zero-point correction (Hartree): 0.108847

TS.HMVKBO2.HO2elim.pZm
----------------------
IRC pathway available
E(CCSD(T)/Aug-CC-pVDZ) (Hartree): -456.31014617
E(CCSD/Aug-CC-pVDZ) (Hartree): -456.24990038
     T1 diagnostic:  0.033259
E(MP2/Aug-CC-pVDZ) (Hartree): -456.19833979
E(MP3/Aug-CC-pVDZ) (Hartree): -456.21898987
E(PMP2/Aug-CC-pVDZ) (Hartree): -456.22754672
E(PMP3/Aug-CC-pVDZ) (Hartree): -456.24442716
E(PUHF/Aug-CC-pVDZ) (Hartree): -454.87061449
E(UHF/Aug-CC-pVDZ) (Hartree): -454.83893501
E(CCSD(T)/Aug-CC-pVTZ) (Hartree): -456.69941482
```

```
E(CCSD/Aug-CC-pVTZ) (Hartree): -456.61634437
     T1 diagnostic:  0.033018
E(MP2/Aug-CC-pVTZ) (Hartree): -456.58459471
E(MP3/Aug-CC-pVTZ) (Hartree): -456.59304969
E(PMP2/Aug-CC-pVTZ) (Hartree): -456.61504853
E(PMP3/Aug-CC-pVTZ) (Hartree): -456.61953681
E(PUHF/Aug-CC-pVTZ) (Hartree): -454.97780129
E(UHF/Aug-CC-pVTZ) (Hartree): -454.94481991
E(UM062X/Aug-CC-pVTZ) (Hartree): -457.33102745
Electronic state : 2-A
Cartesian coordinates (Angs):
     O      -1.600602      1.577093      -0.473492
     O      -0.381432      1.683747      -0.299410
     C       0.007739     -0.031122       0.846214
     C      -1.230978     -0.677766       0.715075
     H      -1.771137      0.353518       0.220605
     O      -1.428894     -1.718010      -0.170292
     H      -0.649465     -1.775960      -0.744313
     H      -1.816856     -0.804403       1.621860
     C       1.177094     -0.322897      -0.012823
     H       0.174297      0.574827       1.725566
     O       1.094585     -1.112130      -0.933774
     C       2.440989      0.424506       0.294026
     H       3.218798      0.143151      -0.408547
     H       2.245208      1.496359       0.230771
     H       2.760839      0.210581       1.314851
Rotational constants (GHz):    2.4029100    1.8353600    1.2661800
Vibrational harmonic frequencies (cm-1): (Scaled by 0.9710)
    i1027.9926                69.8267                111.2287
      131.0264               148.6305                204.2438
      249.0331               340.6202                364.4529
      456.6042               517.6168                550.8328
      624.2639               691.3864                715.6867
      844.1860               909.3656                958.2840
     1003.7957              1022.7406               1110.1159
     1171.2932              1196.2076               1257.0953
     1333.0390              1348.0429               1386.3677
     1423.0189              1429.0542               1434.3050
     1509.3672              1549.4444               1736.7490
     2977.9066              3039.3516               3053.5596
     3095.1894              3128.6717               3590.9805
Zero-point correction (Hartree): 0.109529
```